Large Solar Flares and their Ionospheric D-region Enhancements

Neil R. Thomson and Craig J. Rodger
Physics Department, University of Otago, Dunedin, New Zealand

Mark A. Clilverd
Physical Sciences Division, British Antarctic Survey, Cambridge, UK

On 4 November 2003, the largest solar flare ever recorded saturated the GOES satellite X–ray detectors making an assessment of its size difficult. However, VLF radio phase advances effectively recorded the lowering of the VLF reflection height and hence lowest edge of the Earth's ionosphere. Previously these phase advances were used to extrapolate the GOES 0.1-0.8 nm ('XL') fluxes from saturation at X17 to give a peak magnitude of X45±5 for this great flare. Here it is shown that a similar extrapolation, but using the other GOES X–ray band, 0.05-0.4 nm ('XS'), is also consistent with a magnitude of X45. Also reported here are VLF phase measurements from two paths near dawn: 'Omega Australia' to Dunedin, NZ, (only just all sunlit) and NPM, Hawaii, to Ny Alesund, Svalbard (only partly sunlit) which also give remarkably good extrapolations of the flare flux, suggesting that VLF paths monitoring flares do not necessarily need to be in full daylight. D-region electron densities are modeled as functions of X-ray flux up to the level of the great X45 flare by using flare-induced VLF amplitudes together with the VLF phase changes. During this great flare, the 'Wait' reflection height, *H'*, was found to have been lowered to ~53 km, or ~17 km below the normal mid-day value of ~70 km. Finally, XL/XS ratios are examined during some large flares including the great flare. Plots of such ratios against XL can give quite good estimates of the great flare's size (X45), but without use of VLF measurements.

1. Introduction

During solar flares the X-ray flux received at the Earth increases dramatically, often within a few minutes, and then decays again in times ranging from a few tens of minutes to several hours (http://sec.noaa.gov/Data/goes.html). These X-rays have major effects in the Earth's upper atmosphere but are absorbed before they reach the ground. X-ray detectors on the GOES satellites have been recording the fluxes from solar flares since about 1976. However, during the very largest flares, such as the great flare of 4 November 2003, the GOES detectors saturate thus resulting in considerable uncertainty in the peak X-ray flux.

VLF (Very Low Frequency) radio waves (3-30 kHz) typically propagate with good signal-to-noise ratio over ranges up to 10-15 Mm or more in the Earth-ionosphere waveguide, bounded above by the D-region and below by the Earth's surface [e.g., *Watt*, 1967]. By day, the propagation paths are largely stable and the received phases are reproducible, in quiet conditions away from dawn and dusk, to a very few microseconds or better than about 10 degrees [e.g., *Watt*, 1967; *McRae and Thomson*, 2000; 2004]. However, when a solar flare occurs (on a sunlit path), the extra ionization generated by the X-rays lowers the effective reflection height of the ionosphere and advances the phase at the receiver by an amount that depends on the intensity of the X-ray flux [e.g., *Mitra*, 1974]. For daytime solar flares, both the height lowering and the phase advance (at least for path lengths greater than a few Mm) have been found to be nearly proportional to the logarithm of the X-ray flux [*McRae and Thomson*, 2004] up to at least the level of an X5 flare which lowered the effective reflection height from about 70 km (mid-day) to about 58 km [*McRae and Thomson*, 2004].

These D-region flare-induced ionospheric changes show no saturation effects thus allowing measurements of the received VLF phase changes to be used to extrapolate the GOES X-ray fluxes beyond saturation to the peak of the great flare. *Thomson et al.* [2004] used this technique on the GOES fluxes in the band 0.1-0.8 nm together with the daytime VLF paths across the Pacific to

Dunedin, NZ, from the transmitters NLK (Seattle, 24.8 kHz), NPM (Hawaii, 21.4 kHz), and NDK (North Dakota, 25.2 kHz). They found that this technique gave a magnitude of X45±5 (4.5±0.5 mW/m^2 in the 0.1-0.8 nm band) for the great flare as compared with the value of X28 (2.8 mW/m^2 in the 0.1-0.8 nm band) estimated by NOAA's Space Environment Center (SEC) (http://sec.noaa.gov/weekly/pdf2003/prf1471.pdf).

The two previously largest flares were both about X20 (2.0 mW/m^2 in the 0.1-0.8 nm band), occurring on 16 August 1989 and 2 April 2001. Flares smaller than X1 (0.1 mW/m^2 in the 0.1-0.8 nm band) are designated in the ranges M1.0-M9.9 or C1.0-C9.9 when their 0.1-0.8 nm band fluxes are in the ranges 10-99 $\mu W/m^2$ and 1-9.9 $\mu W/m^2$, respectively (http://sec.noaa.gov/weekly/Usr_guide.pdf). Generally the ionospheric VLF phase technique is sensitive down to about C1 (1 $\mu W/m^2$) [e.g., *McRae and Thomson,* 2004] or about 1/4500 of the flux of the great flare of 4 November 2003. Below this C1 X-ray flux level (i.e., during normal quiet times), the D-region is maintained by day mainly by Lyman-α radiation (121.6 nm) from the Sun ionizing the minor neutral constituent, nitric oxide (in contrast with the flare X-rays which ionize all constituents, including N_2 and O_2) [e.g., *Banks and Kockarts,* 1973].

The GOES satellites record the X-ray fluxes in two wavelength bands: (1) 0.1-0.8 nm, referred to as 'long' or 'XL', and (2) 0.05-0.4 nm, referred to as 'short' or 'XS'. The 'long' band has the greater fluxes and is, as explained above, used in the usual C, M, X flare designations. The 'short' band fluxes are more penetrating and so are more representative of the wavelengths doing the ionizing at the bottom edge of the D-region during a large flare [e.g., *Banks and Kockarts,* 1973]. The XL/XS power ratio varies from around 20-40 at the C1 level down to around 2-3 for the largest flares. This is discussed in more detail in section 5. In the present day GOES satellites (GOES 10 and 12), the 'XL' fluxes saturate at about X17 (1.7 mW/m^2) whereas the 'XS' fluxes saturate just below 0.5 mW/m^2 which typically corresponds to flare sizes of around X8-X12.

In section 2, the use of VLF phase perturbations is extended to extrapolate the 'XS' 0.05-0.4 nm X-ray flux during the great flare, beyond saturation to its peak. By making a reasonable estimate for the XL/XS ratio at the peak, the peak XS flux is translated into a new estimate of peak XL flux, and thus flare magnitude. Later, in section 5, these XL/XS ratios, particularly during large flares, are further examined and found to be able to give surprisingly good estimates of (conventional) flare sizes, in particular the size of the great flare of 4 November 2003.

In section 3, we test the VLF-phase extrapolation technique on VLF paths with higher solar zenith angles (i.e., with the Sun nearer the horizon) to potentially considerably increase the number of suitable VLF observing paths for extrapolating the X-ray fluxes of very large flares.

In section 4, we extend the work of *McRae and Thomson* [2004] who reported H' and β values (measures of the D-region reflection height and 'sharpness' respectively) as functions of X-ray flux from around C1-C2 up to about X5. The VLF amplitudes and phases of three new large flares (X10, X20, and X45) are analyzed here to extend this range of D-region electron density parameters by a further factor of nearly 10 in X-ray flux.

2. X-ray Flux Extrapolation using VLF Phase Records

Figure 1 shows the VLF radio propagation paths used in this study, in particular, the 12.3 Mm path across the sunlit Pacific Ocean to Dunedin, New Zealand from the 24.8 kHz US Navy transmitter, NLK, in Seattle.

Figure 2 [*Thomson et al.,* 2004] shows the 0.1-0.8 nm flux (right hand axis, log scale) as a function of time during the great flare of 4 November 2003. Also shown are the accompanying phase variations of NLK received at Dunedin. The two curves were superposed by linearly scaling the phase, with an appropriate constant factor, and offsetting the phase by another appropriate constant factor.

The phases were recorded with AbsPAL receivers which are similar to OmniPAL VLF data loggers [*Dowden et al*., 1998] but modified so that they lock to GPS 1-second pulses [*Bahr et al*., 2000]. The 3-second resolution X-ray data in figure 2 have been scaled in amplitude to match the 1-minute data on the NOAA-SEC web site, and thus the standard (C,M,X) X-ray flare magnitudes.

The VLF phase in Figure 2 can be seen to track the GOES 0.1-0.8 nm X-ray flux up until the X-ray detector goes into saturation at about X17. Assuming the phase continues to track the (unavailable) XL flux beyond saturation, the peak flux is 4.5±0.5 mW/m^2 or X45±5 as found by *Thomson et al.* [2004] who also found very similar results (including a peak around X45) using the Dunedin recorded phases of NPM (Hawaii, 8.1 Mm, 21.4 kHz) and NDK (North Dakota, 13.5 Mm, 25.2 kHz) to extrapolate the GOES 0.1-0.8 nm X-ray flux.

Figure 3 is similar to Figure 2, except that the VLF phase (NLK to Dunedin) is now fitted to the 'short' or 'XS' band X-ray flux (0.05-0.4 nm). As can be seen, the phase again tracks the XS flux well, enabling the flux to be extrapolated from saturation (about 0.49 mW/m^2) up to the peak which can thus be seen to be about 2.45 mW/m^2 (with an error of about ±0.3 mW/m^2). X-ray flux in this XS band is likely to be doing the bulk of the ionizing in the enhanced lower D–region, at altitudes of 40-70 km [e.g., *Banks and Kockarts*, 1973]. Although there is more energy in the XL band (0.1-0.8 nm), these longer wavelength X–rays do not penetrate so far into the atmosphere.

It is interesting to explore how the ratio of 'long' X-ray flux to 'short' X-ray flux (i.e., XL/XS) varies during the flare. In Figure 4 this XL/XS ratio is plotted against the 'long' band flux, XL. The ('open' circle) data points are from the 3–s X–ray fluxes from NOAA-SEC (scaled in size to match their standard 1-min values). As the flare rises towards its maximum the XL/XS ratio reduces, moving up the lower trace; the XL/XS ratio is lower (i.e., the flux is harder) while the flare fluxes are rising (for given values of XL) as compared with when the flare is decaying.

The cusp on the rising trace at about the X1 level (0.1 mW/m^2) corresponds to where the fluxes happen to briefly plateau, for this particular flare (see Figures 2 and 3), during their otherwise rapid rises. The near 90-degree change of direction of the data points as the flare rises past about X10 (1 mW/m^2) is due to first the XS flux saturating and then, around X17, the XL flux saturating too. When both fluxes come out of saturation, the XL/XS ratio moves down the upper trace as the flare decays.

The dashed line around the peak of the flare is a likely extrapolation of the XL/XS ratio beyond saturation. In making this extrapolation the following (reasonably probable) constraints were used as guides: (1) the slope of the XL/XS versus XL plot should not change suddenly and (2) the general appearance/shape of the XL/XS ratio near the peak should be similar to that for other large flares (as displayed in section 5). Although the peak value of XL is shown (tentatively) at X45 in Figure 4, it would make little difference to the resulting value of the XL/XS ratio at the XL peak if this peak value were anywhere in the range X20-X50. Thus it can be seen that a reasonable estimate of the XL/XS ratio at the peak of the great flare is about 1.92 ± 0.1. However, this ratio, when combined with the 'short' flux peak value of 2.45 mW/m^2 as extrapolated in Figure 3, gives XL = 1.92 x 2.45 = 4.7 mW/m^2 or a magnitude of X47±8 (after allowing for uncertainty in both the XS peak flux and the

XL/XS ratio at the peak). This indirect estimate of X47 is reasonably consistent with the more direct (VLF phase-guided, 'long' flux) extrapolation of X45±5 made by *Thomson et al*. [2004].

3. VLF Phase near Dawn/Dusk and X-ray Flux Extrapolation

The original VLF phase extrapolations of the great flare's (long band) X-ray flux, which gave the peak as X45, used VLF paths from Hawaii, Seattle and North Dakota to New Zealand for which the maximum solar zenith angle was about 65 degrees while the average solar zenith angle was about 40-50 degrees, meaning the paths were well sunlit with the Sun averaging 40-50 degrees above the horizon.

The question arises as to whether it is necessary for the Sun to be so high in the sky in order to get a satisfactory VLF phase extrapolation (in cases where the X-ray flux detectors saturate). Not surprisingly solar zenith angle does affect VLF phase and this occurs progressively with changing daytime solar zenith angle; it is not simply a matter of being either day or night [*McRae and Thomson*, 2000 and 2004]. However, although the effects on the D-region of the ionosphere and hence the changes in VLF phase become smaller for flares at high solar zenith angles (since the X-rays have to travel obliquely and thus further through the atmosphere to penetrate to and ionize at a given height), the effects seem likely to be *proportionately* smaller.

For example, if the solar zenith angle were sufficiently great that the VLF phase change for the X-ray flux increasing from (say) 4 $\mu W/m^2$ to 1.7 mW/m^2 (i.e., GOES detector saturation) was half that for (nearly) overhead Sun, then it seems likely that the VLF phase change from the GOES saturation level to the peak flux (say 4.5 mW/m^2) would also be half that for (nearly) overhead Sun. This would be in

line with the observations of *McRae and Thomson* [2004] who found that the VLF phase perturbations were fairly closely proportional to the logarithm of the X-ray flux at least up to about X5 (0.5 mW/m^2 in the usual 0.1-0.8 nm band). However, their results applied for solar zenith angles less than about 60-70 degrees and fluxes up to X5.

An opportunity to test VLF paths with higher solar zenith angles arises with the 2.2 Mm 'Omega Australia' (13 kHz, 38.5^o S, 146.9^o E) to Dunedin, NZ, path for which the solar zenith angles were in a range of about 64-82 degrees near the time of the great flare peak (1945 UT, 4 November 2003). This is shown in figure 5 where the extrapolation again comes out close to X45 thus suggesting that such high solar zenith angle paths can give good results. The transmitter referred to here as 'Omega Australia' is the transmitter that used to be the real Omega Australia until 30 September 1997. In 2003 it was using 100 baud MSK on a fixed frequency of 13 kHz rather than the old Omega pulse sequence. Unfortunately it was no longer as phase stable as the real Omega transmitters were. However, this does not seem to be a problem because the phase drift is fairly constant (about 46 degrees per hour) and this has been largely removed before Figure 5 was plotted.

It now seems appropriate to test if VLF phase extrapolation at still higher solar zenith angles might give useful, though possibly more approximate, results even when part of the path is in darkness. An OmniPAL receiver in Ny Alesund, Svalbard, recorded the phase of NPM, Hawaii, at the time of the great flare. About one third of the nearly 9 Mm path was in darkness, at the receiver end. A superposed plot of the long band X-ray flux and the NPM phase is shown in Figure 6. It can be seen that, even for this day-night path, the VLF phase fit and extrapolation are quite good. Certainly the flare size would come out at X50±10 rather than X45 but this is only a ~10% difference for this very inhomogeneous path. From Figure 6 it can be seen that the NPM VLF phase changes are about 70 degrees per decade of X-ray flux change for this partly sunlit, 9 Mm, high solar zenith angle path. In

contrast, for the fully sunlit, lower solar zenith angle, 8 Mm, NPM to Dunedin path, the VLF phase changes were about twice as large, at 130 degrees per decade of X-ray flux change [*Thomson et al.*, 2004]. These phase changes are none-the-less both proportional to the corresponding (logarithms of their) X-ray flux changes.

For this path the NPM phase is stable but the OmniPAL receiver phase was drifting about 76 degrees/hour when averaged over a few days. In Figure 6, a correction of just 70 degrees/hour has been applied to get the best fits before and after the flare. This difference between 70 and 76 degrees/hour is partly due to changing solar zenith angle during the flare and partly to measurement uncertainty.

While a highly inhomogeneous day-night VLF path such as NPM to Ny Alesund gives only marginally satisfactory results on extrapolation, it is none-the-less interesting that they are so close to acceptable. This tends to imply that the relatively minor inhomogeneities in an all-day path, even at quite high solar zenith angles, are unlikely to detract significantly from the accuracy of VLF-phase-guided X-ray flux extrapolations.

The nearly satisfactory extrapolation results from the day-night NPM-Ny Alesund path do not imply that all day-night paths will give similarly useful results. Because of the near polar location of Ny Alesund (latitude ~79^{o} N) and the time of the flare, the sunrise/sunset terminator was moving rather slowly (less than about 0.2 Mm/hour) along this path. In contrast, for the nearly 6 Mm day-night path from NWC (19.8 kHz, North West Cape of Australia) to Dunedin, the terminator was moving nearly 1.3 Mm/hour during the flare, and so the day-night phase changes are comparable or greater than the flare induced phase changes. Also, the day-night phase changes during a large flare can be expected to be significantly different from those in unperturbed conditions, because of the much lower D-region

heights (and hence different mode conversions), and thus a useful separation of the flare effects from the day-night effects would be difficult.

4. D-region Electron Density Parameters as a Function of Solar X-ray Flux

The X-rays from solar flares ionize the neutral atmosphere at D-region heights (40-90 km) greatly increasing the electron densities there and thus markedly lowering the effective VLF reflection height. This lowering of the reflection height is the principal cause of the VLF phase advances observed during flares. However, the electron density profile at the lower edge of the D-region also 'sharpens' during flares in the sense that the rate of increase of electron density with height increases, and this also effects the VLF phase and amplitude at the receiver [eg *Thomson and Clilverd*, 2001 ; *McRae and Thomson*, 2004].

The VLF signals used here propagate in the Earth-ionosphere waveguide which is bounded below by the Earth (typically ocean) and above by the D-region. We model this using the NOSC (Naval Ocean Systems Center, San Diego, USA) computer programs (MODESRCH, MODEFINDER, LWPC – long wave propagation capability) which take the input path parameters, calculate appropriate full-wave reflection coefficients for the waveguide boundaries, and then search for those modal angles which give a phase change of 2π across the guide, taking into account the curvature of the Earth [e.g. *Morfitt and Shellman*, 1976]. These NOSC programs can take arbitrary electron density profiles supplied by the user to describe the D-region profile and thus the ceiling of the waveguide. However, for accurately predicting (or explaining) VLF amplitudes and phases, this approach effectively involves too many variables to be manageable in our present state of knowledge of the D-region. We thus follow the work of the NOSC group by characterizing the D-region with a Wait ionosphere defined by

just two parameters, the 'reflection height', H', in km, and the exponential sharpness factor, β, in km^{-1} [*Wait and Spies*, 1964]. This has been found to give very satisfactory results for normal daytime propagation over a good range of solar zenith angles [*Thomson*, 1993; *McRae and Thomson*, 2000] and for solar flares up to about X5 [*Thomson and Clilverd*, 2001; *McRae and Thomson*, 2004]. Here we extend the flare-time VLF phase and amplitude results of *McRae and Thomson* [2004] by nearly a factor of ten in X-ray flux up to the X45 level of the great flare of 4 November 2003.

4.1 VLF Amplitude Changes during the Great Flare

Figure 7 shows the amplitude (left-hand ordinate) of the 24.8 kHz VLF signal recorded at Dunedin, NZ, during the great flare of 4 November 2003. Also plotted, for comparison, is the 'long' (0.1-0.8 nm) GOES-12 X-ray flux (right-hand ordinate). The contrast with the phase plot for the same period in Figure 2 is evident. The phase varies very nearly proportionately with the (logarithm of the) X-ray flux while the amplitude does not. Thus the phase is useful and convenient for extrapolating the X-ray flux when the GOES detectors saturate but the amplitude is not. None-the-less, these flare-time VLF amplitudes and their accompanying phase perturbations readily allow the determination of β and H' at the peak of the flare, as described below.

4.2 Flare Induced VLF Amplitude and Phase Changes up to X45

Figure 8 shows the VLF phase and amplitude perturbations for the NLK to Dunedin path for three recent very large flares as well as the flares (all ≤X5) previously reported by *McRae and Thomson* [2004]. The three new very large flares shown are the X20 of 2 April 01, the X10 of 29 Oct 03, and the great flare of 4 Nov 03. Other recent very large flares such as the X17.2 of 28 Oct 03 and the X14.4 of 15 Apr 01 were not suitably timed for daylight VLF paths for our receivers in Dunedin, NZ.

Special care has been required in establishing and plotting the phase changes for the very large flares in Figure 8, as opposed to the smaller flares. Typically before the smaller flares and away from solar maximum, where the ≤X5 flares were recorded, the X-ray flux preceding the flare is (appreciably) less than the C1 level. In these conditions the pre-flare D-region is maintained principally by Lyman–α and so is at a standard unperturbed 'base' level. The phase changes observed and calculated are thus between this fairly standard unperturbed level [see *McRae and Thomson*, 2004, for details] and the flare peak. However, for flares occurring during periods of high solar activity, such as the very large flares reported here, the pre-flare X-ray flux is normally appreciably greater than C1 and so needs to be taken into account. For example, for the great flare, the pre-flare flux was about C4, and so the observed phase change ('C4-to-peak') needed to be increased by the (small) expected 'unperturbed-to-C4' phase change (from the left-hand side of the phase plot in Figure 8) before plotting the great flare (on the right-hand side of this plot) in Figure 8.

As can be seen in Figure 8, the phase trend evident in the previous work [*McRae and Thomso*n, 2004] continues (for a further factor of ~10 in flare power). However, the amplitude increase, in the lower panel of Figure 8, at high flare powers, does not fully flatten off for flare sizes >X5 as had previously been indicated [*McRae and Thomson*, 2004], but continues to rise slowly.

4.3 Flare Induced β and H' up to X45

Figure 9 shows plots of the values of β and H' required for MODEFINDER to calculate the observed (as shown in figure 8) absolute amplitudes at the flare peaks and the observed (as shown in Figure 8) phase changes at the flare peaks. Although the process of finding β and H' using MODEFINDER has an element of trial and error, the process is none-the-less fairly fast and straightforward. As is found

from MODEFINDER, the phase changes are monotonic in H', and much more dependent on H' than β, while the amplitude changes are typically more dependent on β than H'. This makes it possible to iteratively and quickly find values of β and H' which cause MODEFINDER to output the observed amplitudes and the observed phase changes. The key to this is starting with appropriate values of β and H' for the unperturbed D-region. These are now fairly well established [e.g., *Thomson*, 1993; *McRae and Thomson*, 2004] and, when these are used as the starting points here, the resulting searches for the flare-time values of β and H' prove to be fast (few iterations), stable and unique.

As can be seen in the lower panel of Figure 9, the nearly linear reduction of H' with (the logarithm of the) flare flux (0.1-0.8 nm) continues from the upper limit of X5 in the previous study [*McRae and Thomson*, 2004] to at least the X45 of the great flare in the present study. However, in the upper panel of Figure 9 it can be seen that, although β levels off to a significant degree around X1-X5 as in the previous study, it then starts to rise again with increasing flare power for the very large flares (>>X5).

β increasing with flare power at low flare powers, and the (near) flattening off of β around the X1 flux level are still likely to be caused, as previously suggested [*Thomson and Clilverd*, 2001], by these X-ray fluxes becoming thoroughly dominant over both cosmic rays and Lyman-α as the ionizing source in the D-region, under these conditions. If Lyman-α were the sole source of ionization in the unperturbed D-region then the unperturbed profile slope would be similar to that when X-rays dominate. However, in the real unperturbed D-region, galactic cosmic rays make additional ionization mainly in the lowest parts [*Rishbeth and Garriott*, 1969] so that the unperturbed electron density falls with decreasing height at a rate which is slower than for Lyman-α (or X-rays) alone. Such normal unperturbed profiles, in which the electron density increases relatively slowly with height, result in relatively low values of β when modeling using β and H'.

The discussion in the last paragraph provides an explanation of why β increases with increasing flare power until the effects of the X-ray flux swamp the effects of the galactic cosmic rays (and the Lyman-α) at which point β would be expected to increase no further and thus appear 'saturated'. It is suggested that the fact that β is observed to increase further for very large flares may be due to there being little X-ray flux at wavelengths shorter than about 0.05 nm (the lower wavelength limit of the 'short' GOES band). Only wavelengths shorter than this could penetrate significantly below a height of about 50 km and their absence would result in extremely low electron densities in these lowest parts of the VLF reflection region.

4.4 Flare Time Electron Density Comparisons

Wait and Spies [1964] defined a height dependent conductivity parameter:

$$\omega_r(z) = \omega_0^2(z)/\nu(z) = 2.5 \times 10^5 \exp[\beta(z-H')]$$

where $\omega_0(z)$ is the (angular) electron plasma frequency and $\nu(z)$ is the effective electron-neutral collision frequency, both being functions of the altitude, z, in km. This assumes $\omega_r(z)$ varies exponentially with height at a rate determined by the constant, β (in km^{-1}). H' is the height (in km) at which $\omega_r(z) = 2.5 \times 10^5$ s^{-1} and is often used as a convenient measure of the 'height' of the D-region. The collision frequency depends on the neutral air density which decreases (approximately) exponentially with height. A reasonable expression for the collision frequency, as used in LWPC and MODEFINDER [*Morfitt and Shellman*, 1976], is $\nu(z) = 1.82 \times 10^{11} \exp(-0.15z)$. The (angular)

plasma frequency is related to the electron density by $\omega_o^2(z) = N(z)e^2/(\varepsilon_o m) \approx 3180\ N(z)$. Hence the electron density increases exponentially with height in the D-region as

$$N(z) = 1.43 \times 10^{13} \exp(-0.15H') \exp[(\beta - 0.15)(z - H')\ ].$$

In Figure 10 are plotted the electron densities for (1) a typical unperturbed mid-solar cycle day (β = 0.39 km^{-1}, H' = 71 km [*McRae and Thomson*, 2004]), (2) an X6 flare as determined by *Zinn et al*. [1990] from a set of incoherent scatter observations, (3) an X6 flare from the H' and β values determined from VLF measurements as in Figure 9 [*McRae and Thomson*, 2004], and (4) the great X45 flare of 4 November 2003.

4.5 A Possible Extrapolation to Even Larger Flares

Figure 11 is essentially the same H' versus solar flare X-ray flux plot as in the lower panel of Figure 9 except that the best fit line has been extrapolated to very much larger solar X-ray fluxes than have ever been recorded. This illustrates just how well our atmosphere protects us on the Earth's surface from the X-ray bursts of extremely large flares. Even if a flare were so large that the 0.1-0.8 nm solar X-ray flux reached the level of the total current output of the Sun (i.e., the solar constant, ~1400 W/m^2), the lower edge of the ionosphere, and hence the height of extinction of the X-rays would still be greater than 20 km.

5. Long/Short (XL/XS) X-ray Flux Ratios during Flares

As shown in Figure 4 and discussed in Section 2, the ratio of the 'long' X-ray flux to the 'short' X-ray flux, or XL/XS ratio, varies during the flare reaching a minimum near the flare flux peak. Similar such XL versus XL/XS plots are shown for a number of large flares in Figure 12. Five of the flares come from the same very active period, 20 October 2003 - 5 November 2003, as the great flare of 4 November 2003. They include the X17 flare of 28 October 2003 and the X10 flare of 29 October 2003 which are the 4th and 10th largest flares ever recorded by the GOES satellites (since 1976). Also included in this period are an X8.3, an X5.4, and an X3.9. They have been included partly because of their large sizes, partly because 3-second resolution data was available and partly because they were recorded on the GOES 12 satellite which is designated by NOAA-SEC as the current primary satellite and was the satellite used as the calibration source by *Thomson et al*. [2004] for their ionospherically estimated X45 determination.

Also shown in Figure 12 are the XL/XS ratios plotted against XL for the X20 flare of 2 April 2001, the X14 flare of 15 April 2001, and the X9.4 flare of 6 November 1997. For these three flares the data comes from the GOES 8 satellite at 1-minute resolution.

In all cases the XL/XS ratios are lower for the rising flare fluxes than for the falling fluxes, just as for the great flare in Figure 4. As can be seen, the slopes of the XL/XS curves typically change progressively in the vicinity of the flux peaks. (For the X20, X17 and X14 flares, XS saturated near the peaks and so the curves have been extrapolated as was done for the great flare in Figure 4.) While no two flares have exactly the same XL/XS vs. XL shape, there can be seen to be some general features. The XL/XS ratio falls to a clear minimum shortly before the peak of the flare. No extrapolation is required to get this minimum for XL/XS except for the X45 and X20 flares and even then the extent of the extrapolation required is minimal.

For flares greater than about X10, extrapolation, shown by dashed or solid lines, has been needed in Figure 12 to estimate the XL/XS ratio at the peak because, as previously mentioned, XS saturates at about 0.49 mW/m^2. Obviously there is some uncertainty in the extrapolations but, as in figure 4, account has been taken of the non-saturating cases in Figure 12, including no discontinuities in the rate of change of slope near the peak. Also, in all cases except perhaps the X20 case, the peak XL values are known because XL has not saturated. In the case of the X20 flare (2 April 2001) the XL extrapolation (from X17) is fairly minimal. Thus the XL/XS ratios at the flare peaks have likely been reasonably well estimated.

Both the minimum value of XL/XS for a flare and the XL/XS ratio at the peak are smaller the larger the flare. In Figure 13 the minimum value of the XL/XS ratio, R_{min}, and the XL/XS ratio at the (XL) peak of the flare, R_{peak}, are plotted against XL at the flare peak for some representative flares. Four plot symbols are used. The solid circles and the large X45 symbol are from 3-second GOES 12 data in the active period 22 October to 4 November 2003, plus an X1.3 flare on 27 May 2003. The open circles are from 1-minute GOES 12 data in July, October and November of 2004. The nine solid diamonds are from 1-minute GOES 8 data from 6 Nov 97 (X9), 18 Aug 98 (X5), 14 Jul 00 (X6), 2, 6 and 15 Apr 01 (X20, X5.6, X14), 28 Aug 01 and 13 Dec 01 (X5, X6), and 23 Jul 02 (X5). The solid lines are reasonable fits to the data points.

From Figure 13, it can be seen that the XL/XS ratios for both R_{min} and R_{peak} are consistent with the great flare of 4 November 2003 having a magnitude of about X45 as determined previously by *Thomson et al*. [2004] by VLF phase extrapolation of the XL flux. This XL/XS ratio consistency check is somewhat independent of the VLF ionospheric technique but has a higher uncertainty. A re-examination of the XL/XS ratio plot for the great flare in Figure 4 shows that if it had been

extrapolated to only (say) X30, R_{min} would have hardly changed and so would still have indicated a magnitude of at least X45 in the R_{min} versus peak XL graph in the top panel of Figure 13.

6. Summary and Conclusions

The great solar flare of 4 November 2003 was the largest ever recorded by the X-ray detectors on the GOES satellites which have been in operation since 1976. Unfortunately the current GOES X-ray detectors saturate at about X17.4 and the great flare was markedly larger than this; so some means of extrapolation is needed to estimate its size. NOAA's Space Environment Center, who provide the GOES detectors and hence the most widely recognized international records of solar flare X-ray fluxes, arrived at an estimate of X28 for the peak by extrapolating their recorded fluxes beyond saturation. The flare X-rays create significant extra ionization in the Earth's ionosphere, particularly in the lower D-region where VLF radio waves reflect thus lowering their reflection height. It has been previously shown that the reflection height lowering and the peak VLF phase advances during flares are nearly linearly related to the logarithm of the flare's peak 'long' (0.1-0.8 nm) X-ray flux [*McRae and Thomson*, 2004]. It has also been shown [*Thomson et al.*, 2004] that the phase shifts during large flares are nearly linearly related to the VLF phase changes during the flares. This relation looks likely to apply over a very great range of solar flare X-ray fluxes (and D-region height lowering) without saturation. This has enabled the continuous, smoothly changing VLF phase to be used to extrapolate the 'long' (0.1-0.8 nm) X-ray flux from which a magnitude of X45 was obtained [*Thomson et al.*, 2004].

Because the wavelengths of the dominant ionizing X-rays at the VLF reflection height near the peak of the great flare are likely to be in the 'short' X-ray band (XS), it seemed sensible to also extrapolate

this band's flux and find its peak value for the flare. This was done successfully in Figure 3, but as flare magnitudes are normally given in terms of their 'long' band peak flux (XL) a value of the XL/XS ratio at the peak was needed. This was found and used to show that this route gave a magnitude of X47±8 for the flare, consistent with the previous (long band) VLF ionospheric extrapolation.

VLF long path phase measurements can still provide very good X-ray flux extrapolation from saturation even when the Sun is quite low in the sky (8-26 degrees above the horizon). Further, quite useful extrapolation results were obtained from a completely independent receiver even though the (partly polar) path was partly in darkness (though more than 50% sunlit). However, in such a case it is important that the day/night ratio on the path is changing only very slowly during the flare.

The lowering of the D-region reflection height due to the flare X-ray fluxes was found to continue, essentially linearly, up to the X45 flux level, nearly a factor of 10 further than had previously been found up to X5. At the peak of the X45 flare, H' had lowered to a height of about 53 km, or about 17 km below typical mid-day, unperturbed conditions. The D-region sharpness parameter, β, which was previously thought to increase to saturation at about 0.52 km^{-1}, was found to increase further again up to about 0.57 km^{-1} at X45, possibly due to the X-ray flux spectrum falling off rapidly for wavelengths shorter than about 0.05 nm (the lower limit of the GOES 'short' band).

Finally the XL/XS ratios were examined for a number of flares from small to very large, and it became clear that the XL/XS ratios themselves were reasonably well defined functions of XL, and so could be used to make quite useful estimates of flare peaks (without reference to the ionosphere or VLF measurements). These XL/XS ratio plots were also found to be consistent with the great flare being at least as large as X45.

Acknowledgements. We are very grateful to NOAA's Space Environment Center, particularly to Dr Rodney Viereck, for their help and for providing not only the 1-min but also the 3-s GOES X-ray data, which made possible the (flux) calibration of our VLF phase data. We would also like to thank Mr Dave Hardisty of our institution for the design and implementation of the digital MSK multi-channel modulator/demodulator which carries our VLF signals live from our field station.

References

Bahr, J. L., J. B. Brundell, S. F. Hardman, and R. L. Dowden, Multi-instrument coincident detection of sprites, *Phys. Chem. Earth (B), 25*, 417-422, 2000.

Banks, P. M. and G. Kockarts, *Aeronomy,* Academic Press, N.Y., 1973.

Dowden, R. L., S. F. Hardman, C. J. Rodger, and J. B. Brundell, Logarithmic decay and Doppler shift of plasma associated with sprites, *J. Atmos. Sol-Terr. Phys.*, *60*, 741-753, 1998.

McRae, W. M. and N. R. Thomson, VLF phase and amplitude: daytime ionospheric parameters, *J. Atmos. Sol-Terr. Phys.*, *62*, 609-618, 2000.

McRae, W. M. and N. R. Thomson, Solar flare induced ionospheric D-region enhancements from VLF phase and amplitude observations, *J. Atmos. Sol-Terr. Phys.*, *66*, 77-87, 2004.

Mitra, A. P. *Ionospheric effects of solar flares*, D. Reidel, Dordrecht, 1974.

Morfitt D. G. and C. H. Shellman, MODESRCH, an improved computer program for obtaining ELF/VLF/LF mode constants in an Earth-Ionosphere Waveguide, Naval Electronics Laboratory Center Interim Rep. 77T, NTIS, Accession No. ADA032573, National Technical Information Service Springfield, Va. 22161, USA, 1976.

Rishbeth, H. and O. K. Garriott, *Introduction to Ionospheric Physics*, Academic Press, N.Y. and London, 1969.

Thomson, N. R., Experimental daytime VLF ionospheric parameters. *J. Atmos. Terr. Phys., 55*, 173-184, 1993.

Thomson, N. R. and M. A. Clilverd, Solar flare induced ionospheric D-region enhancements from VLF amplitude observations. *J. Atmos. Sol-Terr. Phys., 63*(16): 1729-1737, 2001.

Thomson, N. R., C. J. Rodger, and R. L. Dowden, Ionosphere gives size of greatest solar flare. *Geophys. Res. Lett.* 31(6), L06803, doi:10.1029/2003GL019345, 2004.

Watt, A. D., *VLF Radio Engineering,* Pergamon Press, Oxford, 1967.

Wait J.R. and K. P. Spies, Characteristics of the Earth-ionosphere waveguide for VLF radio waves. *NBS Tech. Note* 300, 1964.

Zinn, J., C. D. Sutherland, and S. Ganguly, The solar flare of August 18, 1979: incoherent scatter radar data and photochemical model comparisons, *J. Geophys. Res., 95* (D10), 16705-16718, 1990.

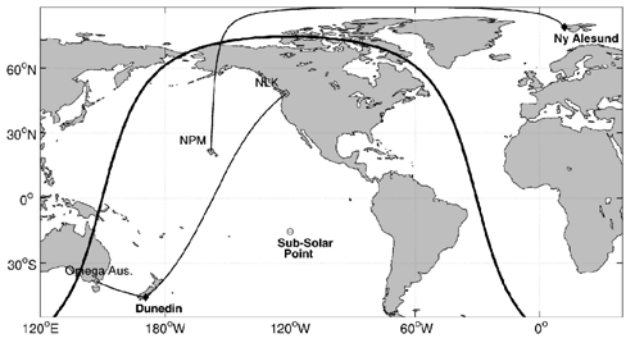

Figure 1. The VLF radio propagation paths used here together with the day-night terminator (bold line).

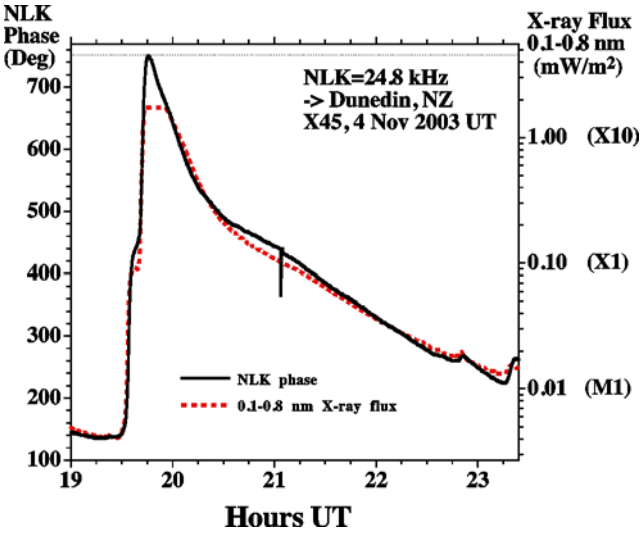

Figure 2. The phase of NLK, Seattle, as received at Dunedin, NZ, during the great flare on 4 November 2003, superposed on the XL (0.1-0.8 nm) GOES X-ray flux.

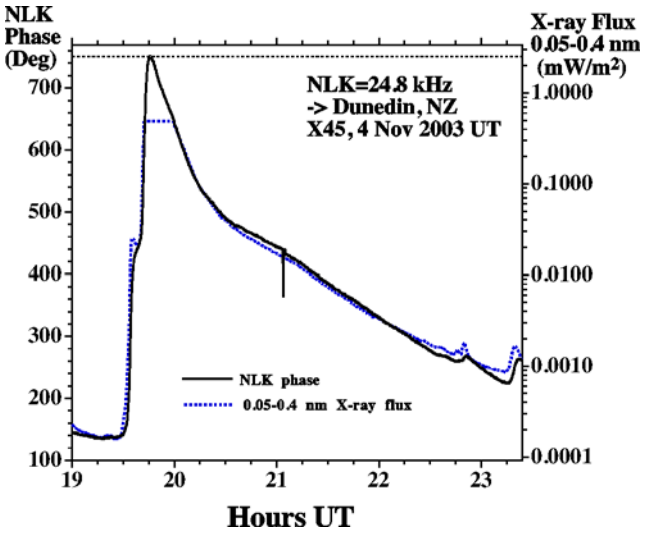

Figure 3. Similar to Figure 2 except that the *XS* band (0.05-0.4 nm) GOES X-ray flux is compared with the VLF phase of NLK, Seattle, as received in Dunedin, NZ.

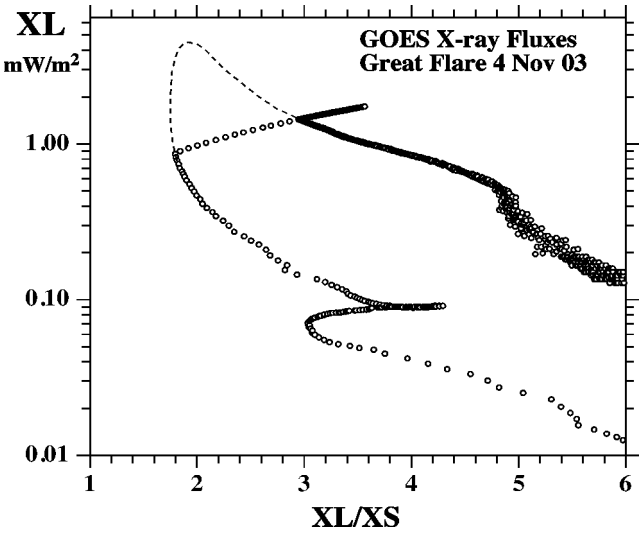

Figure 4. The 'long' band (0.1-0.8 nm) X-ray flux, XL, plotted against the XL/XS ratio, where XS is the 'short' band (0.05-0.4 nm) X-ray Flux, from GOES 12 near the peak of the great flare on 4 November 2003. Time increases clockwise around the plot, starting in the lower right corner.

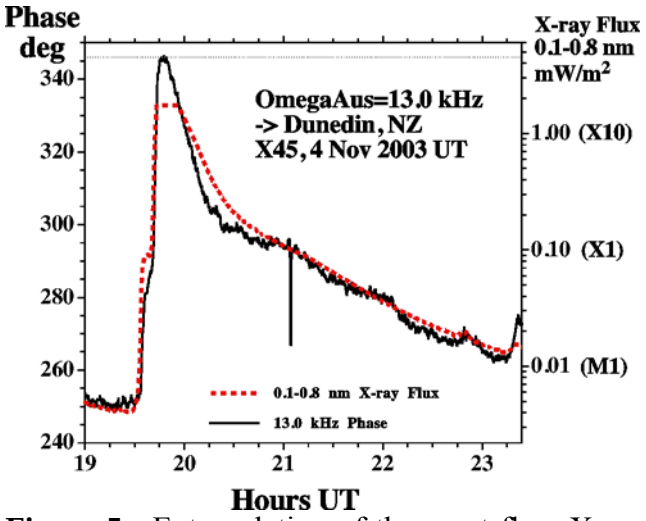

Figure 5. Extrapolation of the great flare X-ray flux using the phase of 'Omega Australia' at Dunedin near dawn.

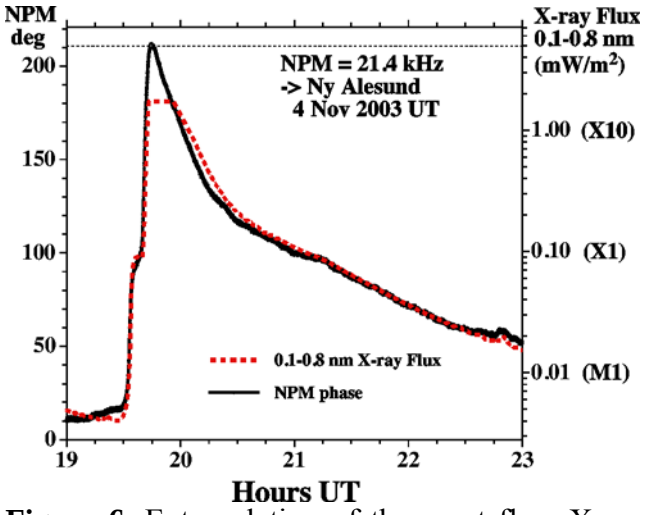

Figure 6. Extrapolation of the great flare X-ray flux using the phase of NPM, Hawaii, at Ny Alesund, Spitzbergen (with about 1/3 of the path in darkness).

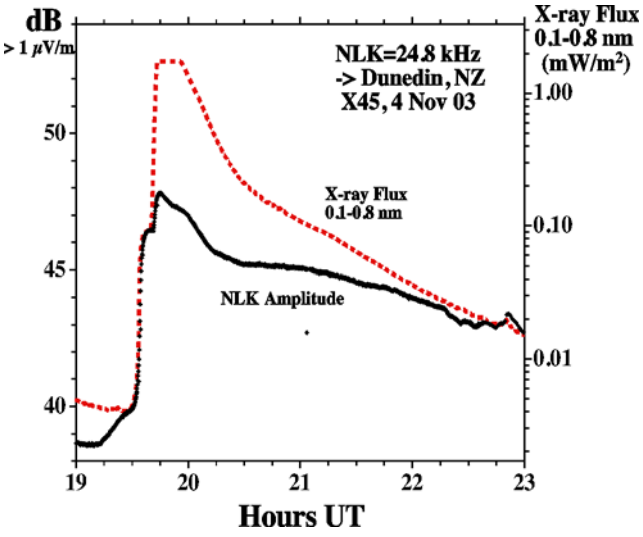

Figure 7. Amplitude of NLK, Seattle, recorded at Dunedin, NZ, together with the GOES X-ray flux during the great flare.

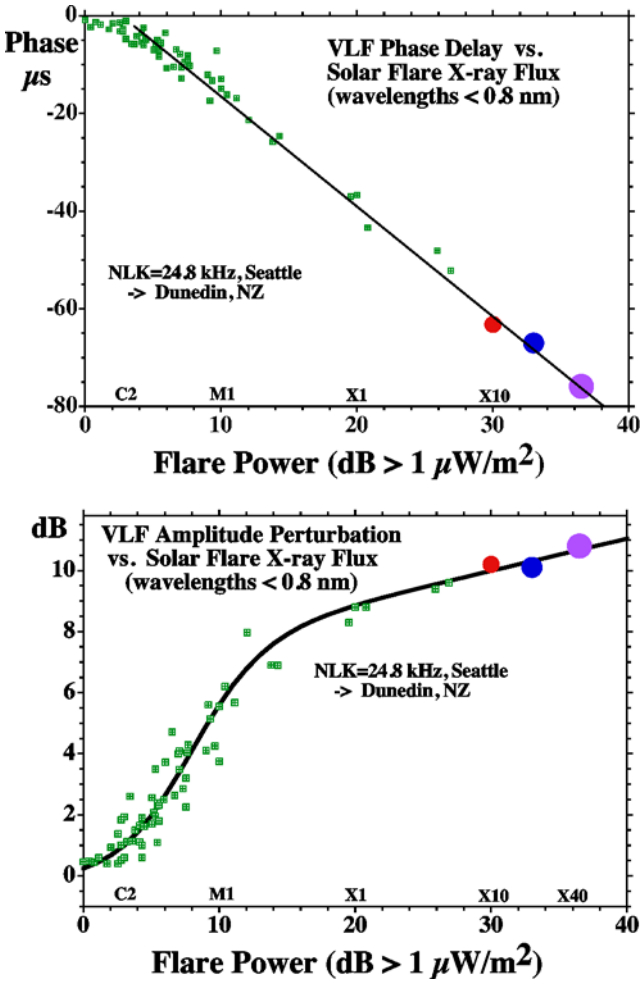

Figure 8. Phase delay perturbations and received VLF amplitude versus peak X-ray flux.

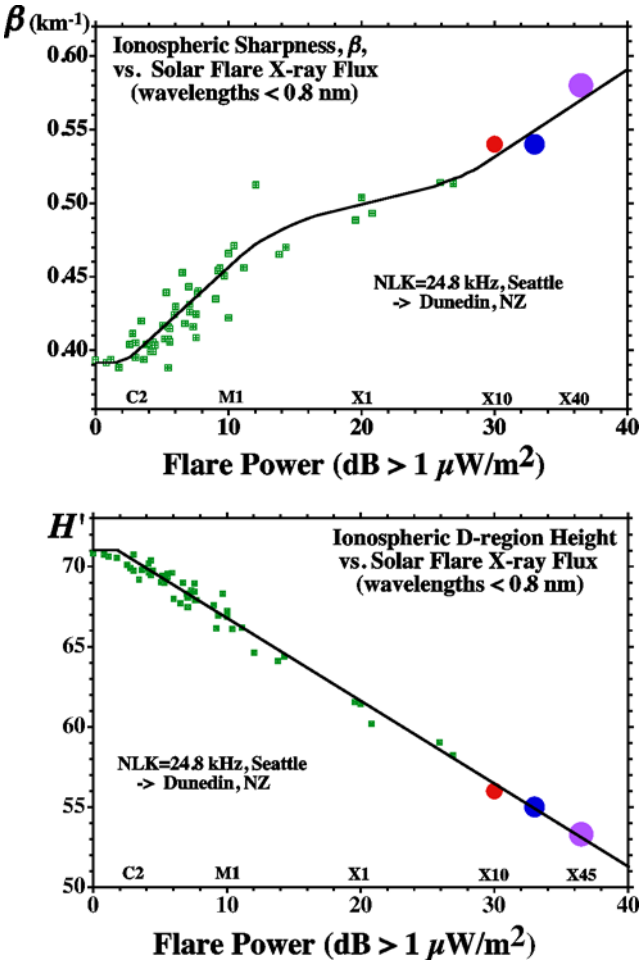

Figure 9. Ionospheric D-region sharpness, β, and height, H', as functions of peak solar flare power.

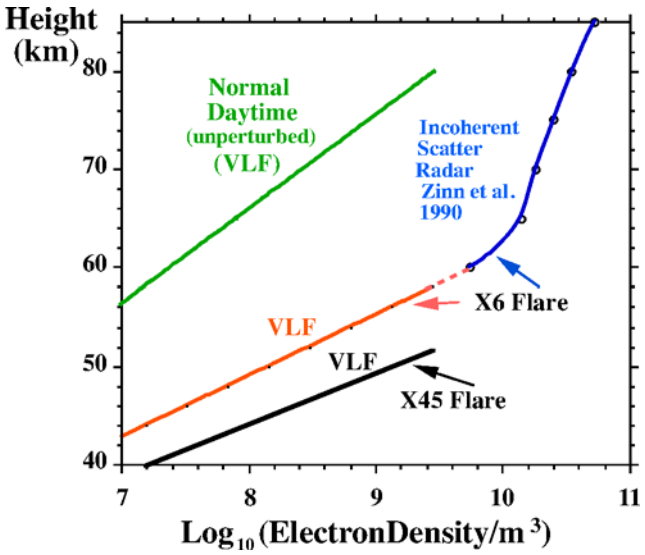

Figure 10. VLF-determined electron densities during the great X45 flare of 4 November 2003 compared with normal unperturbed electron densities. Also shown are electron densities from an incoherent scatter radar during an X6 flare and those predicted from VLF observations.

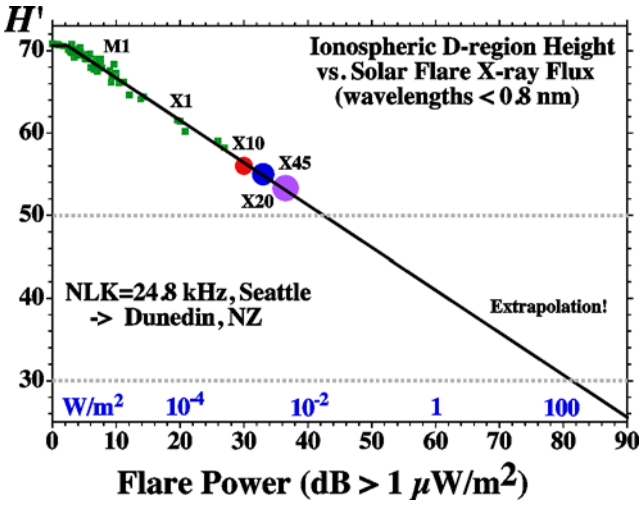

Figure 11. Same as lower panel of Figure 9 except extrapolated to much higher flare magnitudes.

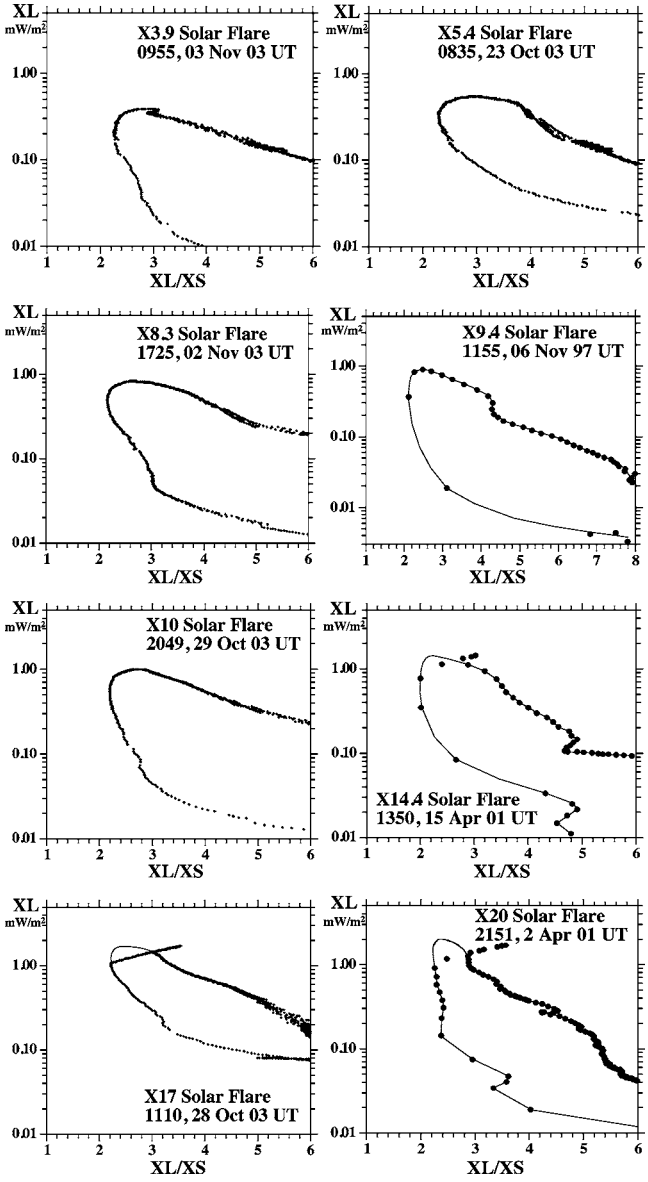

Figure 12. As in Figure 4, XL and XS are the 'long' and 'short' band X-ray fluxes. Again, XL is plotted against the ratio XL/XS. GOES 12 has been used for the five flares from 2003, and GOES 8 for the three earlier flares. Time again increases clockwise around each plot.

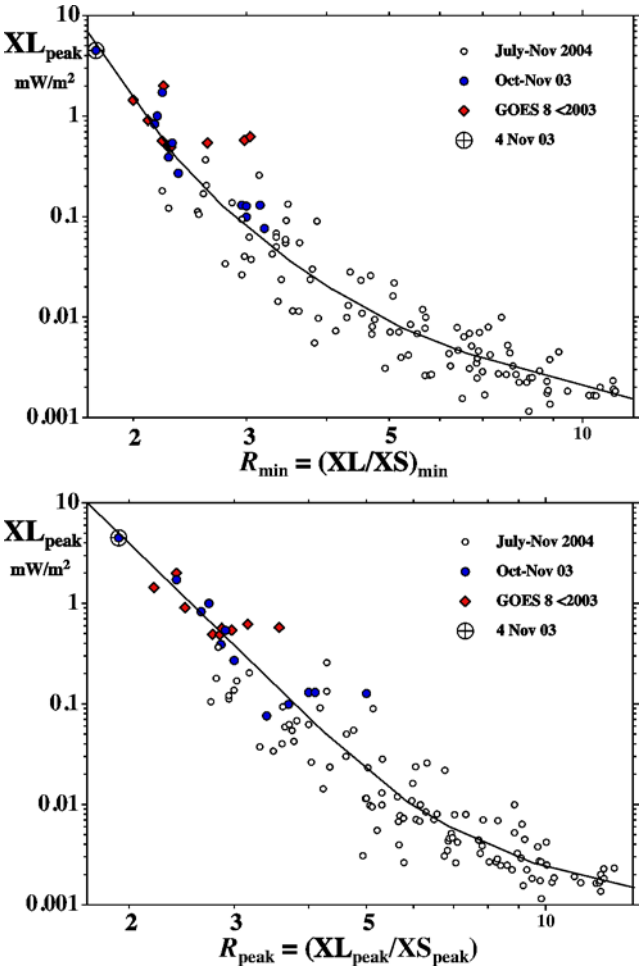

Figure 13. The peak 'long' band X-ray flux, XL_{peak}, plotted against (a) the minimum value of XL/XS near the flare peak and (b) the value of XL/XS at the flare peak.

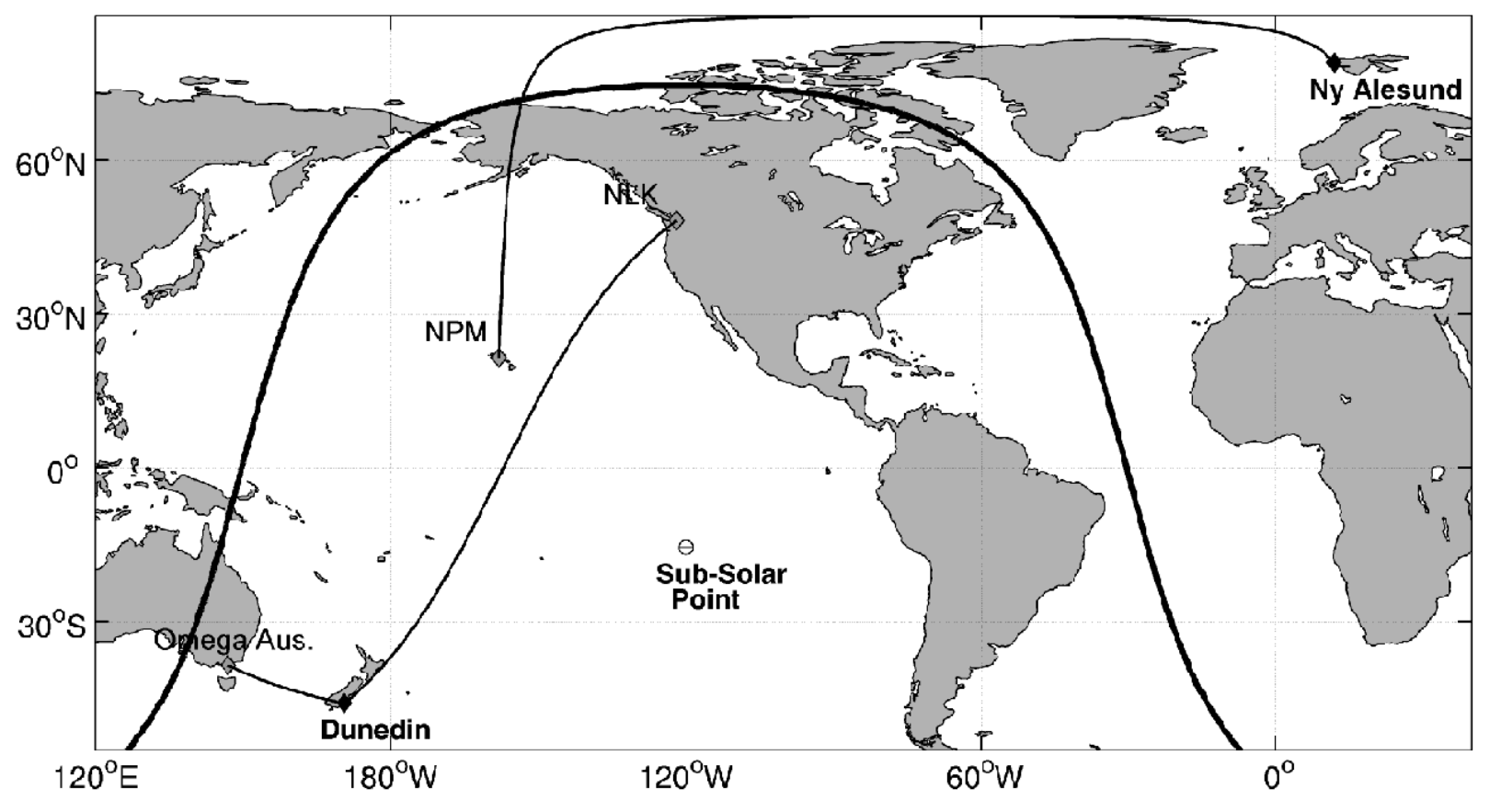
Ny Alesund
NLK
NPM
Sub-Solar
Point
Omega Aus.
Dunedin
60°N
30°N
0°
30°S
120°E
180°W
120°W
60°W
0°

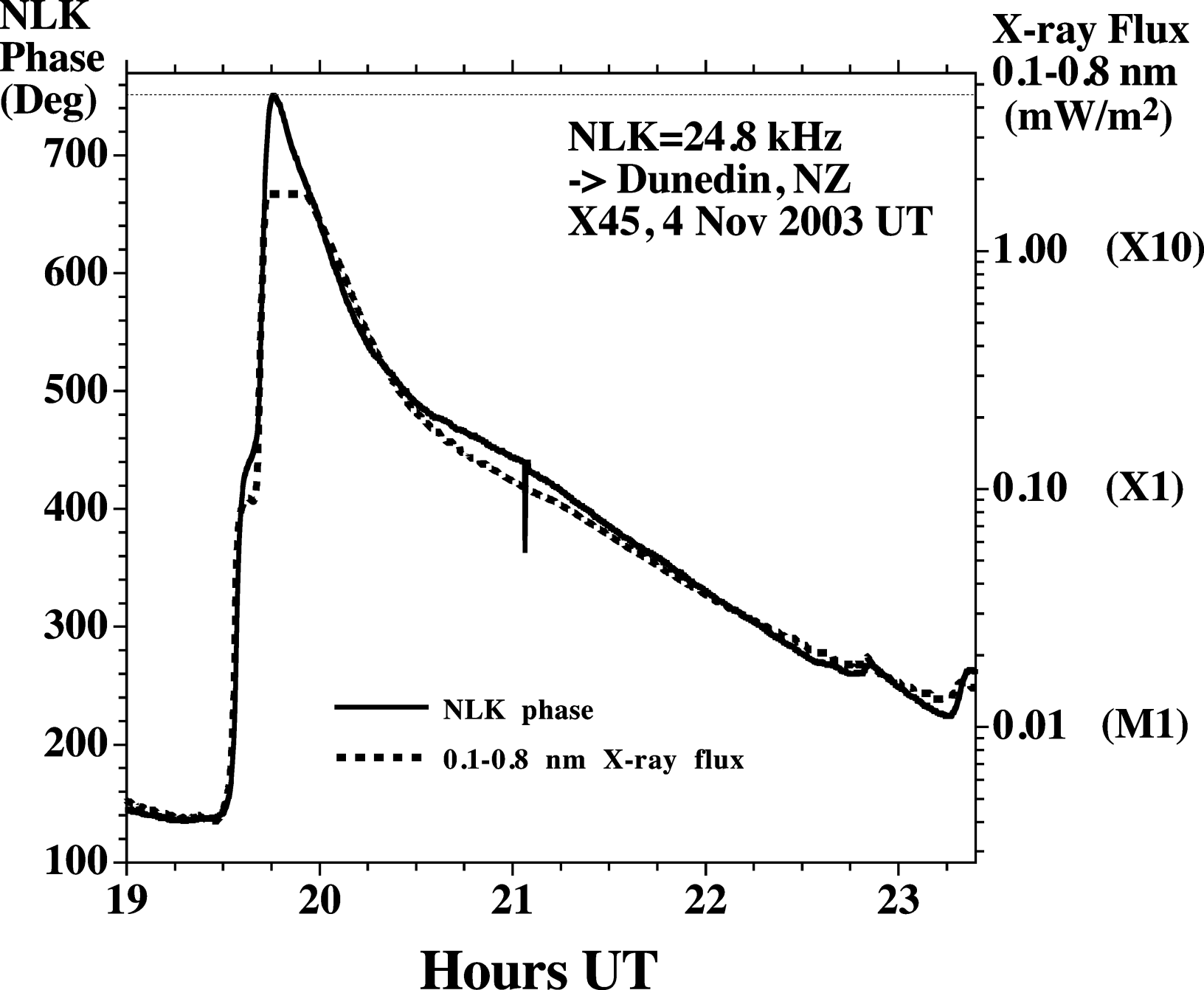
NLK Phase (Deg)
700
600
500
400
300
200
100
X-ray Flux 0.1-0.8 nm (mW/m2)
1.00 (X10)
0.10 (X1)
0.01 (M1)
NLK=24.8 kHz
-> Dunedin, NZ
X45, 4 Nov 2003 UT
NLK phase
0.1-0.8 nm X-ray flux
19
20
21
22
23
Hours UT

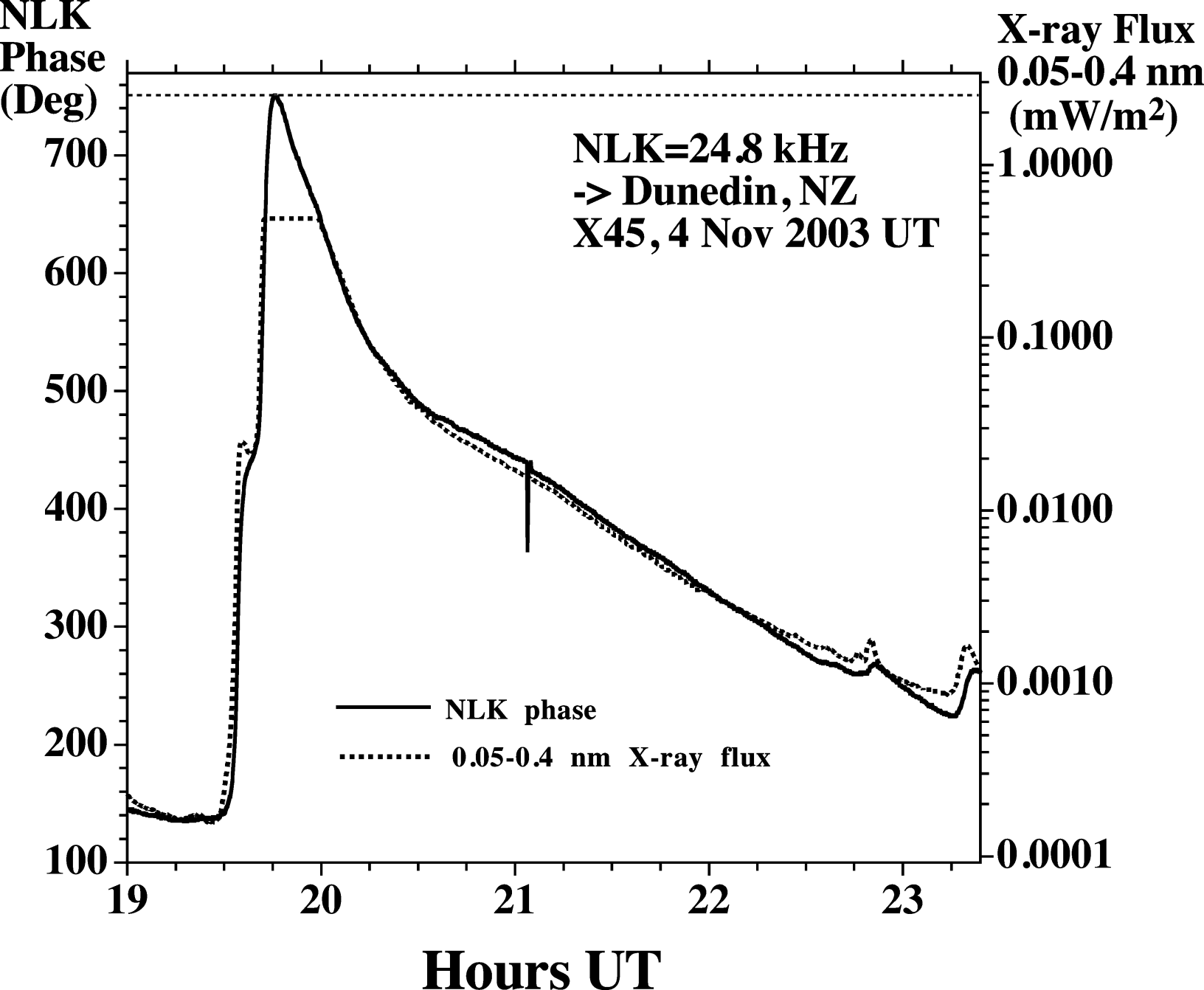
NLK Phase (Deg)
X-ray Flux 0.05-0.4 nm (mW/m²)
NLK=24.8 kHz
-> Dunedin, NZ
X45, 4 Nov 2003 UT
NLK phase
0.05-0.4 nm X-ray flux
700
600
500
400
300
200
100
1.0000
0.1000
0.0100
0.0010
0.0001
19
20
21
22
23
Hours UT

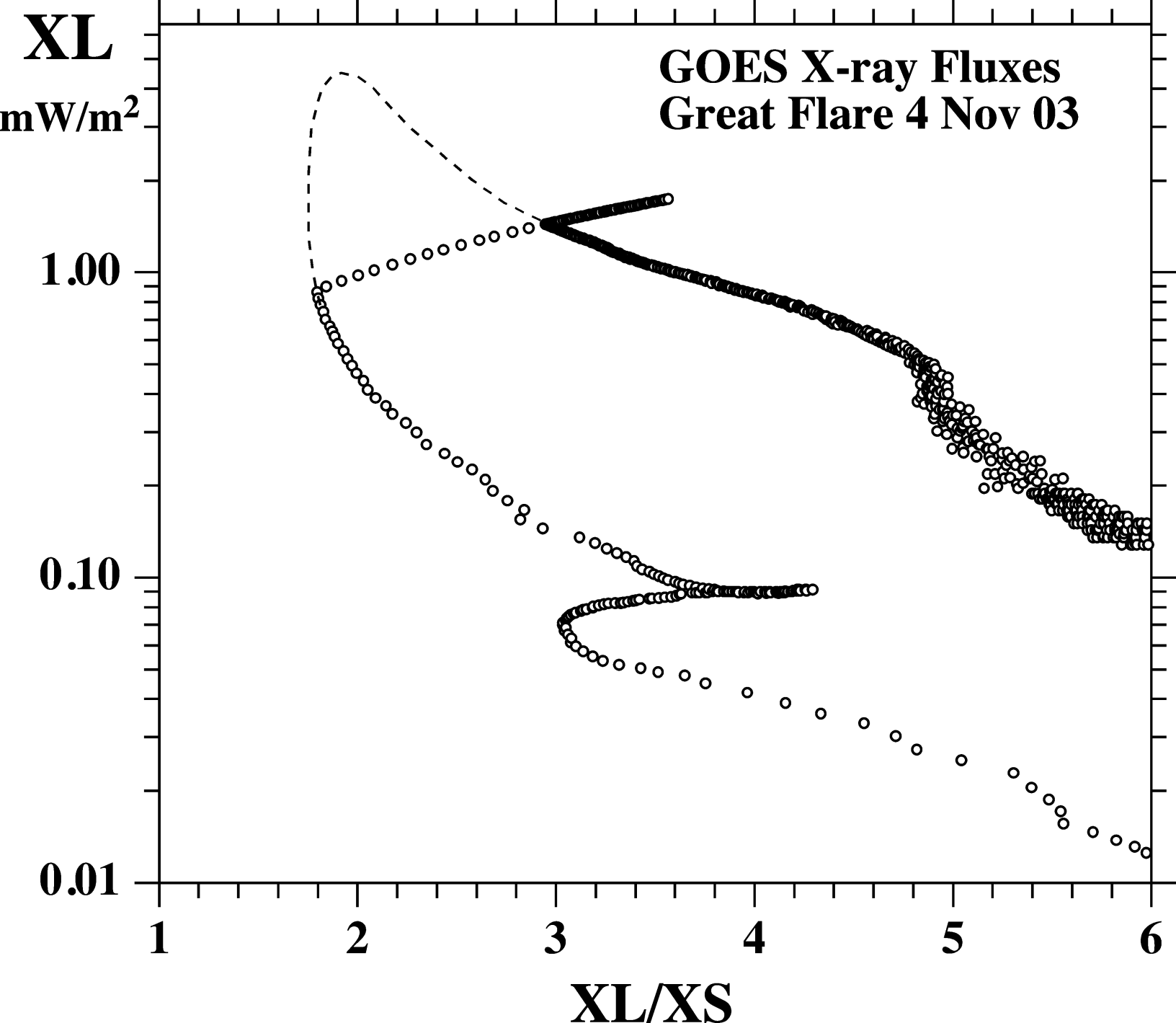
XL
mW/m²
GOES X-ray Fluxes
Great Flare 4 Nov 03
1.00
0.10
0.01
1
2
3
4
5
6
XL/XS

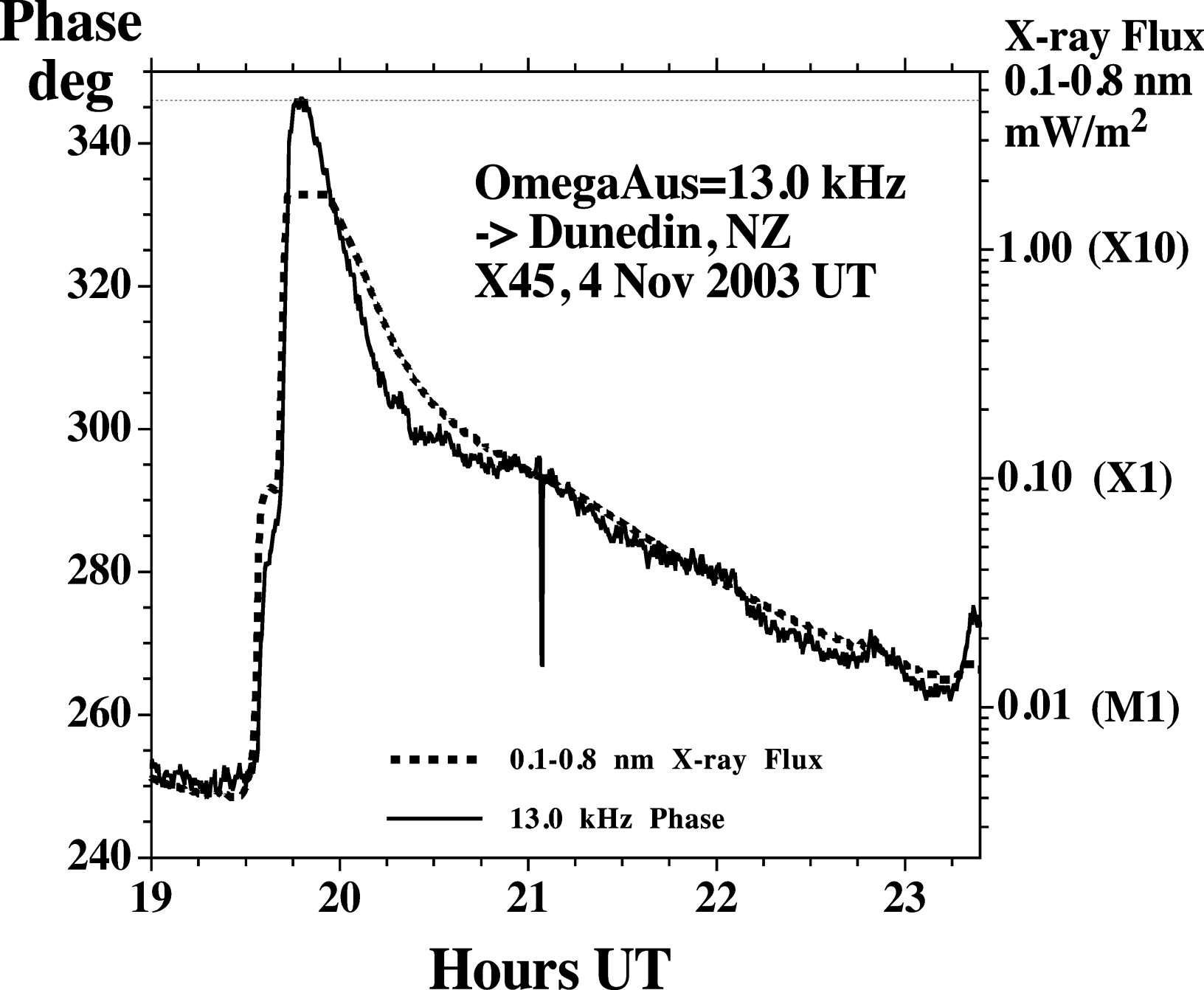
Phase
deg
340
320
300
280
260
240
X-ray Flux
0.1-0.8 nm
mW/m2
1.00 (X10)
0.10 (X1)
0.01 (M1)
OmegaAus=13.0 kHz
-> Dunedin, NZ
X45, 4 Nov 2003 UT
0.1-0.8 nm X-ray Flux
13.0 kHz Phase
19
20
21
22
23
Hours UT

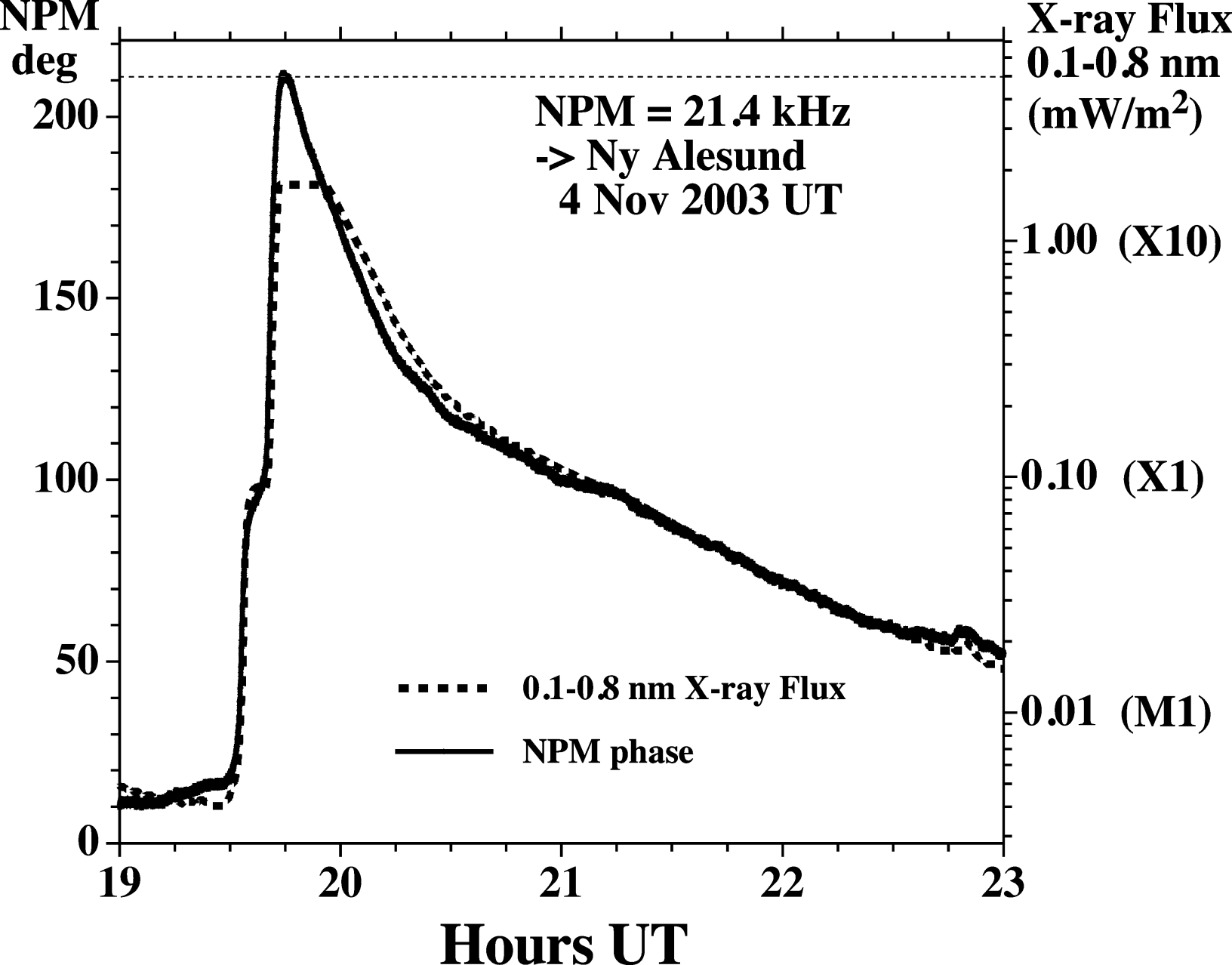
NPM
deg
200
150
100
50
0
X-ray Flux
0.1-0.8 nm
(mW/m2)
1.00 (X10)
0.10 (X1)
0.01 (M1)
NPM = 21.4 kHz
-> Ny Alesund
4 Nov 2003 UT
0.1-0.8 nm X-ray Flux
NPM phase
19
20
21
22
23
Hours UT

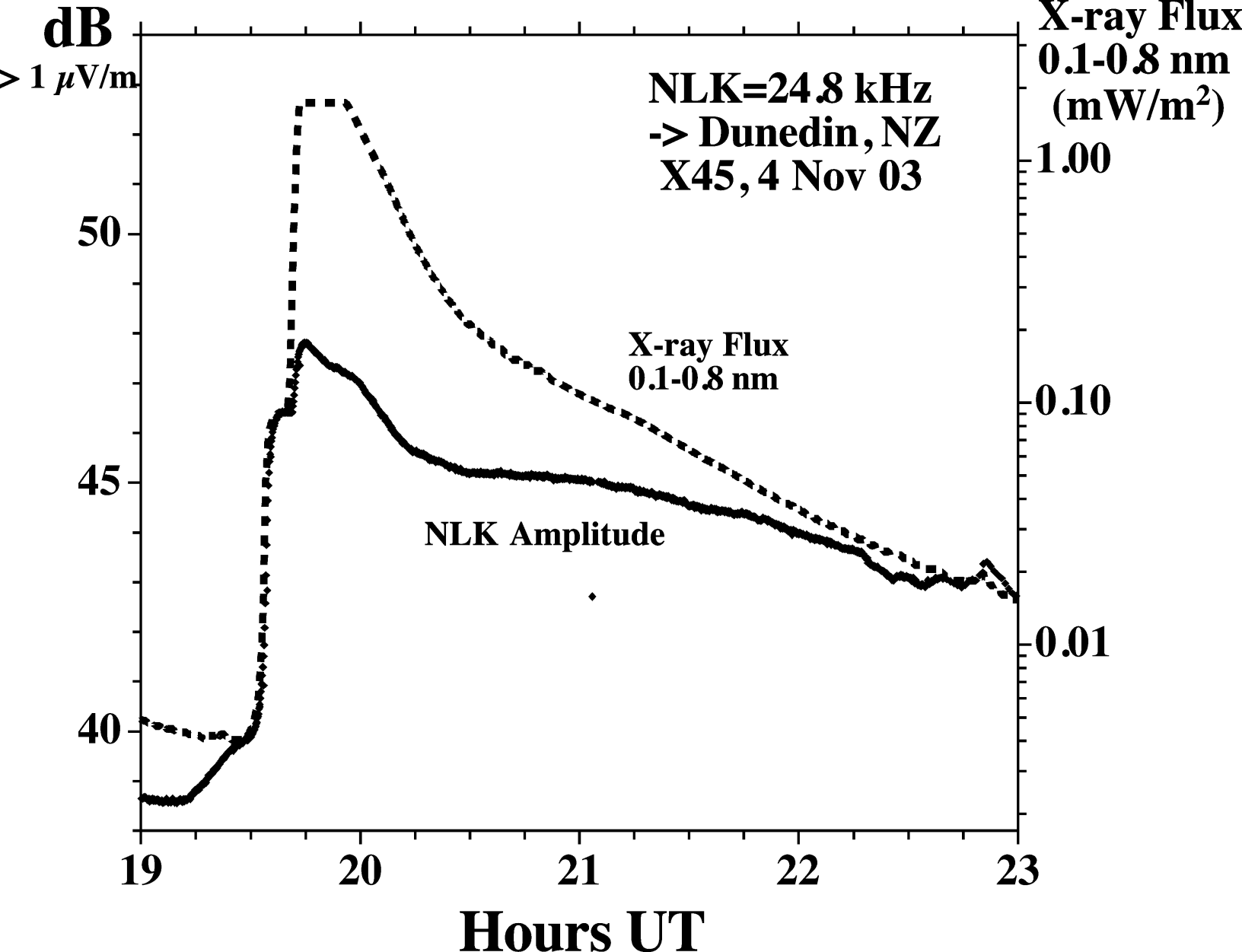
dB
> 1 μV/m
X-ray Flux
0.1-0.8 nm
(mW/m²)
NLK=24.8 kHz
-> Dunedin, NZ
X45, 4 Nov 03
1.00
50
X-ray Flux
0.1-0.8 nm
0.10
45
NLK Amplitude
0.01
40
19
20
21
22
23
Hours UT

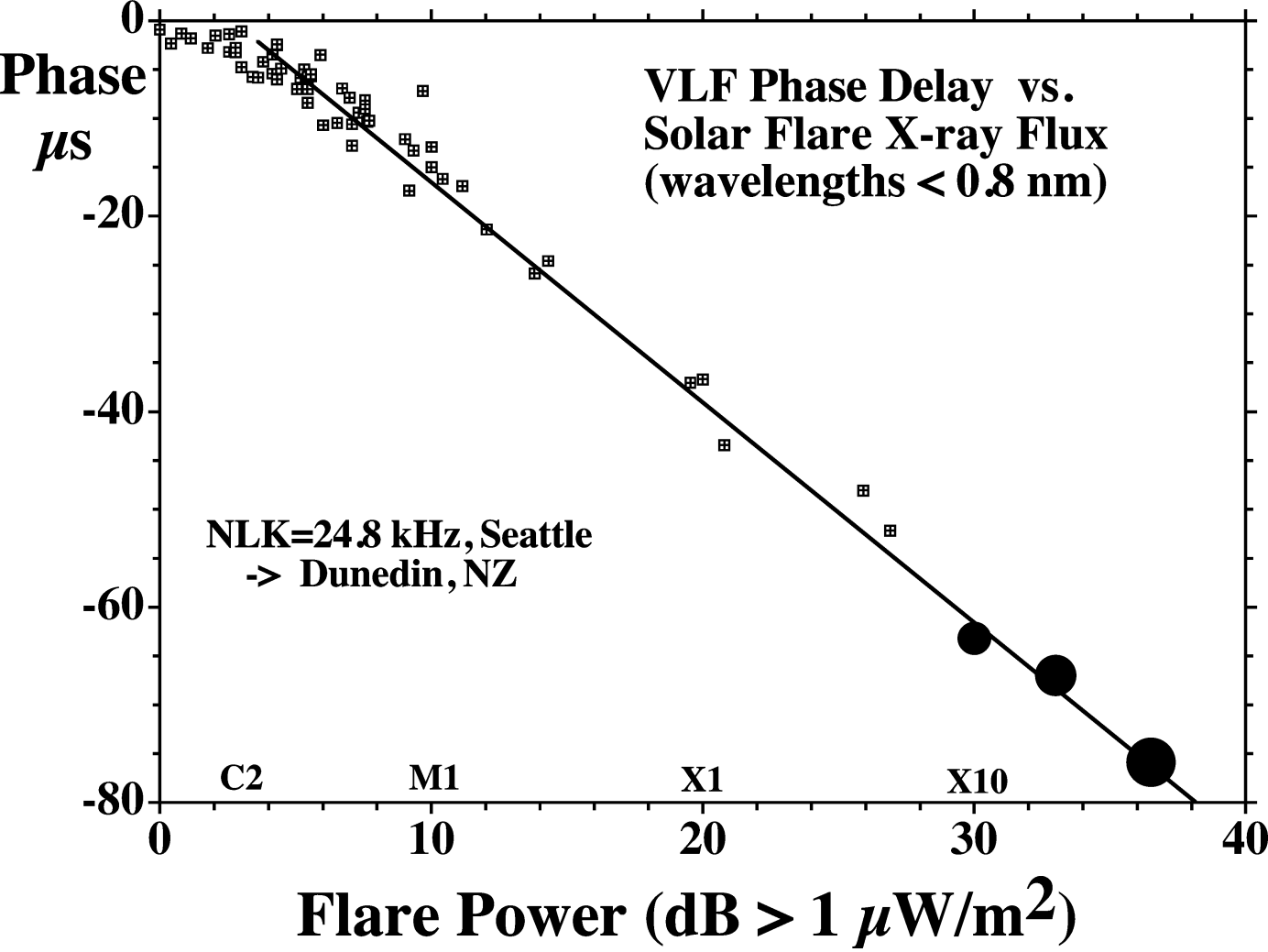
Phase
μs
0
-20
-40
-60
-80
VLF Phase Delay vs.
Solar Flare X-ray Flux
(wavelengths < 0.8 nm)
NLK=24.8 kHz, Seattle
-> Dunedin, NZ
C2
M1
X1
X10
0
10
20
30
40
Flare Power (dB > 1 μW/m2)

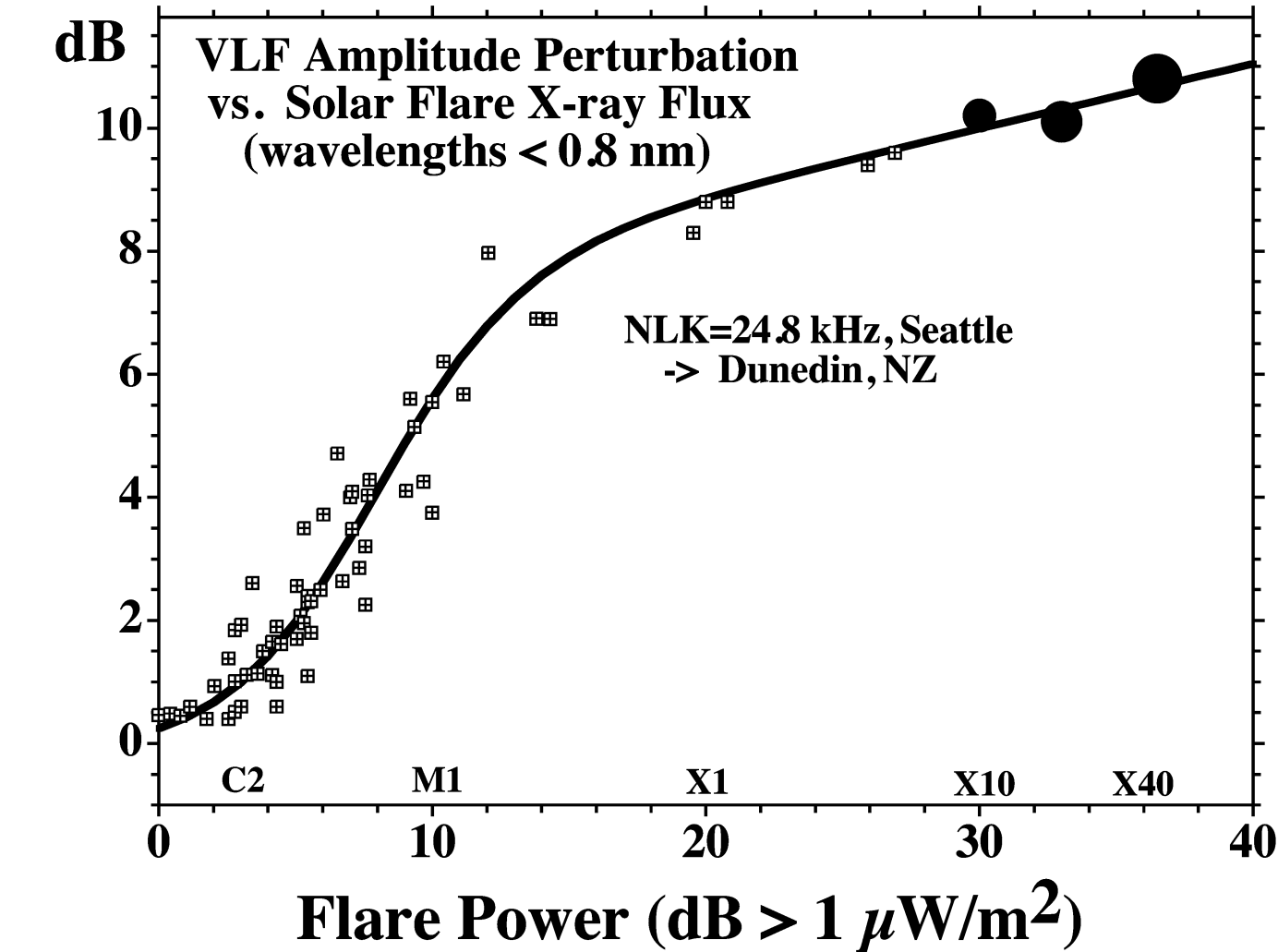
dB
10
8
6
4
2
0
VLF Amplitude Perturbation
vs. Solar Flare X-ray Flux
(wavelengths < 0.8 nm)
NLK=24.8 kHz, Seattle
-> Dunedin, NZ
C2
M1
X1
X10
X40
0
10
20
30
40
Flare Power (dB > 1 μW/m2)

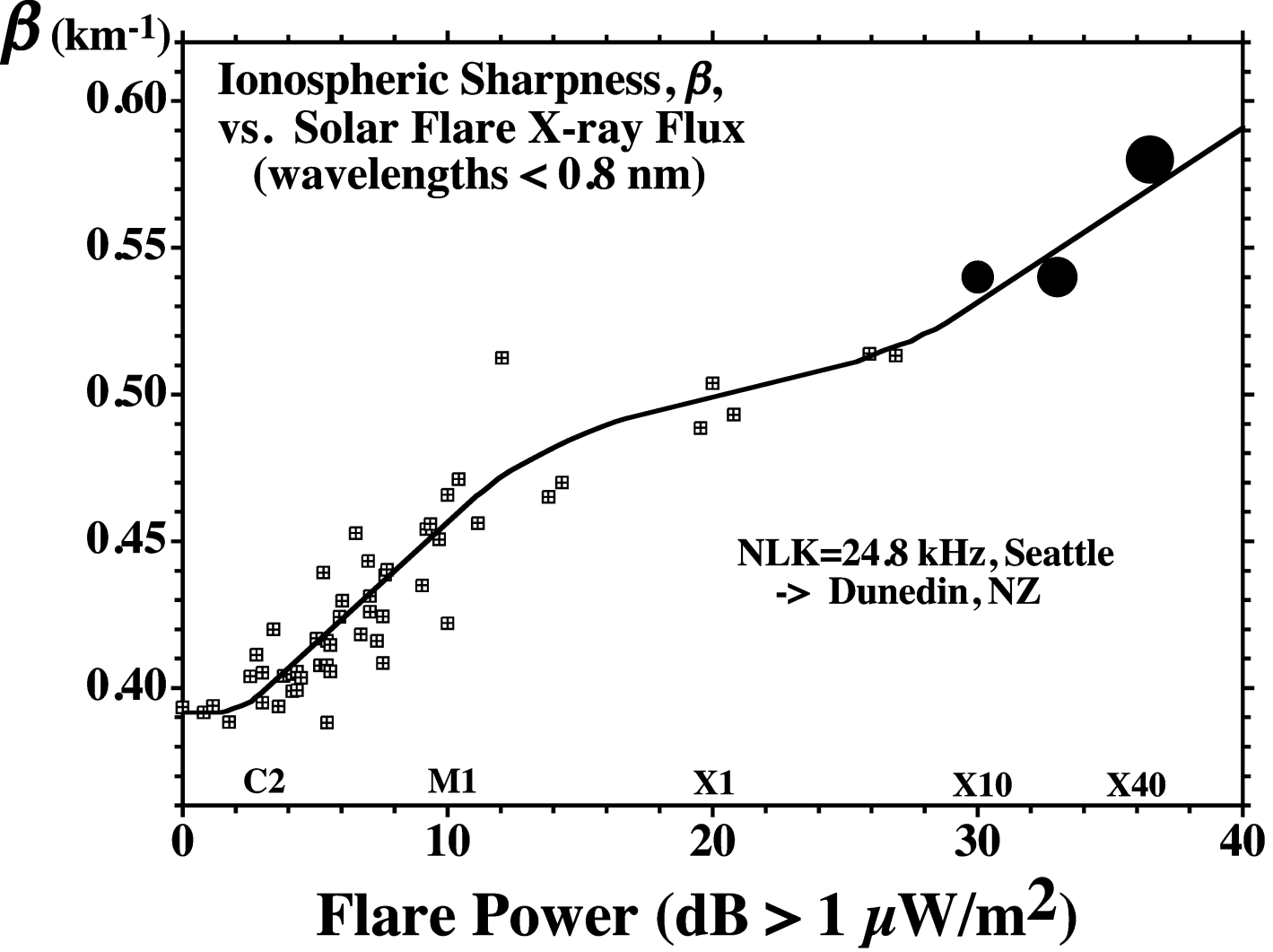
β (km-1)
Ionospheric Sharpness, β,
vs. Solar Flare X-ray Flux
(wavelengths < 0.8 nm)
0.60
0.55
0.50
0.45
0.40
NLK=24.8 kHz, Seattle
-> Dunedin, NZ
C2
M1
X1
X10
X40
0
10
20
30
40
Flare Power (dB > 1 μW/m2)

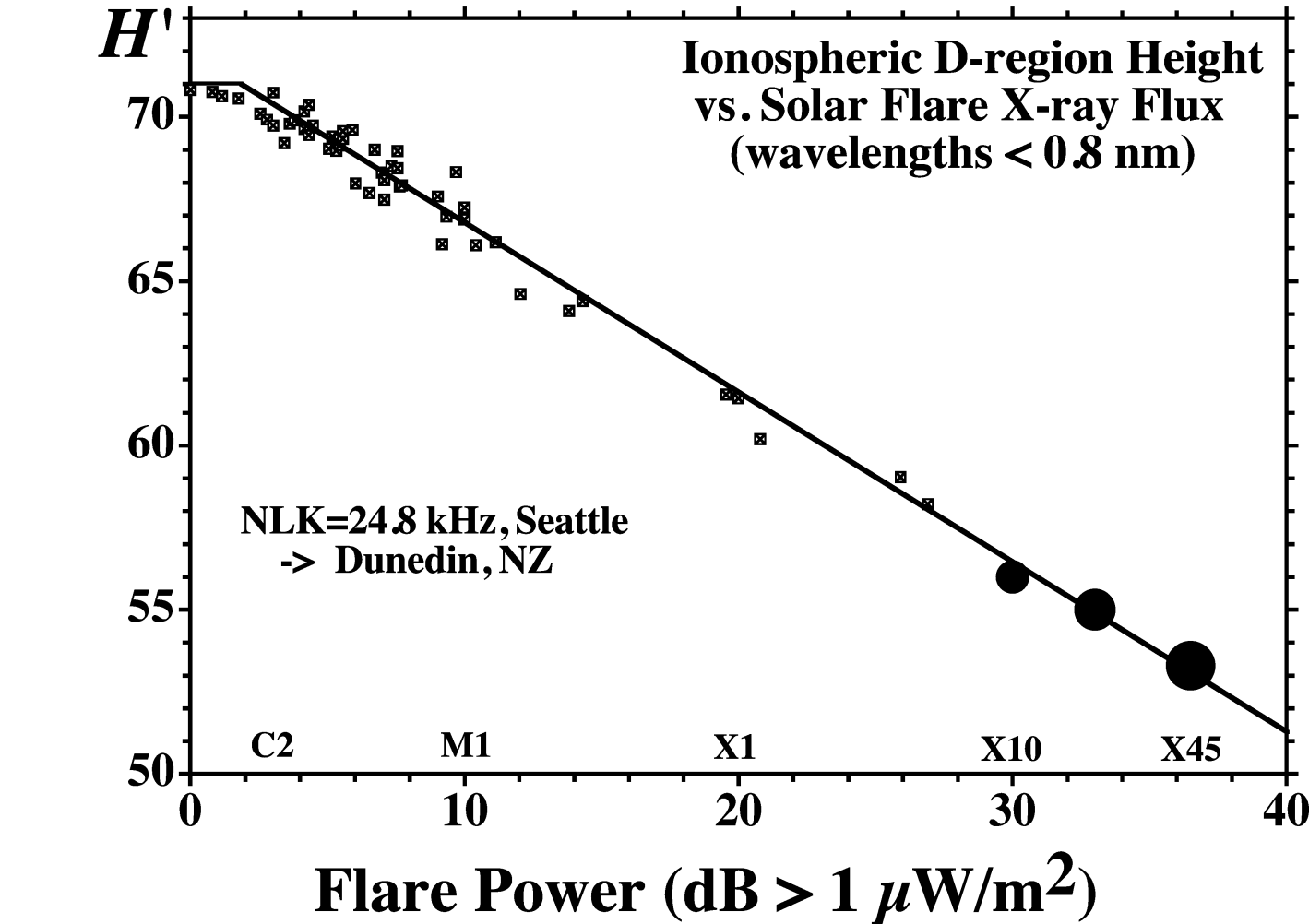
H'
Ionospheric D-region Height
vs. Solar Flare X-ray Flux
(wavelengths < 0.8 nm)
70
65
60
55
50
NLK=24.8 kHz, Seattle
-> Dunedin, NZ
C2
M1
X1
X10
X45
0
10
20
30
40
Flare Power (dB > 1 μW/m2)

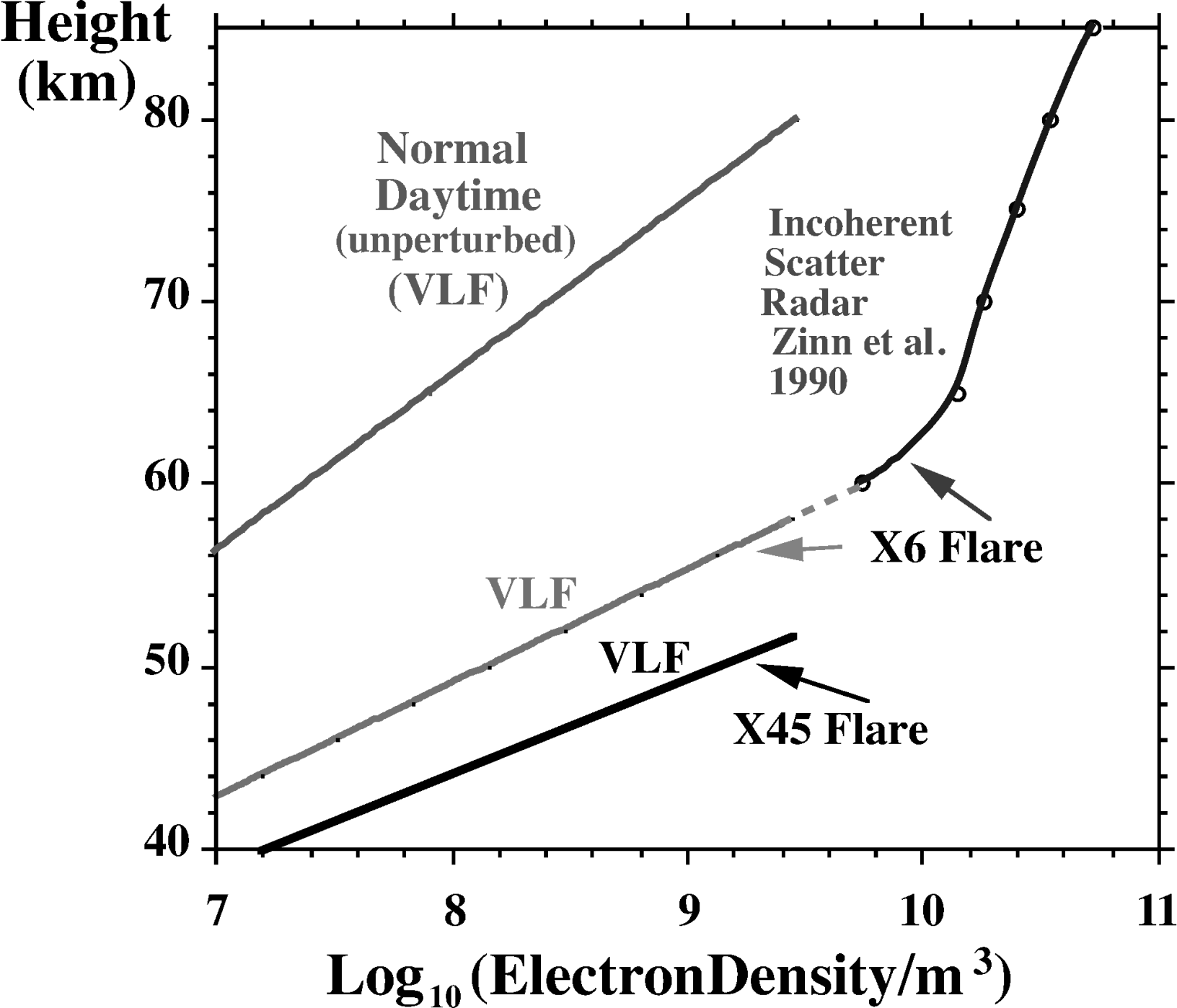
Height (km)
80
70
60
50
40
Normal Daytime (unperturbed) (VLF)
Incoherent Scatter Radar Zinn et al. 1990
X6 Flare
VLF
VLF
X45 Flare
7
8
9
10
11
Log10(ElectronDensity/m3)

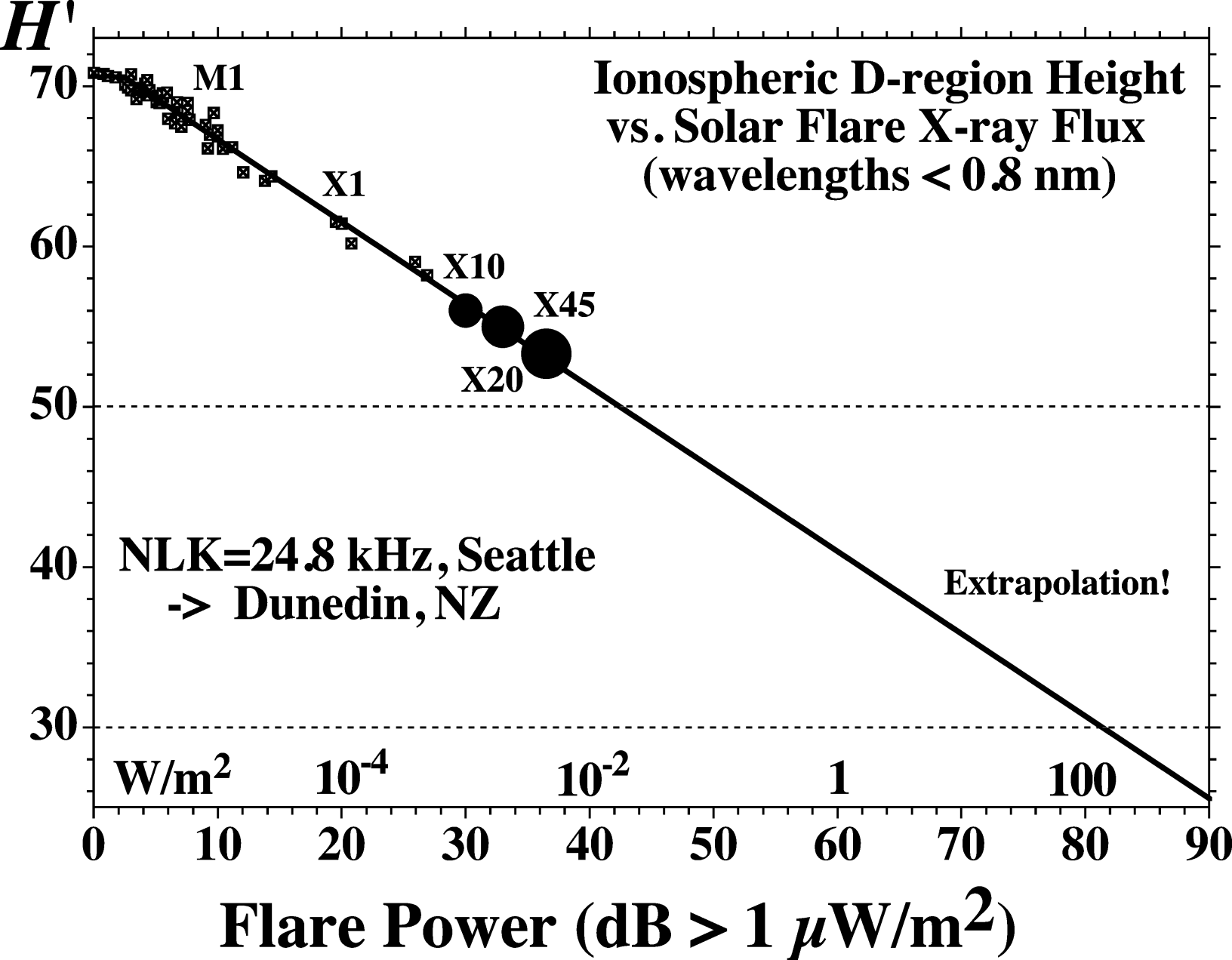
H'
70
60
50
40
30
M1
X1
X10
X45
X20
Ionospheric D-region Height
vs. Solar Flare X-ray Flux
(wavelengths < 0.8 nm)
NLK=24.8 kHz, Seattle
-> Dunedin, NZ
Extrapolation!
W/m2
10-4
10-2
1
100
0
10
20
30
40
50
60
70
80
90
Flare Power (dB > 1 μW/m2)

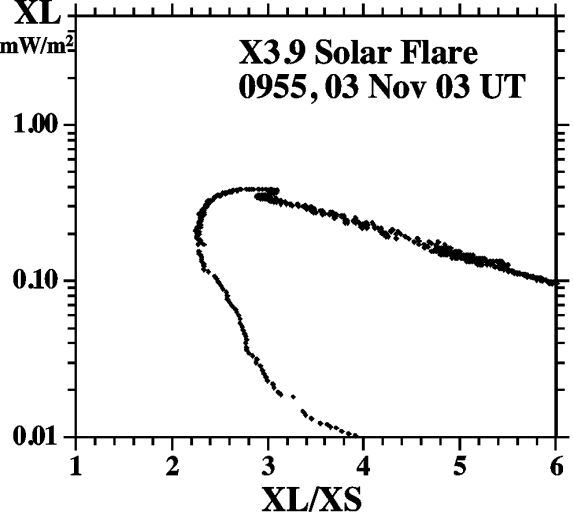
XL
mW/m2
X3.9 Solar Flare
0955, 03 Nov 03 UT
1.00
0.10
0.01
1
2
3
4
5
6
XL/XS

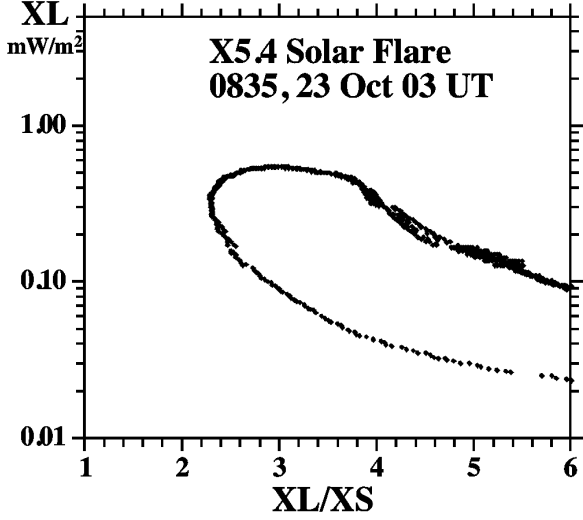
XL
mW/m2
X5.4 Solar Flare
0835, 23 Oct 03 UT
1.00
0.10
0.01
1
2
3
4
5
6
XL/XS

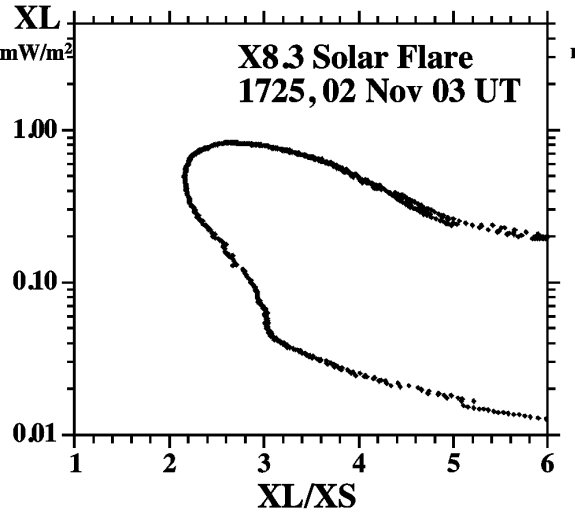
XL
mW/m2
X8.3 Solar Flare
1725, 02 Nov 03 UT
1.00
0.10
0.01
1
2
3
4
5
6
XL/XS

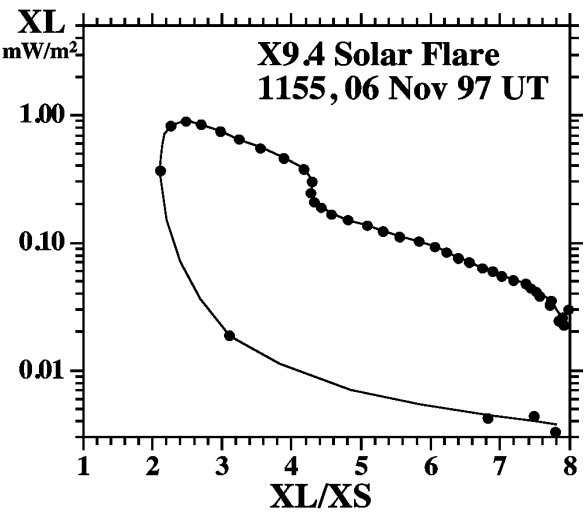
XL
mW/m2
X9.4 Solar Flare
1155, 06 Nov 97 UT
1.00
0.10
0.01
1
2
3
4
5
6
7
8
XL/XS

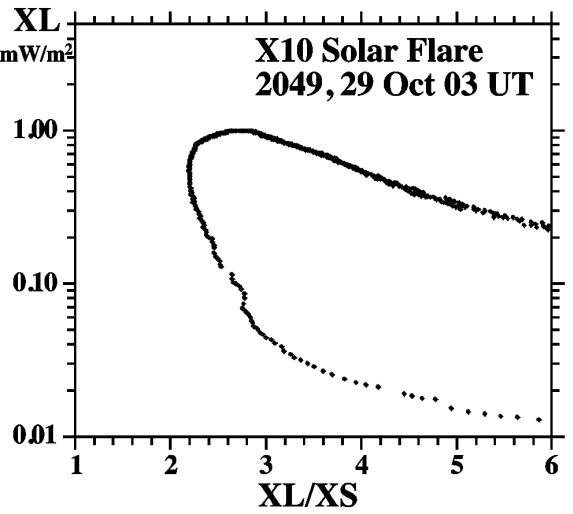
XL
mW/m2
X10 Solar Flare
2049, 29 Oct 03 UT
1.00
0.10
0.01
1
2
3
4
5
6
XL/XS

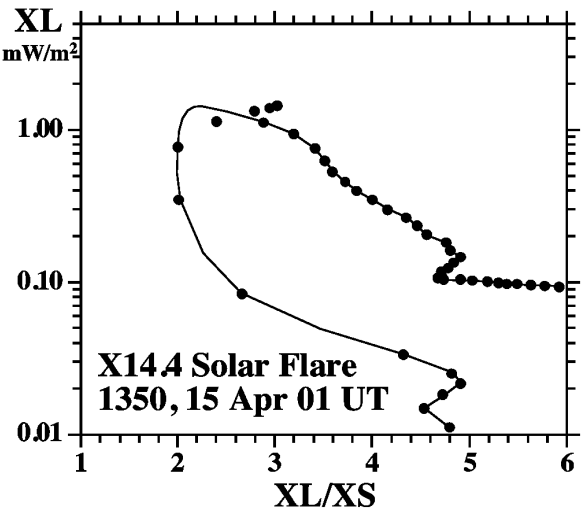
XL
mW/m2
X14.4 Solar Flare
1350, 15 Apr 01 UT
1.00
0.10
0.01
1
2
3
4
5
6
XL/XS

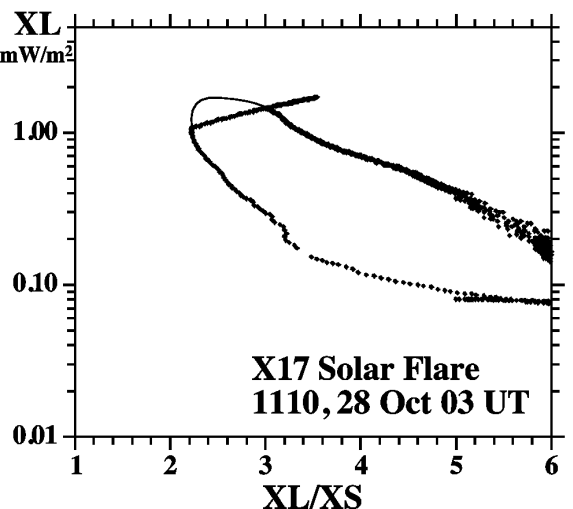
XL
mW/m2
X17 Solar Flare
1110, 28 Oct 03 UT
1.00
0.10
0.01
1
2
3
4
5
6
XL/XS

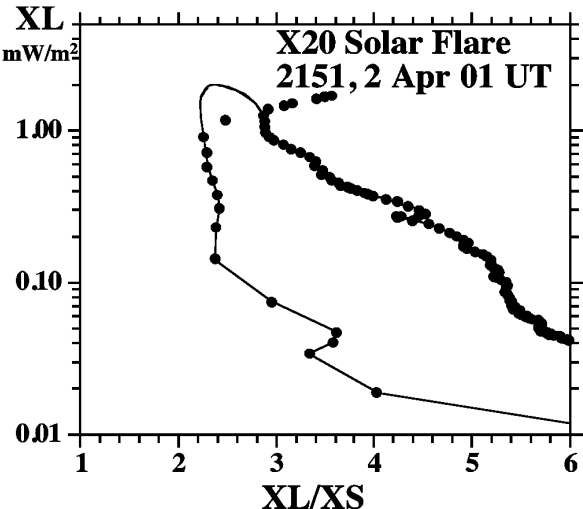
XL
mW/m2
X20 Solar Flare
2151, 2 Apr 01 UT
1.00
0.10
0.01
1
2
3
4
5
6
XL/XS

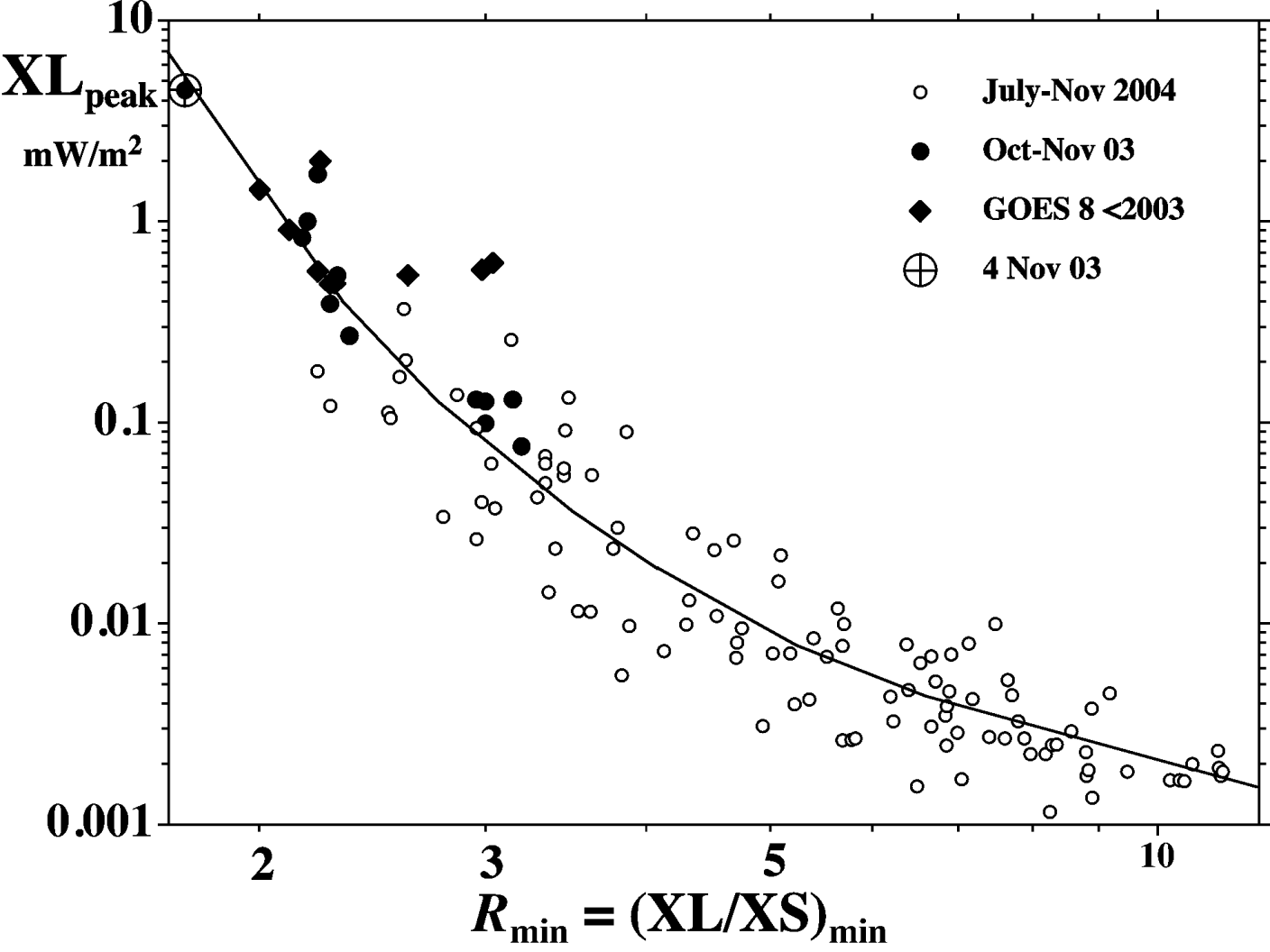
10
1
0.1
0.01
0.001
XL$_{peak}$
mW/m^2
July-Nov 2004
Oct-Nov 03
GOES 8 <2003
4 Nov 03
2
3
5
10
R_{min} = (XL/XS)$_{min}$

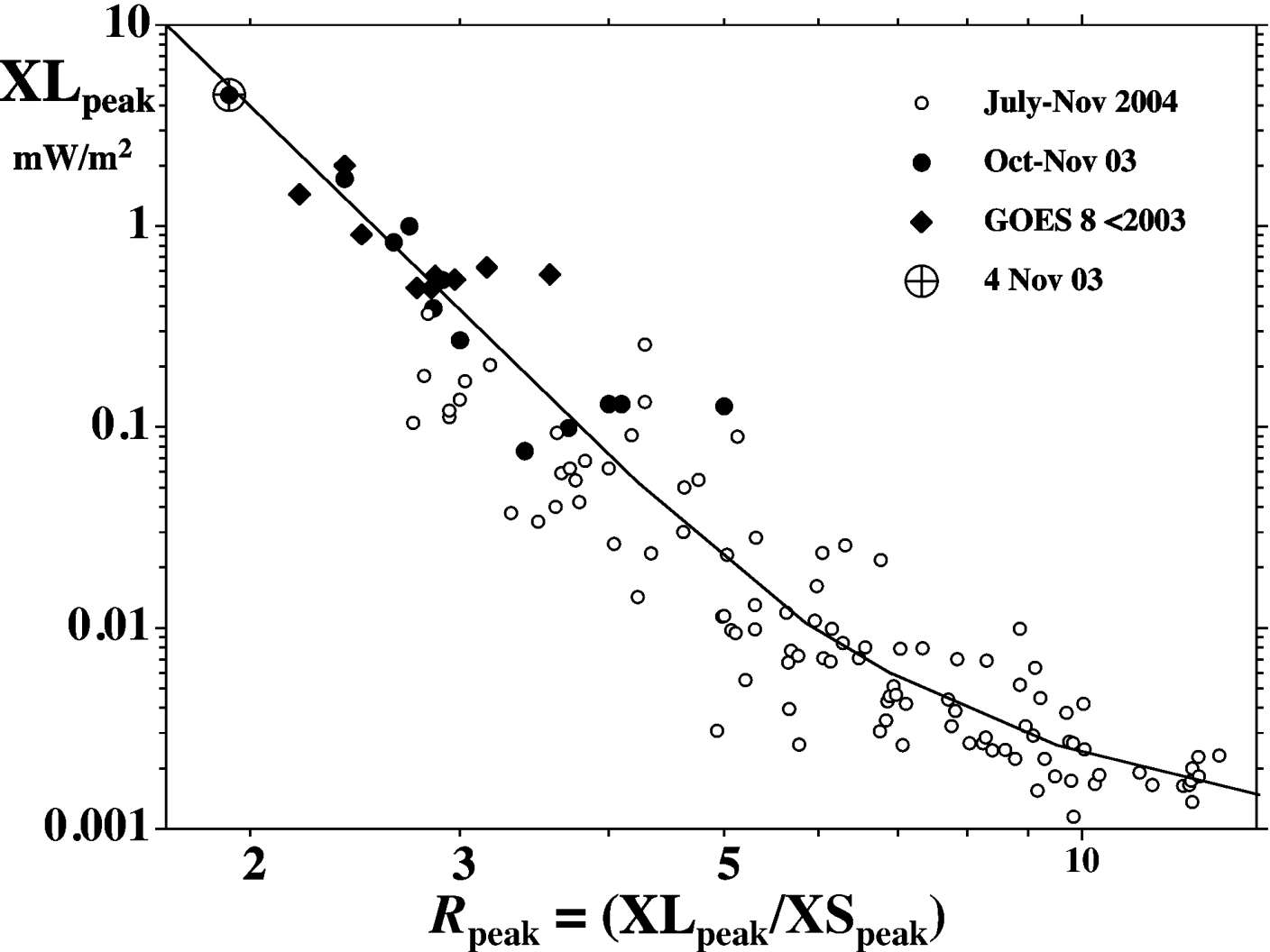
10
1
0.1
0.01
0.001
XL$_{peak}$
mW/m^2
July-Nov 2004
Oct-Nov 03
GOES 8 <2003
4 Nov 03
2
3
5
10
R_{peak} = (XL$_{peak}$/XS$_{peak}$)

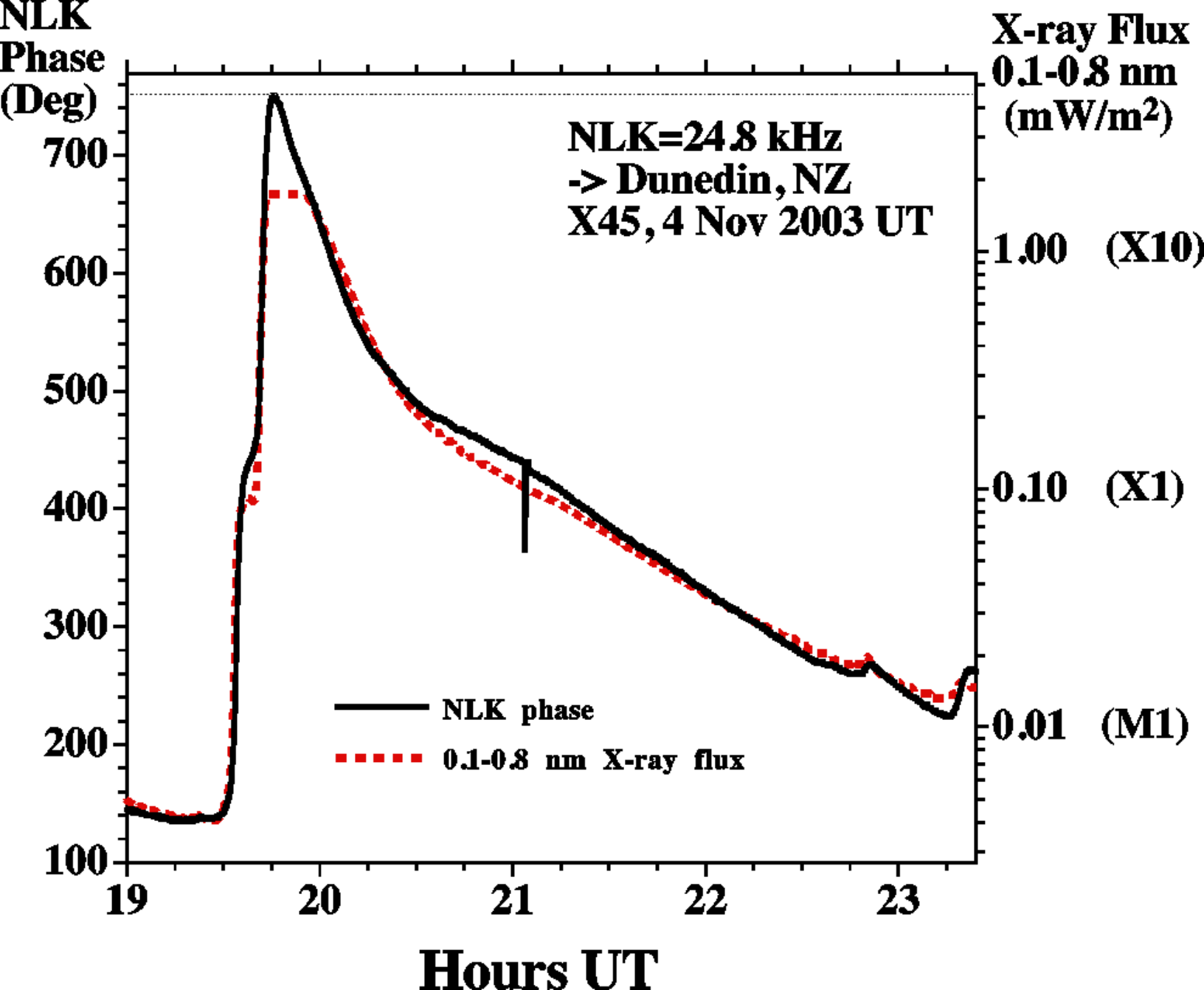
NLK Phase (Deg)
X-ray Flux 0.1-0.8 nm (mW/m²)
NLK=24.8 kHz
-> Dunedin, NZ
X45, 4 Nov 2003 UT
700
600
500
400
300
200
100
1.00 (X10)
0.10 (X1)
0.01 (M1)
NLK phase
0.1-0.8 nm X-ray flux
19
20
21
22
23
Hours UT

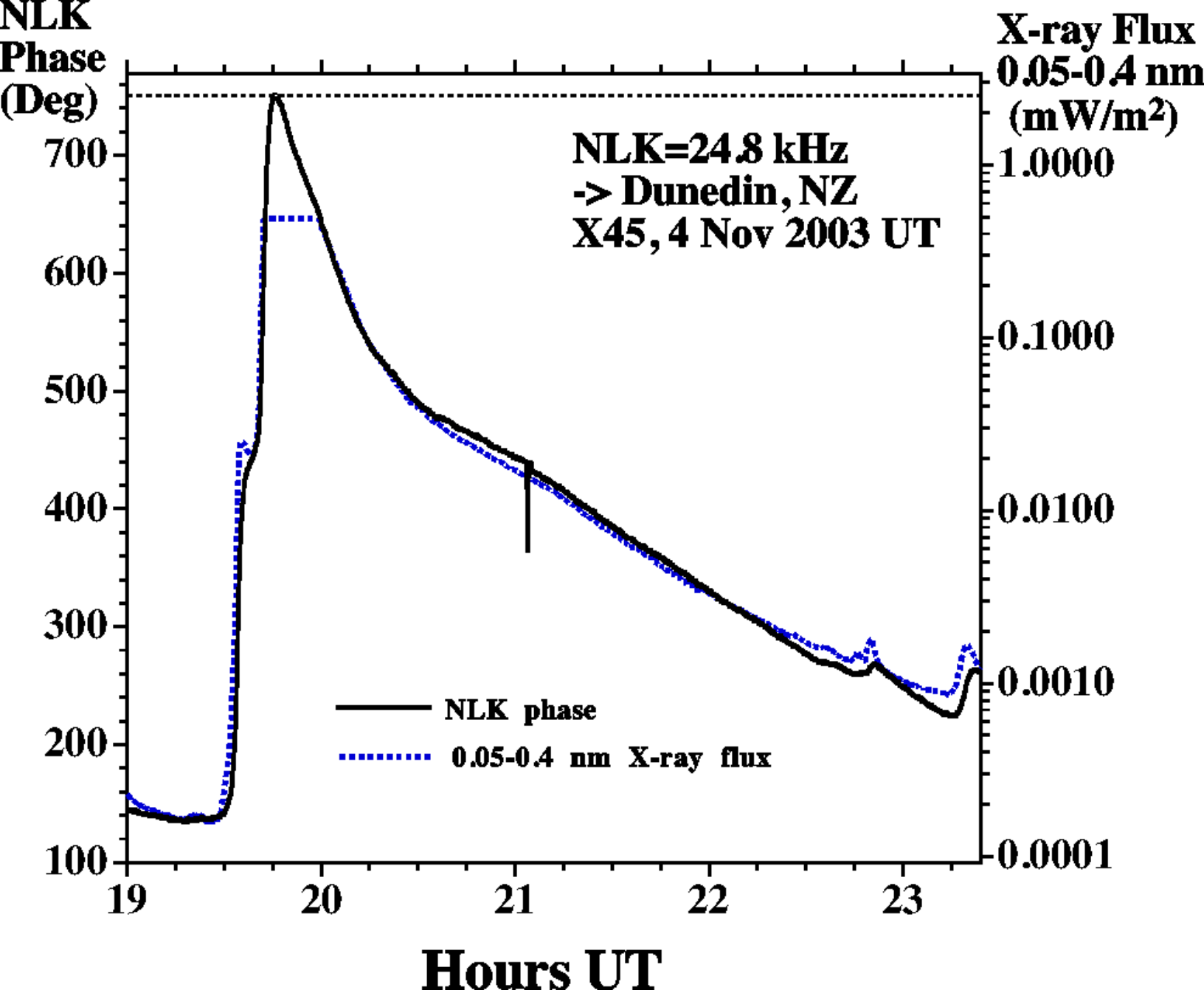
NLK Phase (Deg)
X-ray Flux 0.05-0.4 nm (mW/m²)
NLK=24.8 kHz
-> Dunedin, NZ
X45, 4 Nov 2003 UT
NLK phase
0.05-0.4 nm X-ray flux
700
600
500
400
300
200
100
1.0000
0.1000
0.0100
0.0010
0.0001
19
20
21
22
23
Hours UT

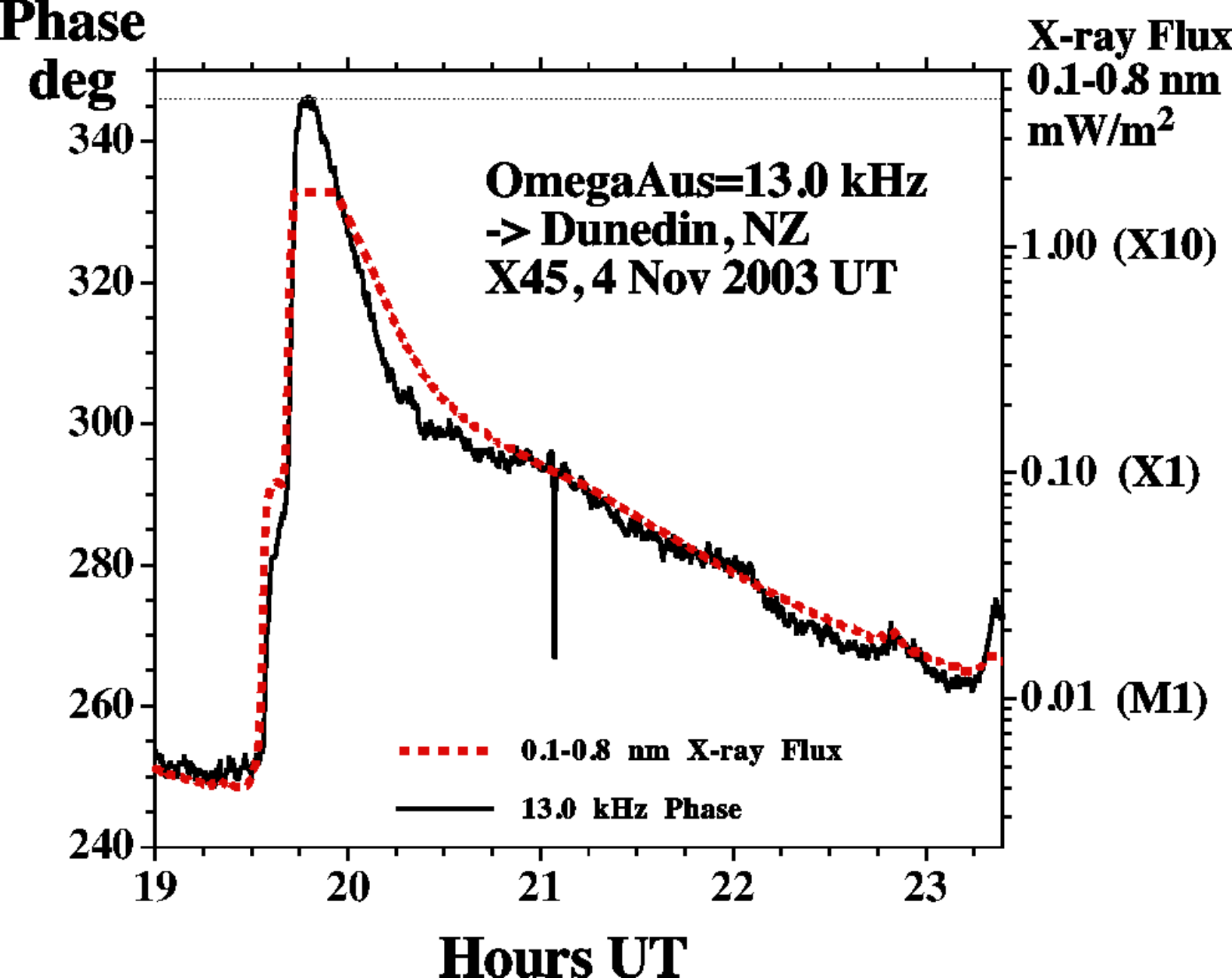
Phase
deg
340
320
300
280
260
240
X-ray Flux
0.1-0.8 nm
mW/m2
1.00 (X10)
0.10 (X1)
0.01 (M1)
OmegaAus=13.0 kHz
-> Dunedin, NZ
X45, 4 Nov 2003 UT
0.1-0.8 nm X-ray Flux
13.0 kHz Phase
19
20
21
22
23
Hours UT

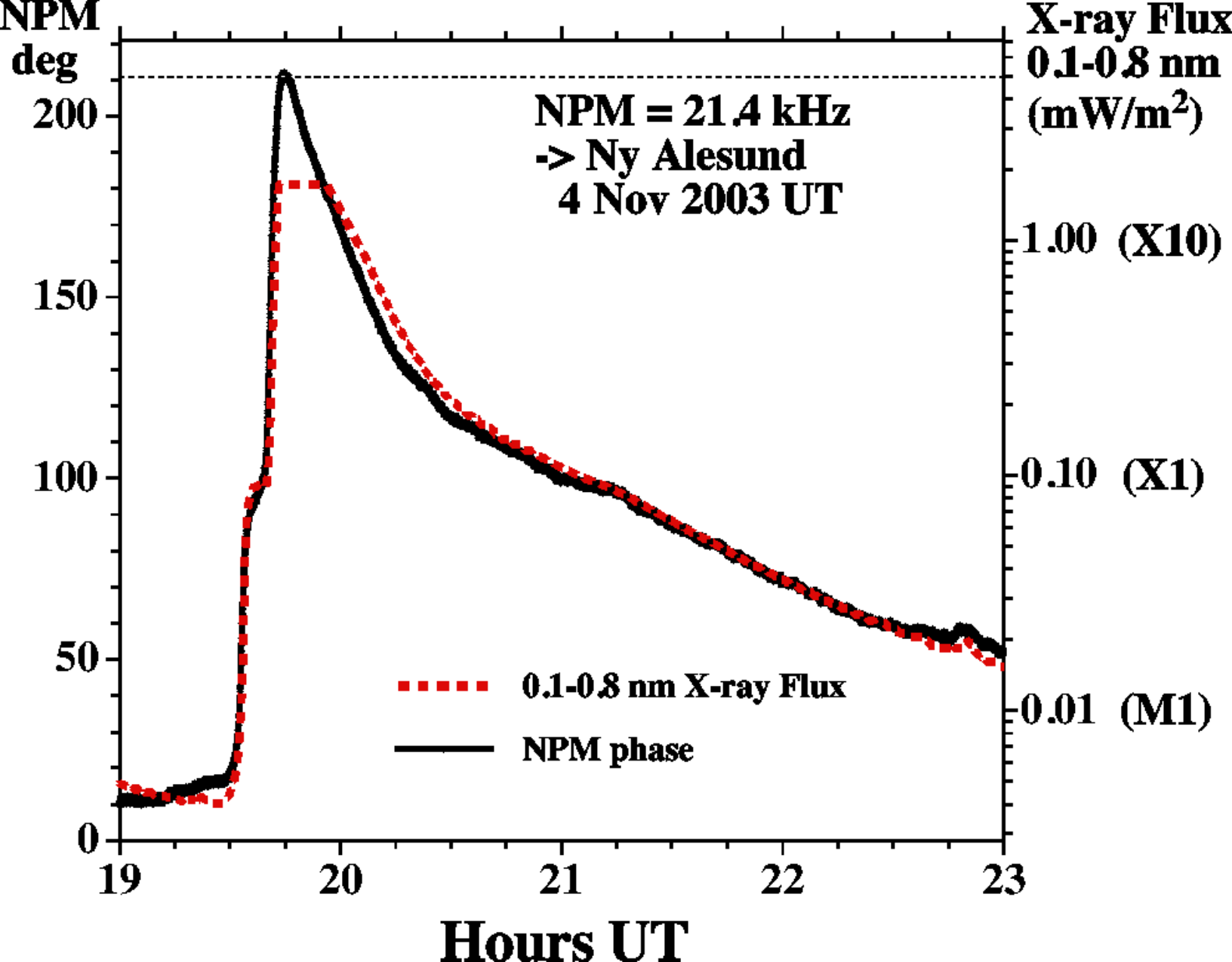
NPM
deg
200
150
100
50
0
X-ray Flux
0.1-0.8 nm
(mW/m2)
1.00 (X10)
0.10 (X1)
0.01 (M1)
NPM = 21.4 kHz
-> Ny Alesund
4 Nov 2003 UT
0.1-0.8 nm X-ray Flux
NPM phase
19
20
21
22
23
Hours UT

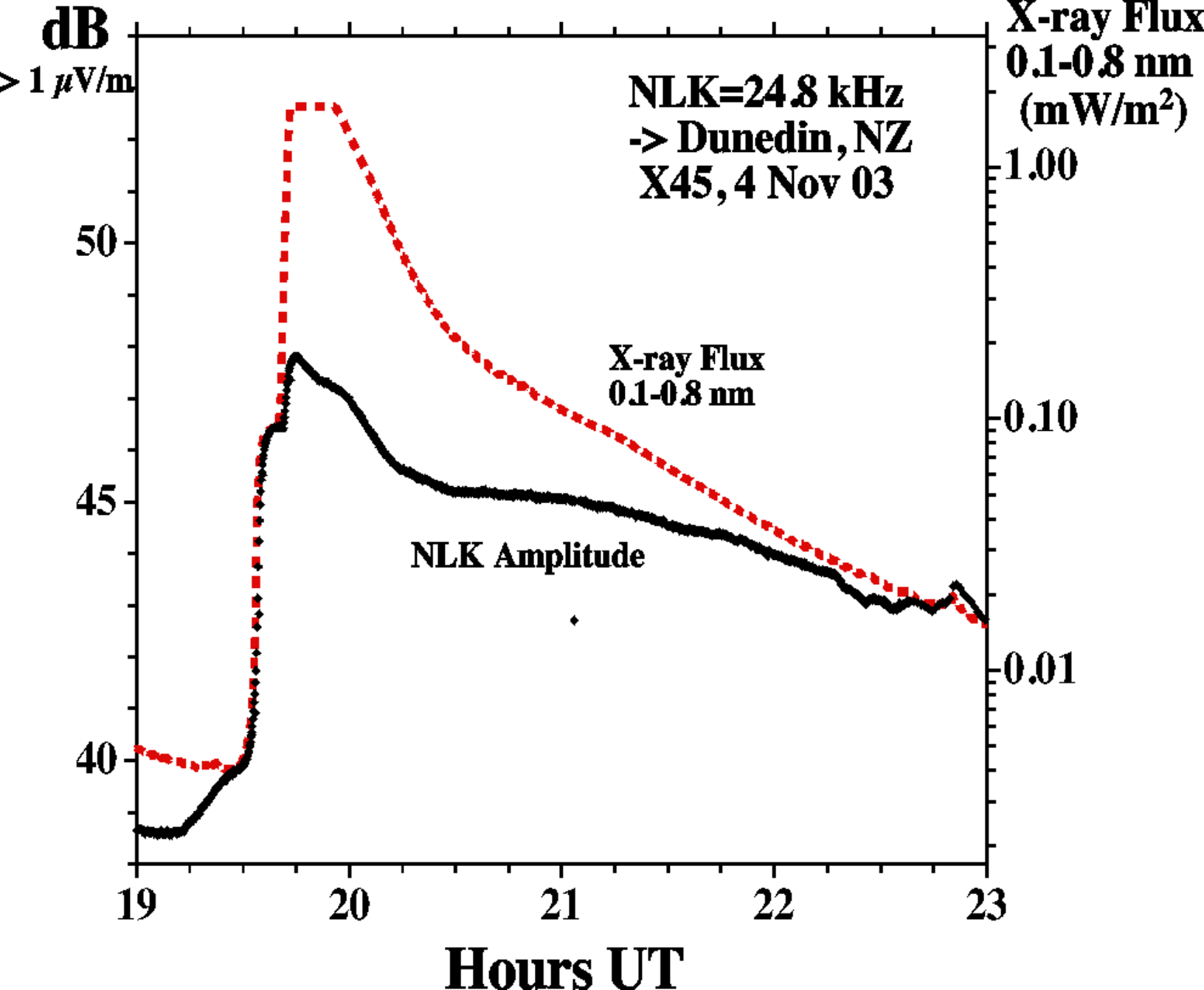
dB
> 1 μV/m
X-ray Flux
0.1-0.8 nm
(mW/m²)
NLK=24.8 kHz
-> Dunedin, NZ
X45, 4 Nov 03
X-ray Flux
0.1-0.8 nm
NLK Amplitude
50
45
40
1.00
0.10
0.01
19
20
21
22
23
Hours UT

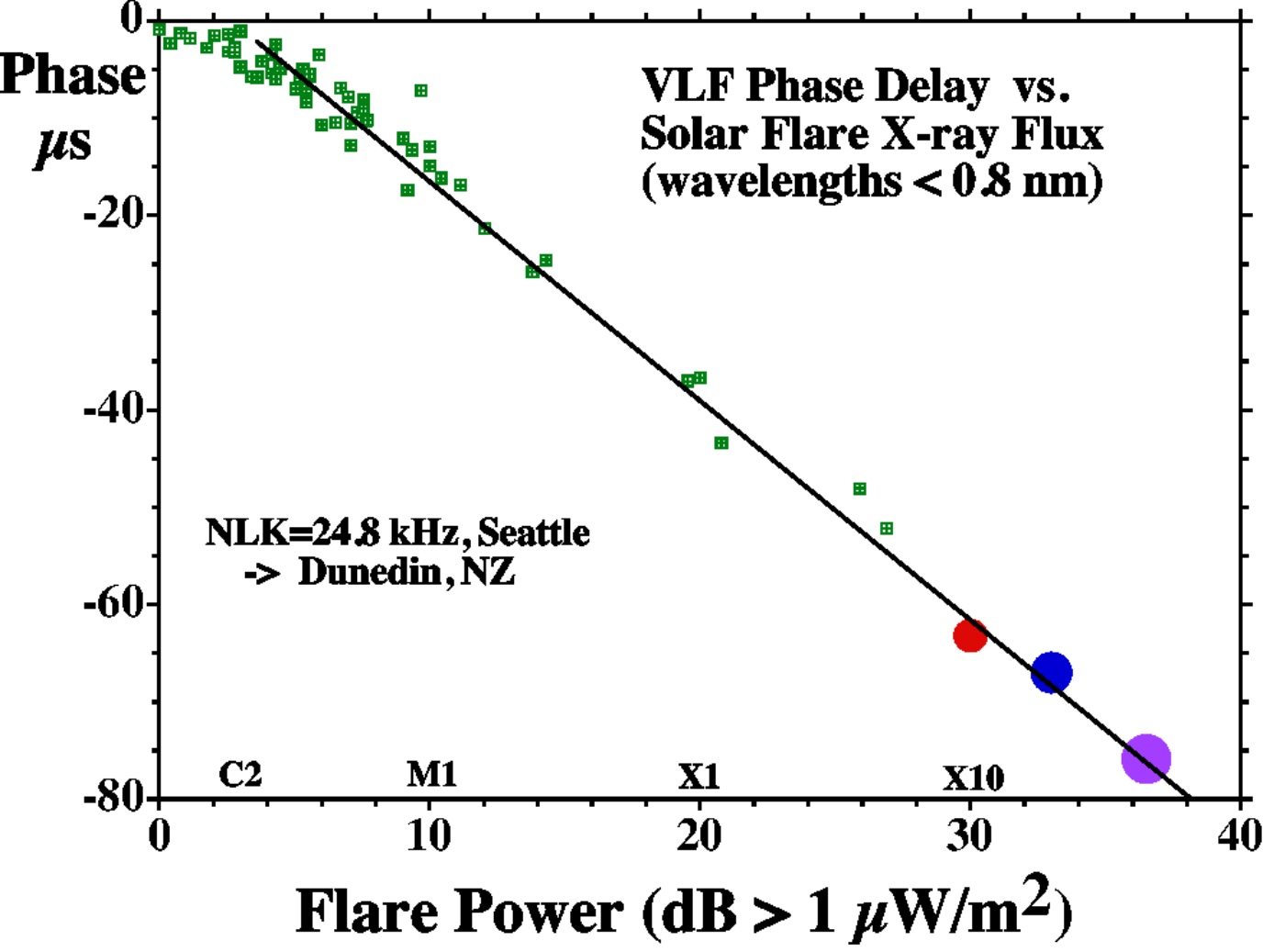
Phase
μs
0
-20
-40
-60
-80
VLF Phase Delay vs.
Solar Flare X-ray Flux
(wavelengths < 0.8 nm)
NLK=24.8 kHz, Seattle
-> Dunedin, NZ
C2
M1
X1
X10
0
10
20
30
40
Flare Power (dB > 1 μW/m2)

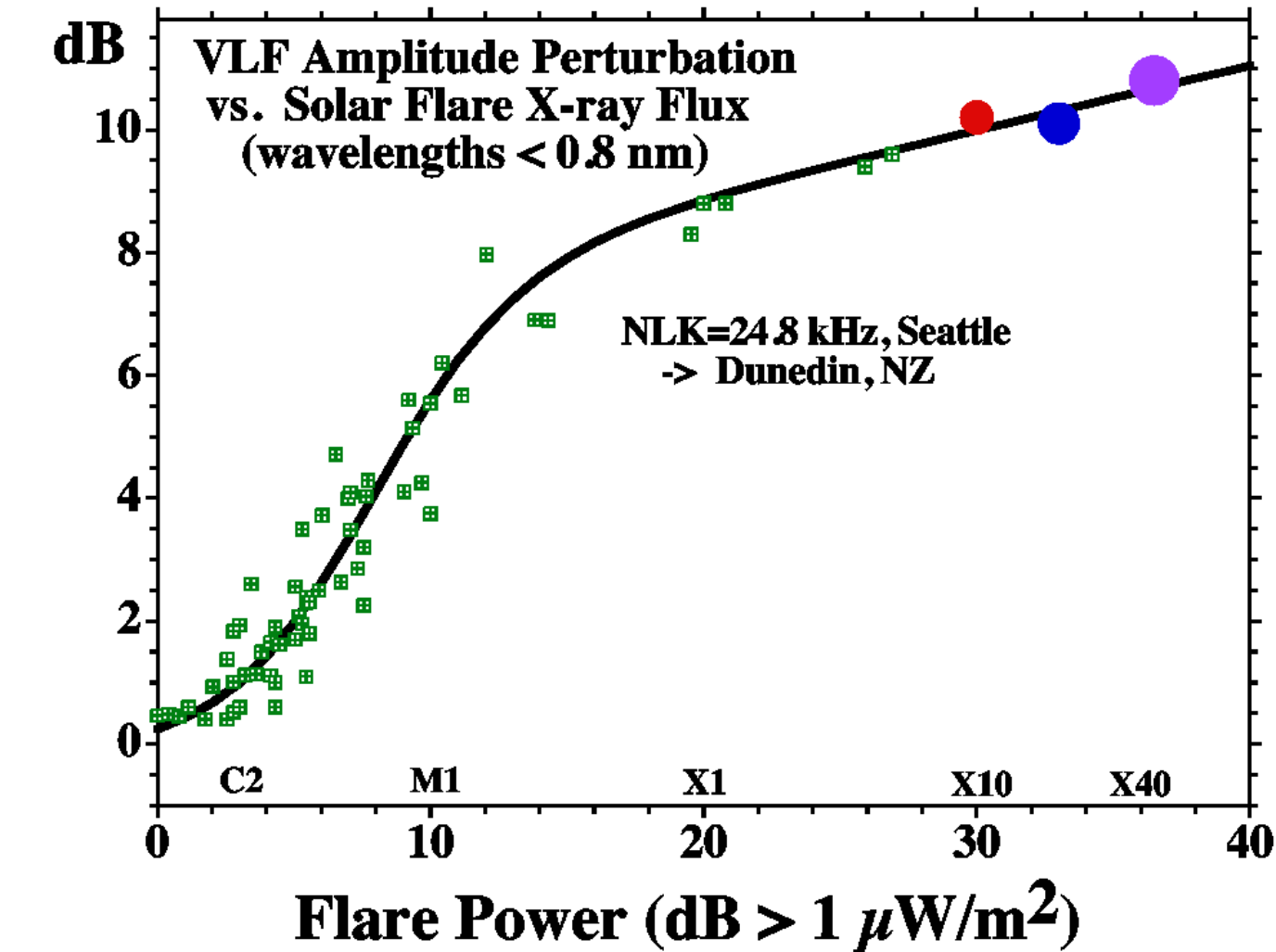
dB
10
8
6
4
2
0
VLF Amplitude Perturbation
vs. Solar Flare X-ray Flux
(wavelengths < 0.8 nm)
NLK=24.8 kHz, Seattle
-> Dunedin, NZ
C2
M1
X1
X10
X40
0
10
20
30
40
Flare Power (dB > 1 μW/m2)

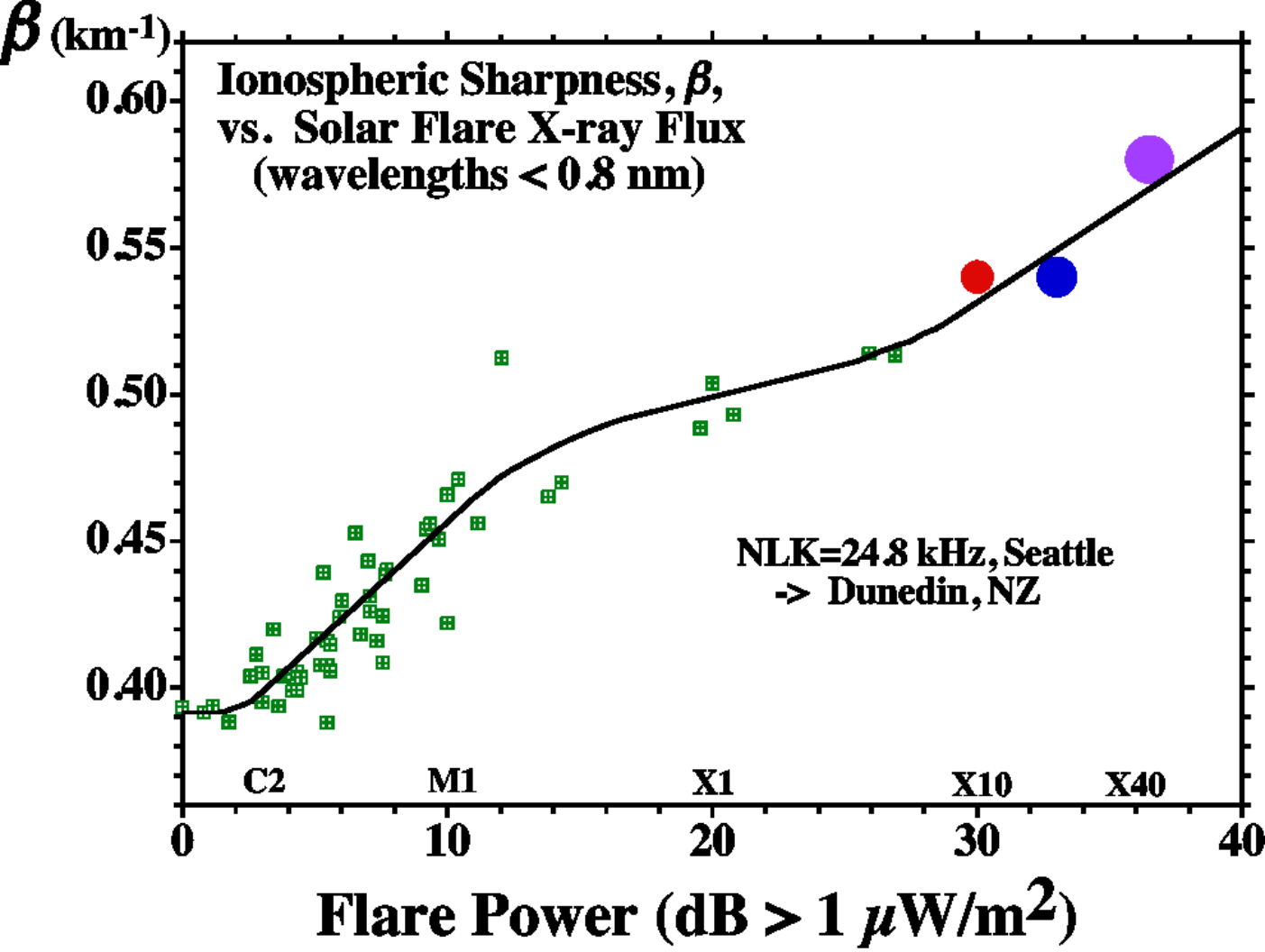
β (km-1)
Ionospheric Sharpness, β,
vs. Solar Flare X-ray Flux
(wavelengths < 0.8 nm)
NLK=24.8 kHz, Seattle
-> Dunedin, NZ
0.60
0.55
0.50
0.45
0.40
C2
M1
X1
X10
X40
0
10
20
30
40
Flare Power (dB > 1 μW/m2)

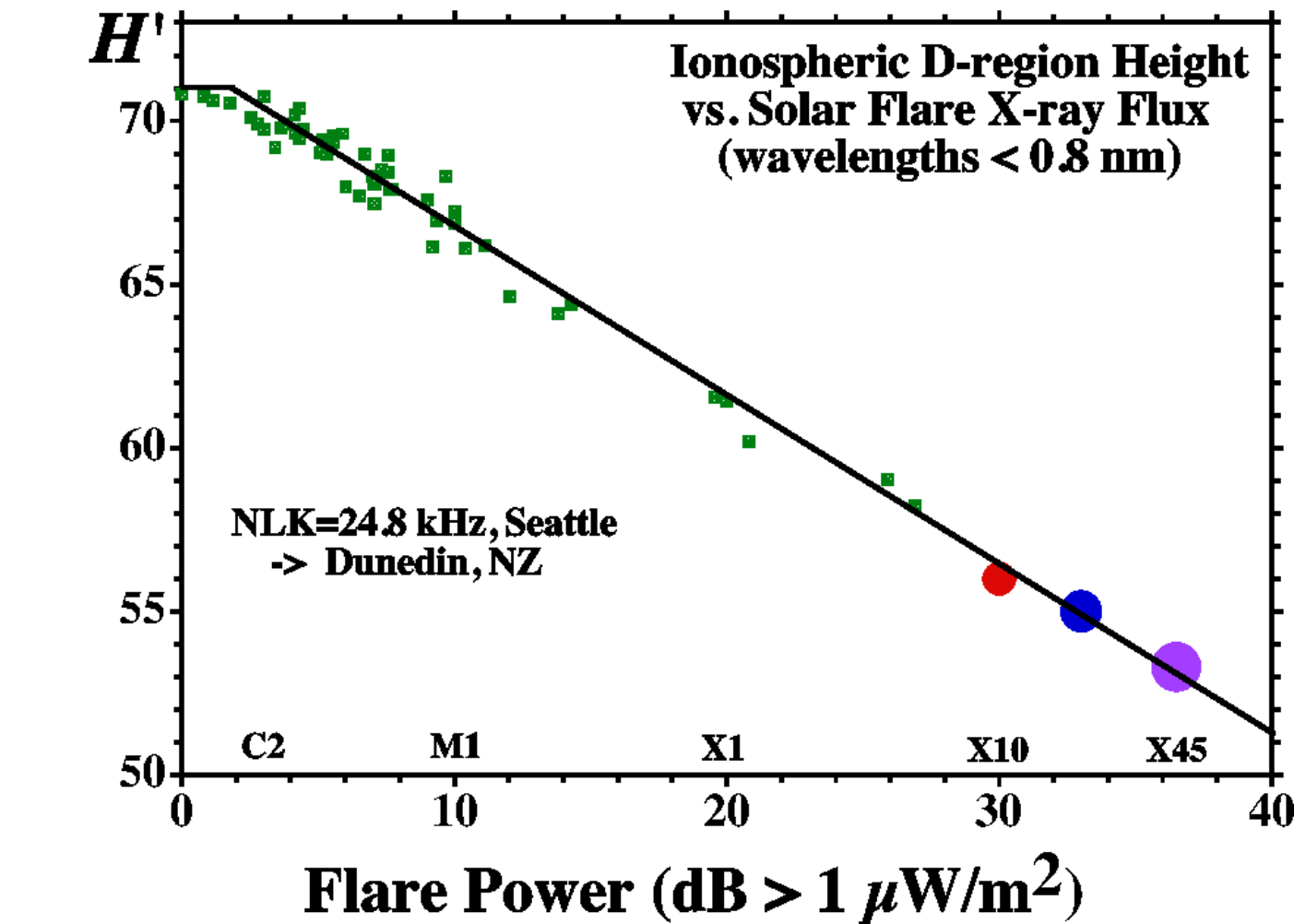
H'
Ionospheric D-region Height
vs. Solar Flare X-ray Flux
(wavelengths < 0.8 nm)
NLK=24.8 kHz, Seattle
-> Dunedin, NZ
70
65
60
55
50
C2
M1
X1
X10
X45
0
10
20
30
40
Flare Power (dB > 1 μW/m2)

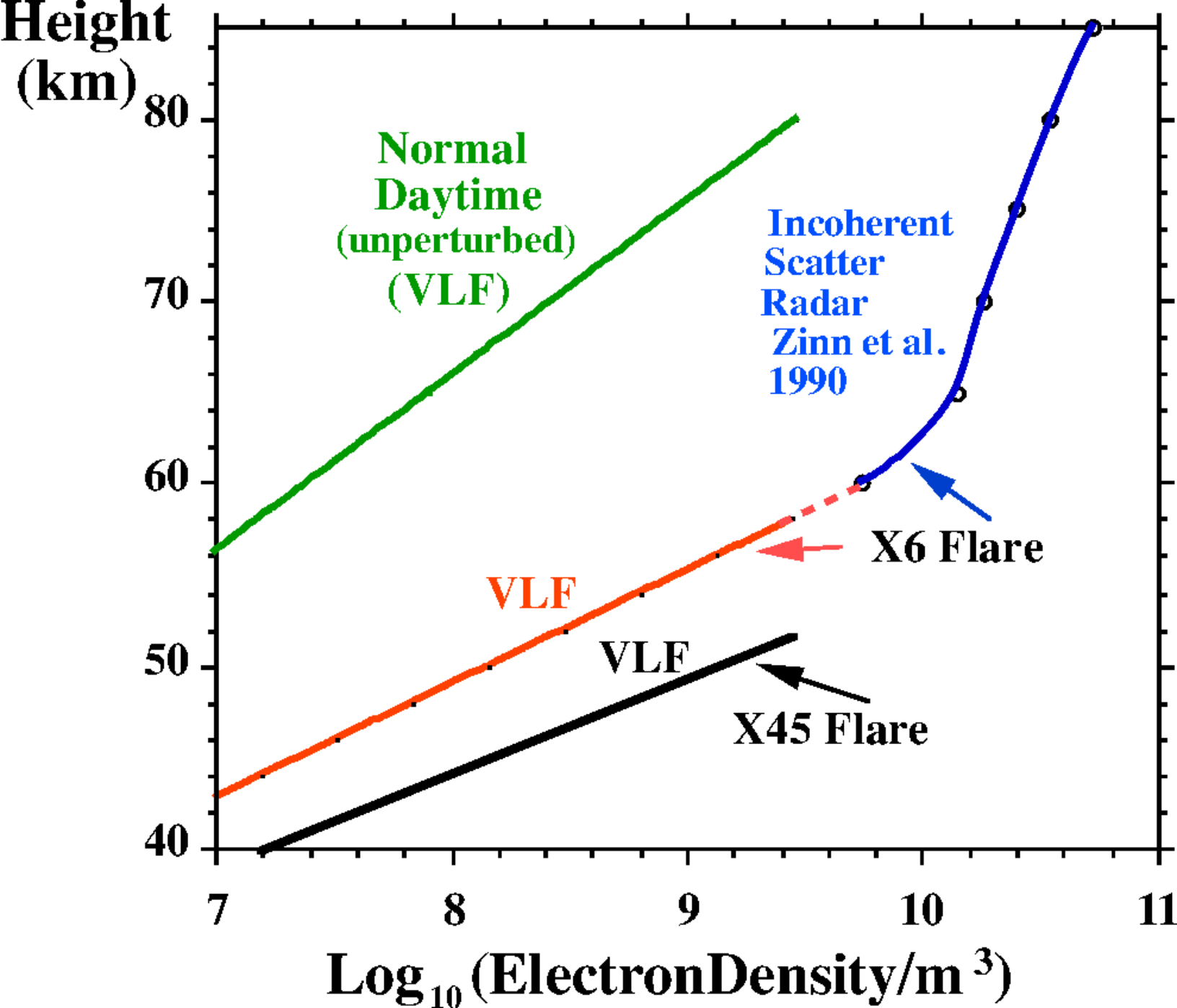
Height (km)
80
70
60
50
40
Normal Daytime (unperturbed) (VLF)
Incoherent Scatter Radar Zinn et al. 1990
X6 Flare
VLF
VLF
X45 Flare
7
8
9
10
11
Log10(ElectronDensity/m3)

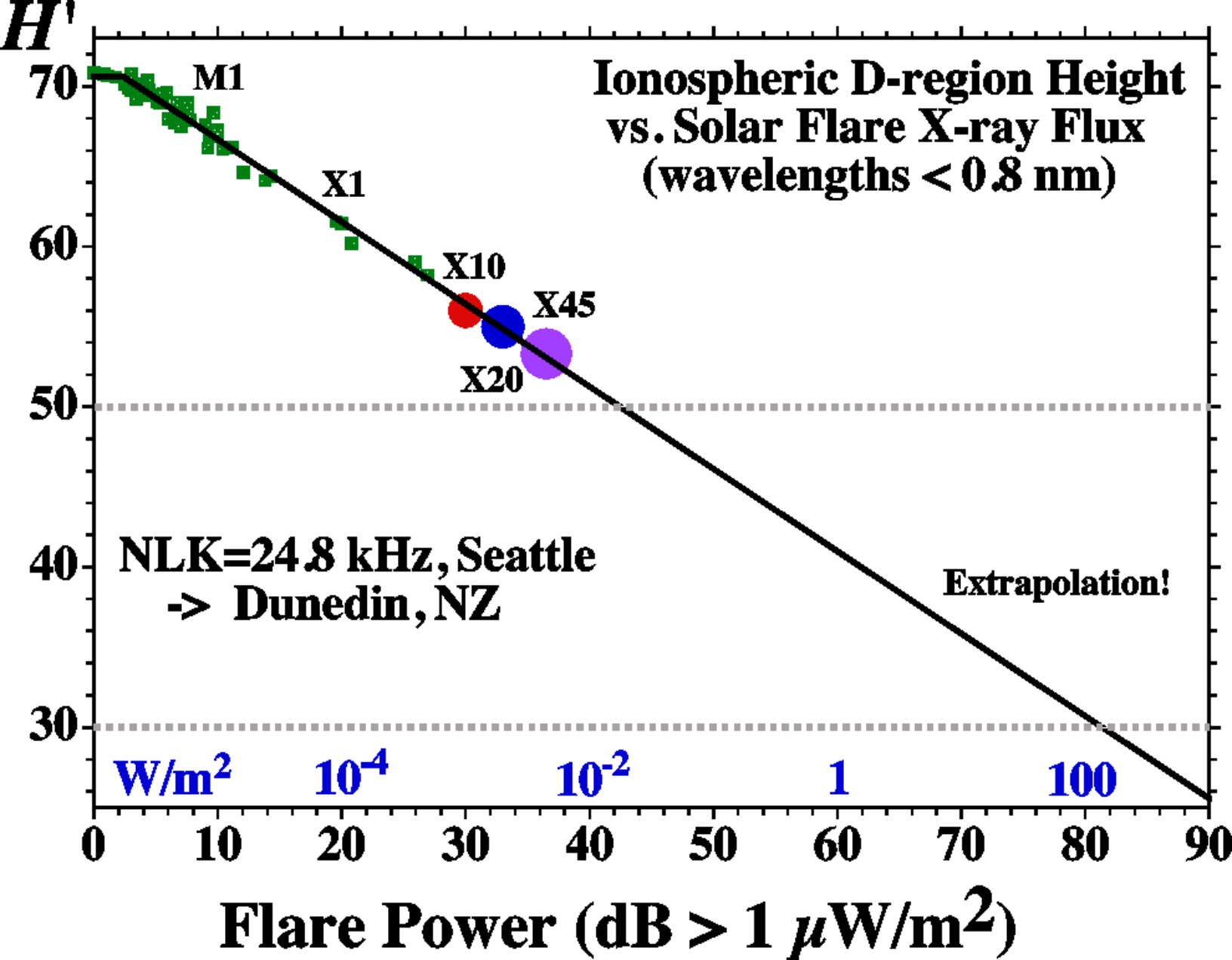
H'
70
60
50
40
30
M1
X1
X10
X45
X20
Ionospheric D-region Height
vs. Solar Flare X-ray Flux
(wavelengths < 0.8 nm)
NLK=24.8 kHz, Seattle
-> Dunedin, NZ
Extrapolation!
W/m2
10-4
10-2
1
100
0
10
20
30
40
50
60
70
80
90
Flare Power (dB > 1 μW/m2)

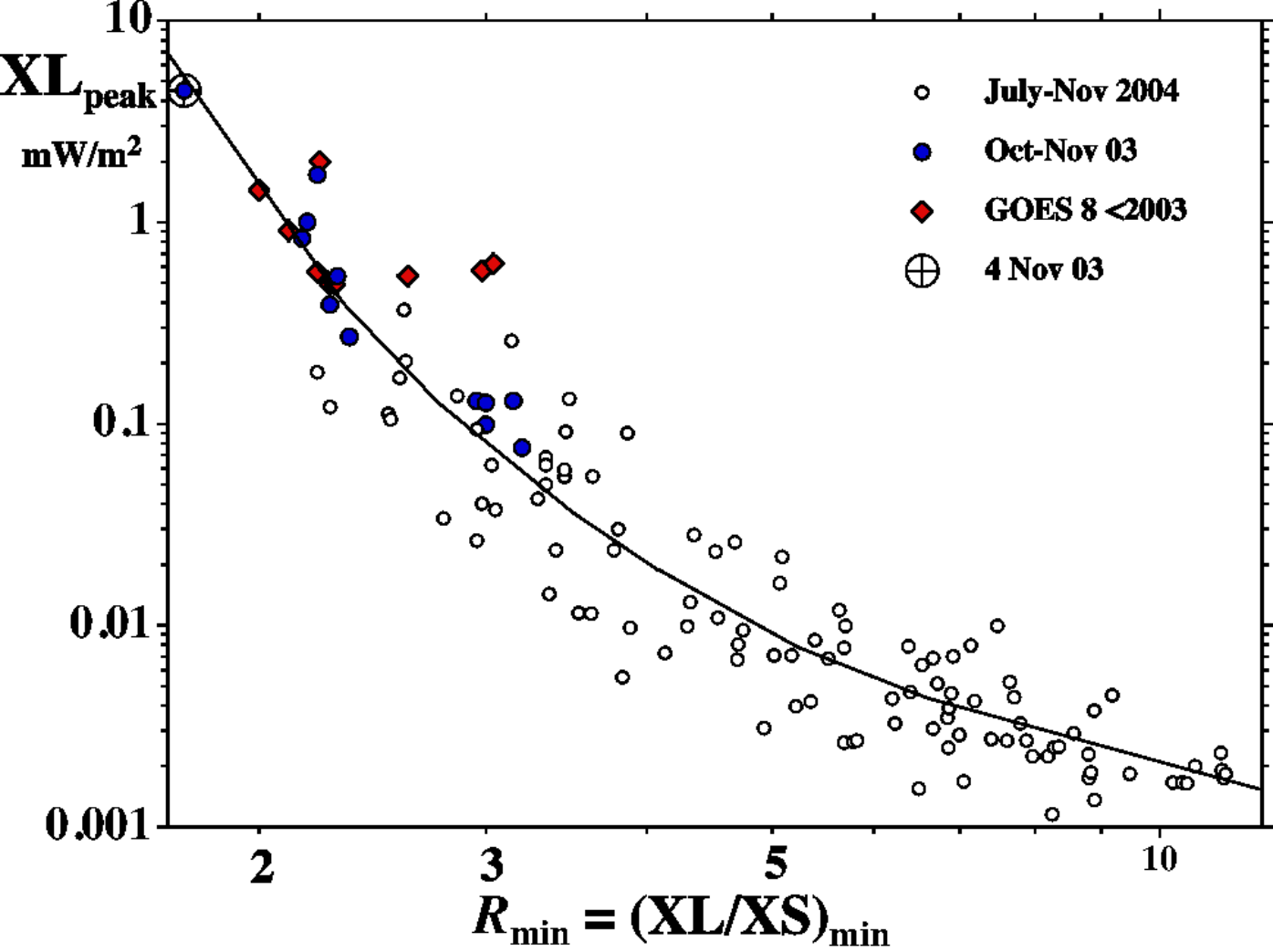
10
1
0.1
0.01
0.001
XL$_{peak}$
mW/m^2
July-Nov 2004
Oct-Nov 03
GOES 8 <2003
4 Nov 03
2
3
5
10
R_{min} = (XL/XS)$_{min}$

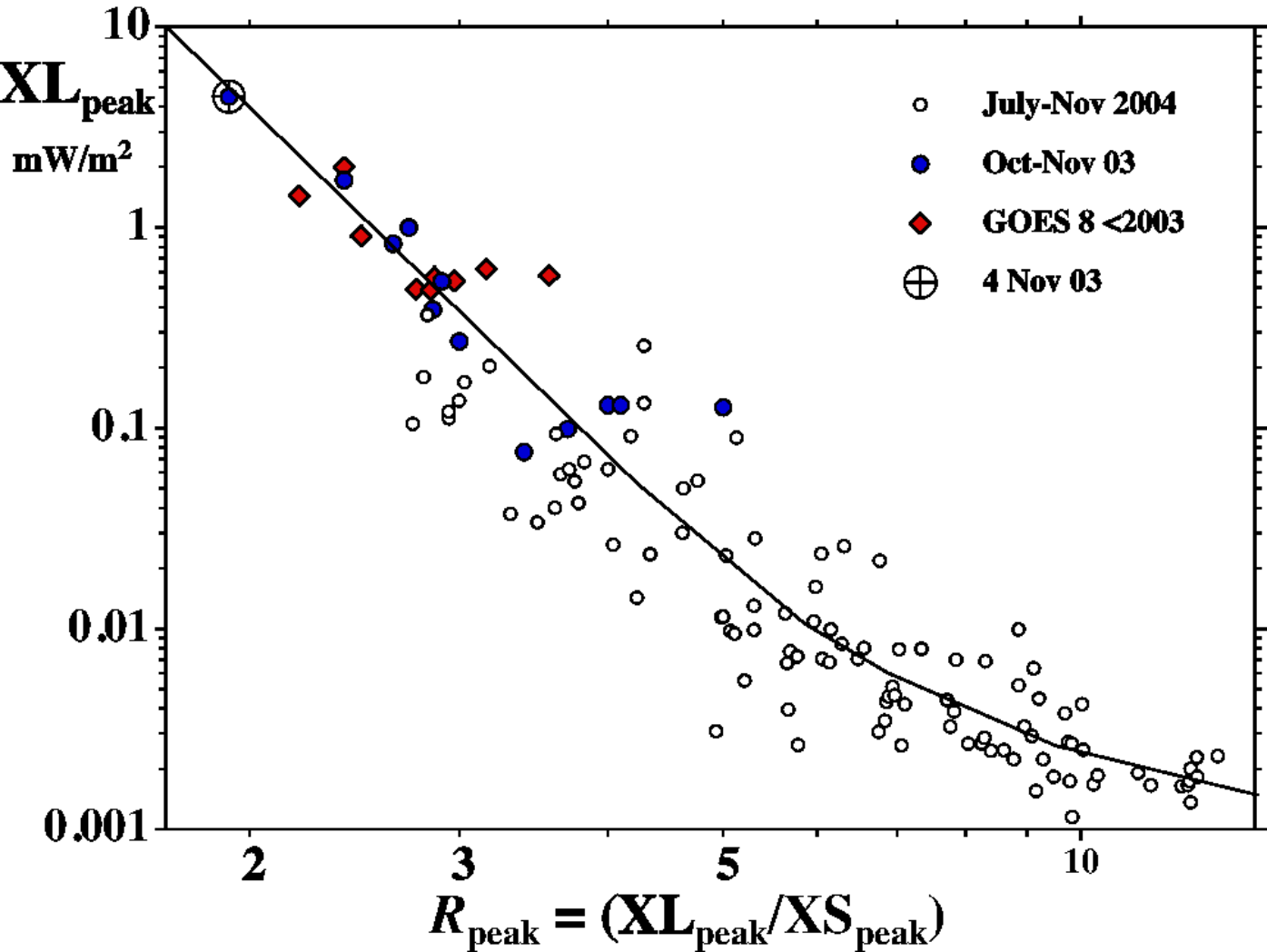
10
1
0.1
0.01
0.001
XL$_{peak}$
mW/m^2
July-Nov 2004
Oct-Nov 03
GOES 8 <2003
4 Nov 03
2
3
5
10
R_{peak} = (XL$_{peak}$/XS$_{peak}$)

Large Solar Flares and their Ionospheric D-region Enhancements

Neil R. Thomson and Craig J. Rodger
Physics Department, University of Otago, Dunedin, New Zealand

Mark A. Clilverd
Physical Sciences Division, British Antarctic Survey, Cambridge, UK

On 4 November 2003, the largest solar flare ever recorded saturated the GOES satellite X–ray detectors making an assessment of its size difficult. However, VLF radio phase advances effectively recorded the lowering of the VLF reflection height and hence lowest edge of the Earth's ionosphere. Previously these phase advances were used to extrapolate the GOES 0.1-0.8 nm ('XL') fluxes from saturation at X17 to give a peak magnitude of X45±5 for this great flare. Here it is shown that a similar extrapolation, but using the other GOES X–ray band, 0.05-0.4 nm ('XS'), is also consistent with a magnitude of X45. Also reported here are VLF phase measurements from two paths near dawn: 'Omega Australia' to Dunedin, NZ, (only just all sunlit) and NPM, Hawaii, to Ny Alesund, Svalbard (only partly sunlit) which also give remarkably good extrapolations of the flare flux, suggesting that VLF paths monitoring flares do not necessarily need to be in full daylight. D-region electron densities are modeled as functions of X-ray flux up to the level of the great X45 flare by using flare-induced VLF amplitudes together with the VLF phase changes. During this great flare, the 'Wait' reflection height, *H'*, was found to have been lowered to ~53 km, or ~17 km below the normal mid-day value of ~70 km. Finally, XL/XS ratios are examined during some large flares including the great flare. Plots of such ratios against XL can give quite good estimates of the great flare's size (X45), but without use of VLF measurements.

1. Introduction

During solar flares the X-ray flux received at the Earth increases dramatically, often within a few minutes, and then decays again in times ranging from a few tens of minutes to several hours (http://sec.noaa.gov/Data/goes.html). These X-rays have major effects in the Earth's upper atmosphere but are absorbed before they reach the ground. X-ray detectors on the GOES satellites have been recording the fluxes from solar flares since about 1976. However, during the very largest flares, such as the great flare of 4 November 2003, the GOES detectors saturate thus resulting in considerable uncertainty in the peak X-ray flux.

VLF (Very Low Frequency) radio waves (3-30 kHz) typically propagate with good signal-to-noise ratio over ranges up to 10-15 Mm or more in the Earth-ionosphere waveguide, bounded above by the D-region and below by the Earth's surface [e.g., *Watt*, 1967]. By day, the propagation paths are largely stable and the received phases are reproducible, in quiet conditions away from dawn and dusk, to a very few microseconds or better than about 10 degrees [e.g., *Watt*, 1967; *McRae and Thomson*, 2000; 2004]. However, when a solar flare occurs (on a sunlit path), the extra ionization generated by the X-rays lowers the effective reflection height of the ionosphere and advances the phase at the receiver by an amount that depends on the intensity of the X-ray flux [e.g., *Mitra*, 1974]. For daytime solar flares, both the height lowering and the phase advance (at least for path lengths greater than a few Mm) have been found to be nearly proportional to the logarithm of the X-ray flux [*McRae and Thomson*, 2004] up to at least the level of an X5 flare which lowered the effective reflection height from about 70 km (mid-day) to about 58 km [*McRae and Thomson*, 2004].

These D-region flare-induced ionospheric changes show no saturation effects thus allowing measurements of the received VLF phase changes to be used to extrapolate the GOES X-ray fluxes beyond saturation to the peak of the great flare. *Thomson et al.* [2004] used this technique on the GOES fluxes in the band 0.1-0.8 nm together with the daytime VLF paths across the Pacific to Dunedin, NZ, from the transmitters NLK (Seattle, 24.8 kHz), NPM (Hawaii, 21.4 kHz), and NDK (North Dakota, 25.2 kHz). They found that this technique gave a magnitude of X45±5 (4.5±0.5 mW/m^2 in the 0.1-0.8 nm band) for the great flare as compared with the value of X28 (2.8 mW/m^2 in the 0.1-0.8 nm band) estimated by NOAA's Space Environment Center (SEC) (http://sec.noaa.gov/weekly/pdf2003/prf1471.pdf).

The two previously largest flares were both about X20 (2.0 mW/m^2 in the 0.1-0.8 nm band), occurring on 16 August 1989 and 2 April 2001. Flares smaller than X1 (0.1 mW/m^2 in the 0.1-0.8 nm band) are designated in the ranges M1.0-M9.9 or C1.0-C9.9 when their 0.1-0.8 nm band fluxes are in the ranges 10-99 μW/m^2 and 1-9.9 μW/m^2, respectively (http://sec.noaa.gov/weekly/Usr_guide.pdf). Generally the ionospheric VLF phase technique is sensitive down to about C1 (1 μW/m^2) [e.g., *McRae and Thomson,* 2004] or about 1/4500 of the flux of the great flare of 4 November 2003. Below this C1 X-ray flux level (i.e., during normal quiet times), the D-region is maintained by day mainly by Lyman-α radiation (121.6 nm) from the Sun ionizing the minor neutral constituent, nitric oxide (in contrast with the flare X-rays which ionize all constituents, including N_2 and O_2) [e.g., *Banks and Kockarts,* 1973].

The GOES satellites record the X-ray fluxes in two wavelength bands: (1) 0.1-0.8 nm, referred to as 'long' or 'XL', and (2) 0.05-0.4 nm, referred to as 'short' or 'XS'. The 'long' band has the greater fluxes and is, as explained above, used in the usual C, M, X flare designations. The 'short' band fluxes are more penetrating and so are more representative of the wavelengths doing the ionizing at the bottom edge of the D-region during a large flare [e.g., *Banks and Kockarts,* 1973]. The XL/XS power ratio varies from around 20-40 at the C1 level down to around 2-3 for the largest flares. This is discussed in more detail in section 5. In the present day GOES satellites (GOES 10 and 12), the 'XL' fluxes saturate at about X17 (1.7 mW/m^2) whereas the 'XS' fluxes saturate just below 0.5 mW/m^2 which typically corresponds to flare sizes of around X8-X12.

In section 2, the use of VLF phase perturbations is extended to extrapolate the 'XS' 0.05-0.4 nm X-ray flux during the great flare, beyond saturation to its peak. By making a reasonable estimate for the XL/XS ratio at the peak, the peak XS flux is translated into a new estimate of peak XL flux, and thus flare magnitude. Later, in section 5, these XL/XS ratios, particularly during large flares, are further examined and found to be able to give surprisingly good estimates of (conventional) flare sizes, in particular the size of the great flare of 4 November 2003.

In section 3, we test the VLF-phase extrapolation technique on VLF paths with higher solar zenith angles (i.e., with the Sun nearer the horizon) to potentially considerably increase the number of suitable VLF observing paths for extrapolating the X-ray fluxes of very large flares.

In section 4, we extend the work of *McRae and Thomson* [2004] who reported H' and β values (measures of the D-region reflection height and 'sharpness' respectively) as functions of X-ray flux from around C1-C2 up to about X5. The VLF amplitudes and phases of three new large flares (X10, X20, and X45) are analyzed here to extend this range of D-region electron density parameters by a further factor of nearly 10 in X-ray flux.

2. X-ray Flux Extrapolation using VLF Phase Records

Figure 1 shows the VLF radio propagation paths used in this study, in particular, the 12.3 Mm path across the sunlit Pacific Ocean to Dunedin, New Zealand from the 24.8 kHz US Navy transmitter, NLK, in Seattle.

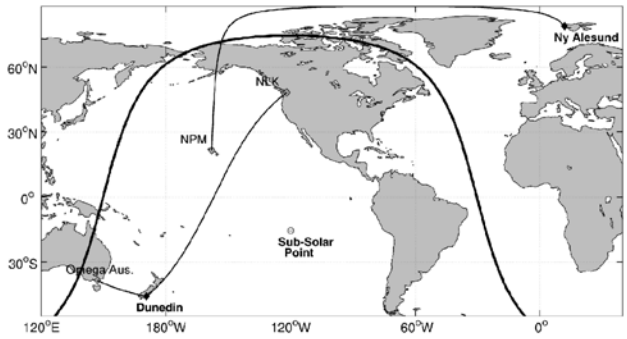

Figure 1. The VLF radio propagation paths used here together with the day-night terminator (bold line).

Figure 2 [*Thomson et al.,* 2004] shows the 0.1-0.8 nm flux (right hand axis, log scale) as a function of time during the great flare of 4 November 2003. Also shown are the accompanying phase variations of NLK received at Dunedin. The two curves were superposed by linearly scaling the phase, with an appropriate constant factor, and offsetting the phase by another appropriate constant factor.

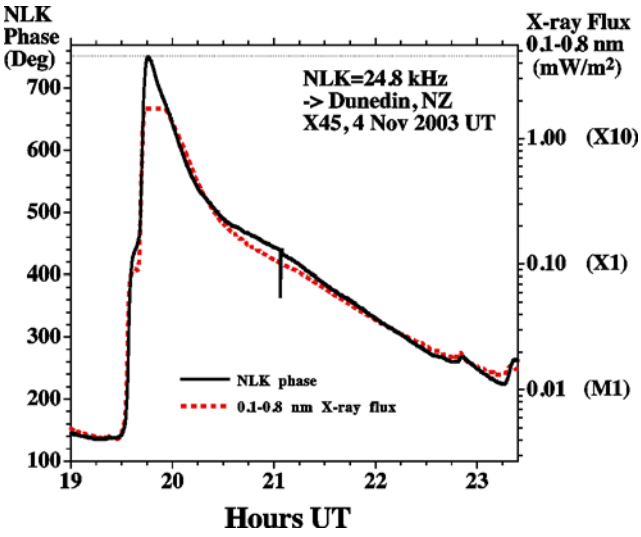

Figure 2. The phase of NLK, Seattle, as received at Dunedin, NZ, during the great flare on 4 November 2003, superposed on the XL (0.1-0.8 nm) GOES X-ray flux.

The phases were recorded with AbsPAL receivers which are similar to OmniPAL VLF data loggers [*Dowden et al.*, 1998] but modified so that they lock to GPS 1-second pulses [*Bahr et al.*, 2000]. The 3-second resolution X-ray data in figure 2 have been scaled in amplitude to match the 1-minute data on the NOAA-SEC web site, and thus the standard (C,M,X) X-ray flare magnitudes.

The VLF phase in Figure 2 can be seen to track the GOES 0.1-0.8 nm X-ray flux up until the X-ray detector goes into saturation at about X17. Assuming the phase continues to track the (unavailable) XL flux beyond saturation, the peak flux is 4.5±0.5 mW/m^2 or X45±5 as found by *Thomson et al.* [2004] who also found very similar results (including a peak around X45) using the Dunedin recorded phases of NPM

(Hawaii, 8.1 Mm, 21.4 kHz) and NDK (North Dakota, 13.5 Mm, 25.2 kHz) to extrapolate the GOES 0.1-0.8 nm X-ray flux.

Figure 3 is similar to Figure 2, except that the VLF phase (NLK to Dunedin) is now fitted to the 'short' or 'XS' band X-ray flux (0.05-0.4 nm). As can be seen, the phase again tracks the XS flux well, enabling the flux to be extrapolated from

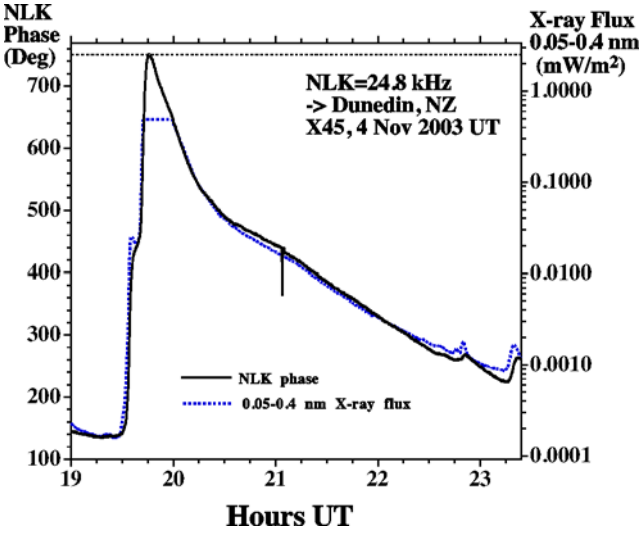

Figure 3. Similar to Figure 2 except that the *XS* band (0.05-0.4 nm) GOES X-ray flux is compared with the VLF phase of NLK, Seattle, as received in Dunedin, NZ.

saturation (about 0.49 mW/m^2) up to the peak which can thus be seen to be about 2.45 mW/m^2 (with an error of about ±0.3 mW/m^2). X-ray flux in this XS band is likely to be doing the bulk of the ionizing in the enhanced lower D–region, at altitudes of 40-70 km [e.g., *Banks and Kockarts*, 1973]. Although there is more energy in the XL band (0.1-0.8 nm), these longer wavelength X–rays do not penetrate so far into the atmosphere.

It is interesting to explore how the ratio of 'long' X-ray flux to 'short' X-ray flux (i.e., XL/XS) varies during the flare. In Figure 4 this XL/XS ratio is plotted against the 'long' band flux, XL. The ('open' circle) data points are from the 3–s X–ray fluxes from NOAA-SEC (scaled in size to match their standard 1-min values). As the flare rises towards its maximum the XL/XS ratio reduces, moving up the lower trace; the XL/XS ratio is lower (i.e., the flux is harder) while the flare fluxes are rising (for given values of XL) as compared with when the flare is decaying.

The cusp on the rising trace at about the X1 level (0.1 mW/m^2) corresponds to where the fluxes happen to briefly plateau, for this particular flare (see Figures 2 and 3), during their otherwise rapid rises. The near 90-degree change of direction of the data points as the flare rises past about X10 (1 mW/m^2) is due to first the XS flux saturating and then, around X17, the XL flux saturating too. When both fluxes come out of saturation, the XL/XS ratio moves down the upper trace as the flare decays.

The dashed line around the peak of the flare is a likely extrapolation of the XL/XS ratio beyond saturation. In making this extrapolation the following (reasonably probable)

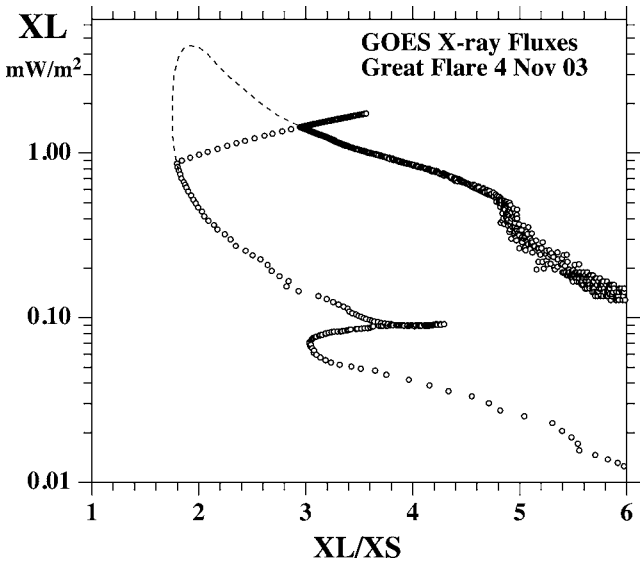

Figure 4. The 'long' band (0.1-0.8 nm) X-ray flux, XL, plotted against the XL/XS ratio, where XS is the 'short' band (0.05-0.4 nm) X-ray Flux, from GOES 12 near the peak of the great flare on 4 November 2003. Time increases clockwise around the plot, starting in the lower right corner.

constraints were used as guides: (1) the slope of the XL/XS versus XL plot should not change suddenly and (2) the general appearance/shape of the XL/XS ratio near the peak should be similar to that for other large flares (as displayed in section 5). Although the peak value of XL is shown (tentatively) at X45 in Figure 4, it would make little difference to the resulting value of the XL/XS ratio at the XL peak if this peak value were anywhere in the range X20-X50. Thus it can be seen that a reasonable estimate of the XL/XS ratio at the peak of the great flare is about 1.92 ± 0.1. However, this ratio, when combined with the 'short' flux peak value of 2.45 mW/m^2 as extrapolated in Figure 3, gives XL = 1.92 x 2.45 = 4.7 mW/m^2 or a magnitude of X47±8 (after allowing for uncertainty in both the XS peak flux and the XL/XS ratio at the peak). This indirect estimate of X47 is reasonably consistent with the more direct (VLF phase-guided, 'long' flux) extrapolation of X45±5 made by *Thomson et al*. [2004].

3. VLF Phase near Dawn/Dusk and X-ray Flux Extrapolation

The original VLF phase extrapolations of the great flare's (long band) X-ray flux, which gave the peak as X45, used VLF paths from Hawaii, Seattle and North Dakota to New Zealand for which the maximum solar zenith angle was about 65 degrees while the average solar zenith angle was about 40-50 degrees, meaning the paths were well sunlit with the Sun averaging 40-50 degrees above the horizon.

The question arises as to whether it is necessary for the Sun to be so high in the sky in order to get a satisfactory VLF phase extrapolation (in cases where the X-ray flux detectors saturate). Not surprisingly solar zenith angle does affect VLF phase and this occurs progressively with changing daytime solar zenith angle; it is not simply a matter of being either day or night [*McRae and Thomson*, 2000 and 2004]. However,

although the effects on the D-region of the ionosphere and hence the changes in VLF phase become smaller for flares at high solar zenith angles (since the X-rays have to travel obliquely and thus further through the atmosphere to penetrate to and ionize at a given height), the effects seem likely to be *proportionately* smaller.

For example, if the solar zenith angle were sufficiently great that the VLF phase change for the X-ray flux increasing from (say) 4 $\mu W/m^2$ to 1.7 mW/m^2 (i.e., GOES detector saturation) was half that for (nearly) overhead Sun, then it seems likely that the VLF phase change from the GOES saturation level to the peak flux (say 4.5 mW/m^2) would also be half that for (nearly) overhead Sun. This would be in line with the observations of *McRae and Thomson* [2004] who found that the VLF phase perturbations were fairly closely proportional to the logarithm of the X-ray flux at least up to about X5 (0.5 mW/m^2 in the usual 0.1-0.8 nm band). However, their results applied for solar zenith angles less than about 60-70 degrees and fluxes up to X5.

An opportunity to test VLF paths with higher solar zenith angles arises with the 2.2 Mm 'Omega Australia' (13 kHz, 38.5° S, 146.9° E) to Dunedin, NZ, path for which the solar zenith angles were in a range of about 64-82 degrees near the time of the great flare peak (1945 UT, 4 November 2003). This is shown in figure 5 where the extrapolation again comes out close to X45 thus suggesting that such high solar zenith angle paths can give good results. The transmitter referred to

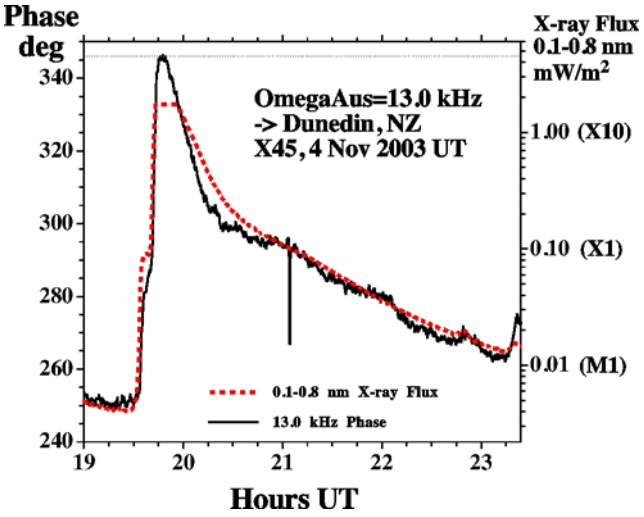

Figure 5. Extrapolation of the great flare X-ray flux using the phase of 'Omega Australia' at Dunedin near dawn.

here as 'Omega Australia' is the transmitter that used to be the real Omega Australia until 30 September 1997. In 2003 it was using 100 baud MSK on a fixed frequency of 13 kHz rather than the old Omega pulse sequence. Unfortunately it was no longer as phase stable as the real Omega transmitters were. However, this does not seem to be a problem because the phase drift is fairly constant (about 46 degrees per hour) and this has been largely removed before Figure 5 was plotted.

It now seems appropriate to test if VLF phase extrapolation at still higher solar zenith angles might give useful, though possibly more approximate, results even when part of the path is in darkness. An OmniPAL receiver in Ny Alesund, Svalbard, recorded the phase of NPM, Hawaii, at the time of the great flare. About one third of the nearly 9 Mm path was in darkness at the receiver end. A superposed plot of the long band X-ray flux and the NPM phase is shown in Figure 6. It can be seen that, even for this day-night path, the VLF phase fit and extrapolation is quite good. Certainly the flare size would come out at X50±10 rather than X45 but this is only a ~10% difference for this very inhomogeneous path. From Figure 6 it can be seen that the NPM VLF phase changes are about 70 degrees per decade of X-ray flux change for this partly sunlit, 9 Mm, high solar zenith angle path. In contrast, for the fully sunlit, lower solar zenith angle, 8 Mm, NPM to Dunedin path, the VLF phase changes were about twice as large, at 130 degrees per decade of X-ray flux change [*Thomson et al.*, 2004]. These phase changes are none-the-less both proportional to the corresponding (logarithms of their) X-ray flux changes.

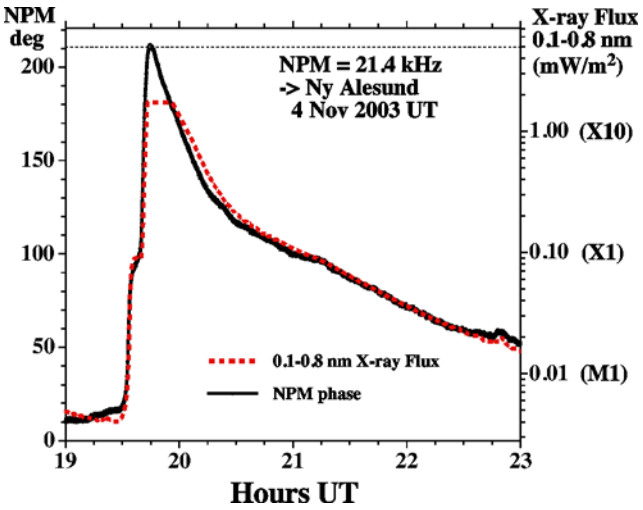

Figure 6. Extrapolation of the great flare X-ray flux using the phase of NPM, Hawaii, at Ny Alesund, Spitzbergen (with about 1/3 of the path in darkness).

For this path the NPM phase is stable but the OmniPAL receiver phase was drifting about 76 degrees/hour when averaged over a few days. In Figure 6, a correction of just 70 degrees/hour has been applied to get the best fits before and after the flare. This difference between 70 and 76 degrees/hour is partly due to changing solar zenith angle during the flare and partly to measurement uncertainty.

While a highly inhomogeneous day-night VLF path such as NPM to Ny Alesund gives only marginally satisfactory results on extrapolation, it is none-the-less interesting that they are so close to acceptable. This tends to imply that the relatively minor inhomogeneities in an all-day path, even at quite high solar zenith angles, are unlikely to detract significantly from the accuracy of VLF-phase-guided X-ray flux extrapolations.

The nearly satisfactory extrapolation results from the day-night NPM-Ny Alesund path do not imply that all day-night paths will give similarly useful results. Because of the near polar location of Ny Alesund (latitude ~79° N) and the time of the flare, the sunrise/sunset terminator was moving rather slowly (less than about 0.2 Mm/hour) along this path.

In contrast, for the nearly 6 Mm day-night path from NWC (19.8 kHz, North West Cape of Australia) to Dunedin, the terminator was moving nearly 1.3 Mm/hour during the flare, and so the day-night phase changes are comparable or greater than the flare induced phase changes. Also, the day-night phase changes during a large flare can be expected to be significantly different from those in unperturbed conditions, because of the much lower D-region heights (and hence different mode conversions), and thus a useful separation of the flare effects from the day-night effects would be difficult.

4. D-region Electron Density Parameters as a Function of Solar X-ray Flux

The X-rays from solar flares ionize the neutral atmosphere at D-region heights (40-90 km) greatly increasing the electron densities there and thus markedly lowering the effective VLF reflection height. This lowering of the reflection height is the principal cause of the VLF phase advances observed during flares. However, the electron density profile at the lower edge of the D-region also 'sharpens' during flares in the sense that the rate of increase of electron density with height increases, and this also effects the VLF phase and amplitude at the receiver [eg *Thomson and Clilverd*, 2001 ; *McRae and Thomson*, 2004].

The VLF signals used here propagate in the Earth-ionosphere waveguide which is bounded below by the Earth (typically ocean) and above by the D-region. We model this using the NOSC (Naval Ocean Systems Center, San Diego, USA) computer programs (MODESRCH, MODEFINDER, LWPC – long wave propagation capability) which take the input path parameters, calculate appropriate full-wave reflection coefficients for the waveguide boundaries, and then search for those modal angles which give a phase change of 2π across the guide, taking into account the curvature of the Earth [e.g. *Morfitt and Shellman*, 1976]. These NOSC programs can take arbitrary electron density profiles supplied by the user to describe the D-region profile and thus the ceiling of the waveguide. However, for accurately predicting (or explaining) VLF amplitudes and phases, this approach effectively involves too many variables to be manageable in our present state of knowledge of the D-region. We thus follow the work of the NOSC group by characterizing the D-region with a Wait ionosphere defined by just two parameters, the 'reflection height', H', in km, and the exponential sharpness factor, β, in km^{-1} [*Wait and Spies*, 1964]. This has been found to give very satisfactory results for normal daytime propagation over a good range of solar zenith angles [*Thomson*, 1993; *McRae and Thomson*, 2000] and for solar flares up to about X5 [*Thomson and Clilverd*, 2001; *McRae and Thomson*, 2004]. Here we extend the flare-time VLF phase and amplitude results of *McRae and Thomson* [2004] by nearly a factor of ten in X-ray flux up to the X45 level of the great flare of 4 November 2003.

4.1 VLF Amplitude Changes during the Great Flare

Figure 7 shows the amplitude (left-hand ordinate) of the 24.8 kHz VLF signal recorded at Dunedin, NZ, during the great flare of 4 November 2003. Also plotted, for comparison, is the 'long' (0.1-0.8 nm) GOES-12 X-ray flux (right-hand ordinate). The contrast with the phase plot for the same period in Figure 2 is evident. The phase varies very nearly proportionately with

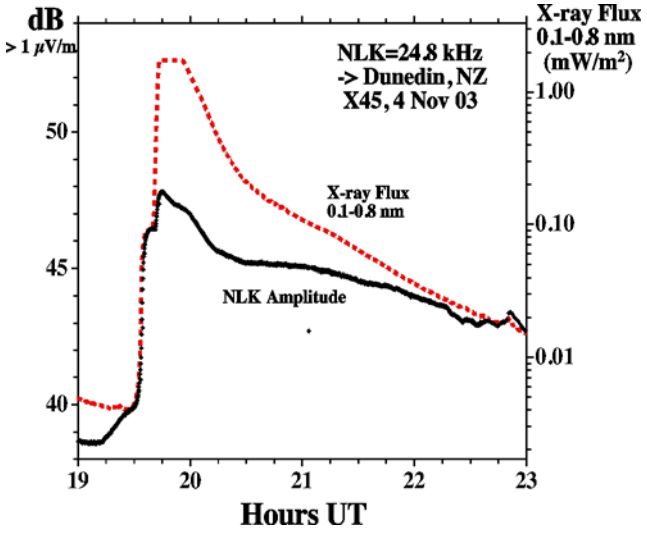

Figure 7. Amplitude of NLK, Seattle, recorded at Dunedin, NZ, together with the GOES X-ray flux during the great flare.

the (logarithm of the) X-ray flux while the amplitude does not. Thus the phase is useful and convenient for extrapolating the X-ray flux when the GOES detectors saturate but the amplitude is not. None-the-less, these flare-time VLF amplitudes and their accompanying phase perturbations readily allow the determination of β and H' at the peak of the flare, as described below.

4.2 Flare Induced VLF Amplitude and Phase Changes up to X45

Figure 8 shows the VLF phase and amplitude perturbations for the NLK to Dunedin path for three recent very large flares as well as the flares (all ≤X5) previously reported by *McRae and Thomson* [2004]. The three new very large flares shown are the X20 of 2 April 01, the X10 of 29 Oct 03, and the great flare of 4 Nov 03. Other recent very large flares such as the X17.2 of 28 Oct 03 and the X14.4 of 15 Apr 01 were not suitably timed for daylight VLF paths for our receivers in Dunedin, NZ.

Special care has been required in establishing and plotting the phase changes for the very large flares in Figure 8, as opposed to the smaller flares. Typically before the smaller flares and away from solar maximum, where the ≤X5 flares were recorded, the X-ray flux preceding the flare is (appreciably) less than the C1 level. In these conditions the pre-flare D-region is maintained principally by Lyman–α and so is at a standard unperturbed 'base' level. The phase changes observed and calculated are thus between this fairly standard unperturbed level [see *McRae and Thomson*, 2004, for details] and the flare peak. However, for flares occurring during periods of high solar activity, such as the very large flares reported here, the pre-flare X-ray flux is normally appreciably greater than C1 and so needs to be taken into account. For example, for the great flare, the pre-flare flux was about C4, and so the observed phase change ('C4-to-peak') needed to be increased by the (small) expected 'unperturbed-to-C4' phase change (from the left-hand side of the phase plot in Figure 8) before plotting the great flare (on the right-hand side of this plot) in Figure 8.

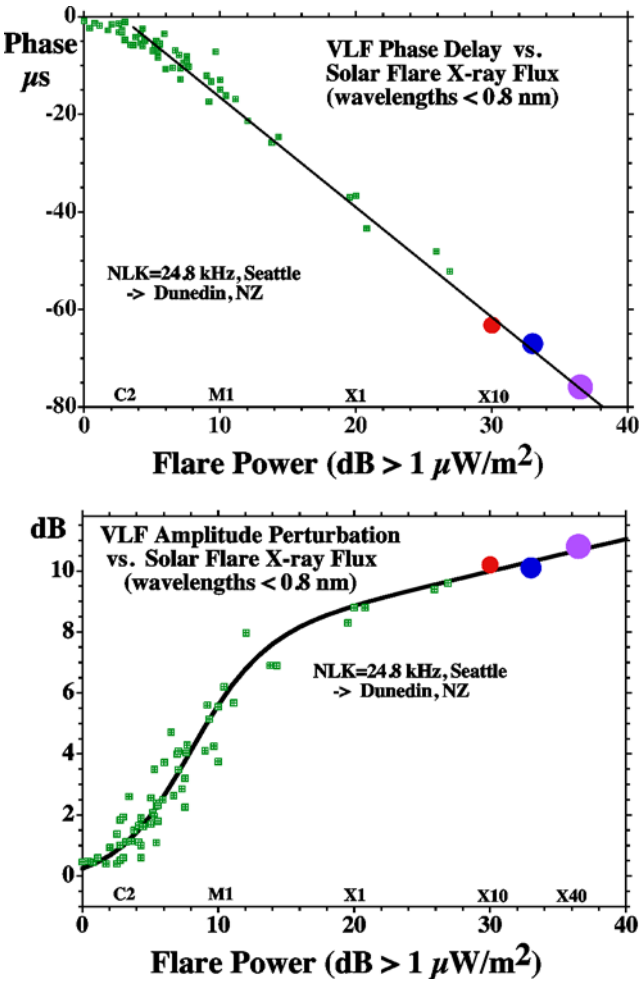

Figure 8. Phase delay perturbations and received VLF amplitude versus peak X-ray flux.

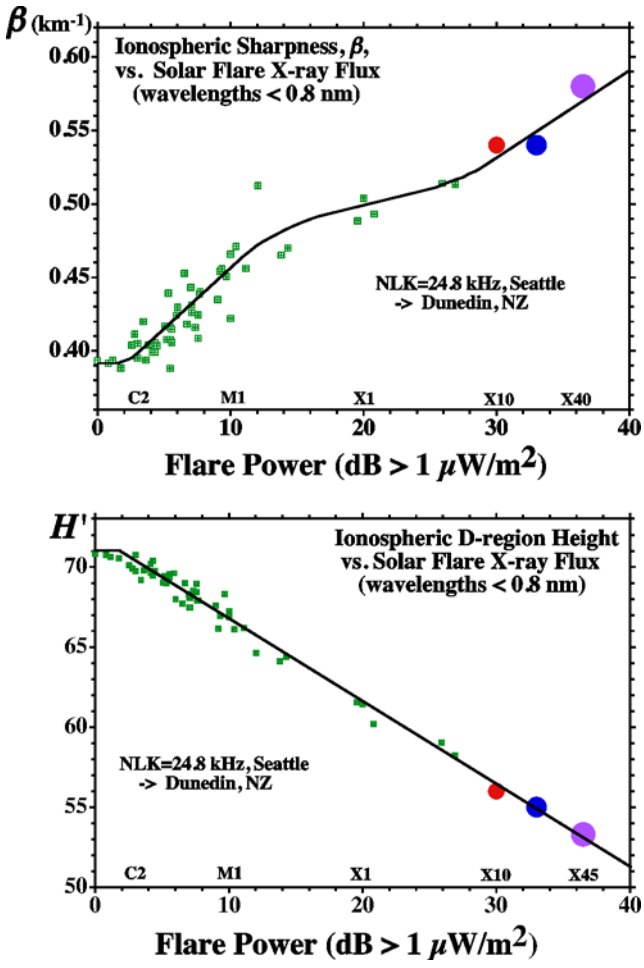

Figure 9. Ionospheric D-region sharpness, β, and height, H', as functions of peak solar flare power.

As can be seen in Figure 8, the phase trend evident in the previous work [*McRae and Thomson*, 2004] continues (for a further factor of ~10 in flare power). However, the amplitude increase, in the lower panel of Figure 8, at high flare powers, does not fully flatten off for flare sizes >X5 as had previously been indicated [*McRae and Thomson*, 2004], but continues to rise slowly.

4.3 Flare Induced β and H' up to X45

Figure 9 shows plots of the values of β and H' required for MODEFINDER to calculate the observed (as shown in figure 8) absolute amplitudes at the flare peaks and the observed (as shown in Figure 8) phase changes at the flare peaks. Although the process of finding β and H' using MODEFINDER has an element of trial and error, the process is none-the-less fairly fast and straightforward. As is found from MODEFINDER, the phase changes are monotonic in H', and much more dependent on H' than β, while the amplitude changes are typically more dependent on β than H'. This makes it possible to iteratively and quickly find values of β and H' which cause MODEFINDER to output the observed amplitudes and the observed phase changes. The key to this is starting with appropriate values of β and H' for the unperturbed D-region. These are now fairly well established [e.g., *Thomson*, 1993; *McRae and Thomson*, 2004] and, when these are used as the starting points here, the resulting searches for the flare-time values of β and H' prove to be fast (few iterations), stable and unique.

As can be seen in the lower panel of Figure 9, the nearly linear reduction of H' with (the logarithm of the) flare flux (0.1-0.8 nm) continues from the upper limit of X5 in the previous study [*McRae and Thomson*, 2004] to at least the X45 of the great flare in the present study. However, in the upper panel of Figure 9 it can be seen that, although β levels off to a significant degree around X1-X5 as in the previous study, it then starts to rise again with increasing flare power for the very large flares (>>X5).

β increasing with flare power at low flare powers, and the (near) flattening off of β around the X1 flux level are still likely to be caused, as previously suggested [*Thomson and Clilverd*, 2001], by these X-ray fluxes becoming thoroughly dominant over both cosmic rays and Lyman-α as the ionizing source in the D-region, under these conditions. If Lyman-α were the sole source of ionization in the unperturbed D-region then the unperturbed profile slope would be similar to that when X-rays dominate. However, in the real unperturbed D-region, galactic cosmic rays make additional ionization mainly in the lowest parts [*Rishbeth and Garriott*, 1969] so that the unperturbed electron density falls with decreasing height at a

rate which is slower than for Lyman-α (or X-rays) alone. Such normal unperturbed profiles, in which the electron density increases relatively slowly with height, result in relatively low values of β when modeling using β and H'.

The discussion in the last paragraph provides an explanation of why β increases with increasing flare power until the effects of the X-ray flux swamp the effects of the galactic cosmic rays (and the Lyman-α) at which point β would be expected to increase no further and thus appear 'saturated'. It is suggested that the fact that β is observed to increase further for very large flares may be due to there being little X-ray flux at wavelengths shorter than about 0.05 nm (the lower wavelength limit of the 'short' GOES band). Only wavelengths shorter than this could penetrate significantly below a height of about 50 km and their absence would result in extremely low electron densities in these lowest parts of the VLF reflection region.

4.4 Flare Time Electron Density Comparisons

Wait and Spies [1964] defined a height dependent conductivity parameter:

$$\omega_r(z) = \omega_0^2(z)/\nu(z) = 2.5 \times 10^5 \exp[\beta(z-H')]$$

where $\omega_0(z)$ is the (angular) electron plasma frequency and $\nu(z)$ is the effective electron-neutral collision frequency, both being functions of the altitude, z, in km. This assumes $\omega_r(z)$ varies exponentially with height at a rate determined by the constant, β (in km^{-1}). H' is the height (in km) at which $\omega_r(z) = 2.5 \times 10^5$ s^{-1} and is often used as a convenient measure of the 'height' of the D-region. The collision frequency depends on the neutral air density which decreases (approximately) exponentially with height. A reasonable expression for the collision frequency, as used in LWPC and MODEFINDER is

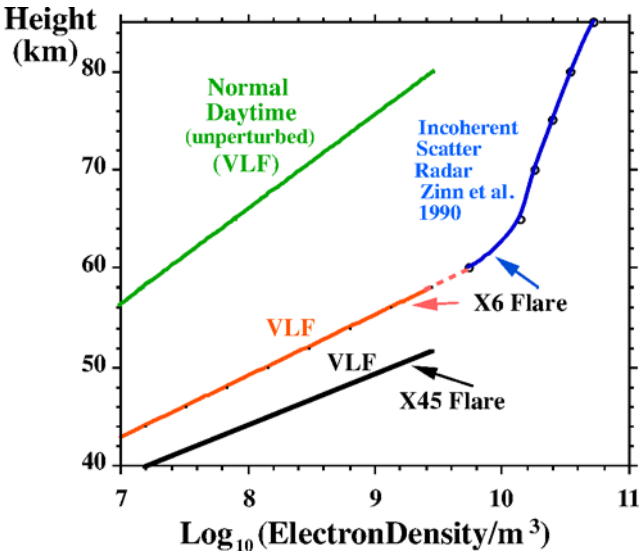

Figure 10. VLF-determined electron densities during the great X45 flare of 4 November 2003 compared with normal unperturbed electron densities. Also shown are electron densities from an incoherent scatter radar during an X6 flare and those predicted from VLF observations.

$\nu(z) = 1.82 \times 10^{11} \exp(-0.15z)$ [*Morfitt and Shellman*, 1976]. The (angular) plasma frequency is related to the electron density by $\omega_0^2(z) = N(z)e^2/(\varepsilon_0 m) \approx 3180\ N(z)$. Hence the electron density increases exponentially with height in the D-region as

$$N(z) = 1.43 \times 10^{13} \exp(-0.15H') \exp[(\beta - 0.15)(z - H')].$$

In Figure 10 are plotted the electron densities for (1) a typical unperturbed mid-solar cycle day ($\beta = 0.39$ km^{-1}, $H' = 71$ km [*McRae and Thomson*, 2004]), (2) an X6 flare as determined by *Zinn et al.* [1990] from a set of incoherent scatter observations, (3) an X6 flare from the H' and β values determined from VLF measurements as in Figure 9 [*McRae and Thomson*, 2004], and (4) the great X45 flare of 4 November 2003.

4.5 A Possible Extrapolation to Even Larger Flares

Figure 11 is essentially the same H' versus solar flare X-ray flux plot as in the lower panel of Figure 9 except that the best fit line has been extrapolated to very much larger solar X-ray fluxes than have ever been recorded. This illustrates just how well our atmosphere protects us on the Earth's surface from the X-ray bursts of extremely large flares. Even if a flare were so large that the 0.1-0.8 nm solar X-ray flux reached the level of the total current output of the Sun (i.e., the solar constant, ~1400 W/m^2), the lower edge of the ionosphere, and hence the height of extinction of the X-rays would still be greater than 20 km.

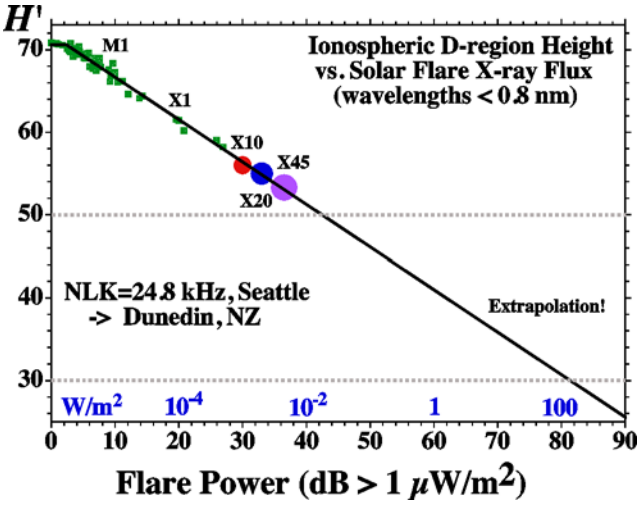

Figure 11. Same as lower panel of Figure 9 except extrapolated to much higher flare magnitudes.

5. Long/Short (XL/XS) X-ray Flux Ratios during Flares

As shown in Figure 4 and discussed in Section 2, the ratio of the 'long' X-ray flux to the 'short' X-ray flux, or XL/XS ratio, varies during the flare reaching a minimum near the flare flux peak. Similar such XL versus XL/XS plots are shown for a number of large flares in Figure 12. Five of the flares come from the same very active period, 20 October 2003 – 5 November 2003, as the great flare of 4 November 2003. They

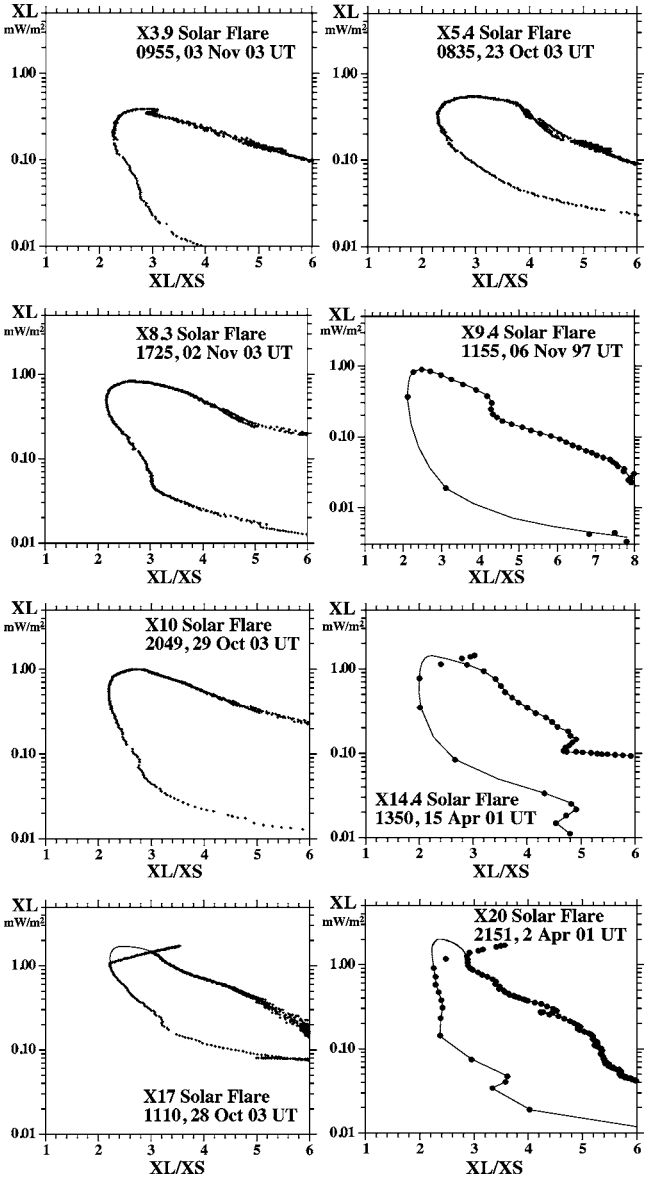

Figure 12. As in Figure 4, XL and XS are the 'long' and 'short' band X-ray fluxes. Again, XL is plotted against the ratio XL/XS. GOES 12 has been used for the five flares from 2003, and GOES 8 for the three earlier flares. Time again increases clockwise around each plot.

include the X17 flare of 28 October 2003 and the X10 flare of 29 October 2003 which are the 4th and 10th largest flares ever recorded by the GOES satellites (since 1976). Also included in this period are an X8.3, an X5.4, and an X3.9. They have been included partly because of their large sizes, partly because 3-second resolution data was available and partly because they were recorded on the GOES 12 satellite which is designated by NOAA-SEC as the current primary satellite and was the satellite used as the calibration source by *Thomson et al.* [2004] for their ionospherically estimated X45 determination.

Also shown in Figure 12 are the XL/XS ratios plotted against XL for the X20 flare of 2 April 2001, the X14 flare of 15 April 2001, and the X9.4 flare of 6 November 1997. For these three

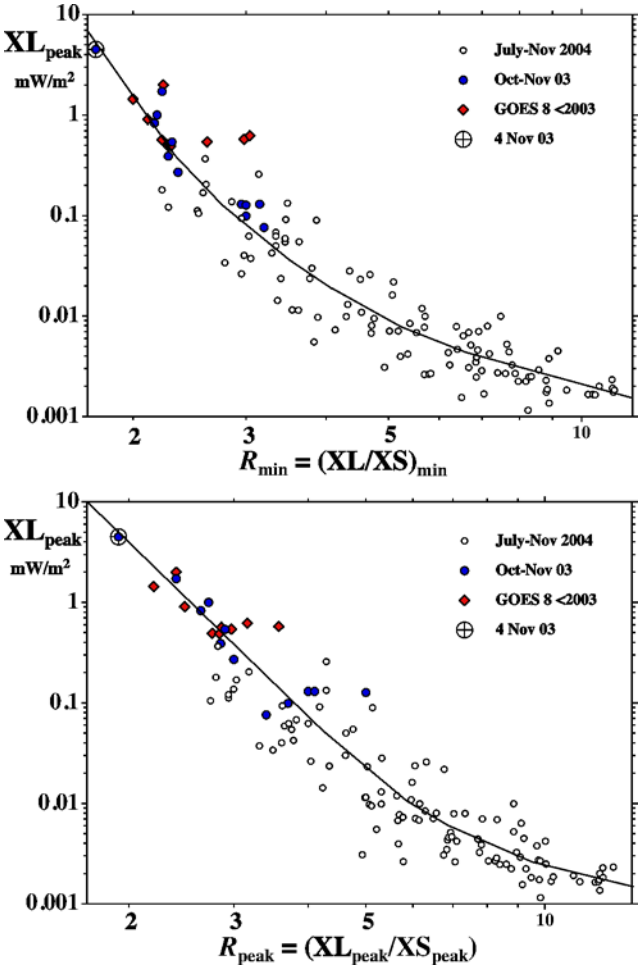

Figure 13. The peak 'long' band X-ray flux, XL_{peak}, plotted against (a) the minimum value of XL/XS near the flare peak and (b) the value of XL/XS at the flare peak.

flares the data comes from the GOES 8 satellite at 1-minute resolution.

In all cases the XL/XS ratios are lower for the rising flare fluxes than for the falling fluxes, just as for the great flare in Figure 4. As can be seen, the slopes of the XL/XS curves typically change progressively in the vicinity of the flux peaks. (For the X20, X17 and X14 flares, XS saturated near the peaks and so the curves have been extrapolated as was done for the great flare in Figure 4.) While no two flares have exactly the same XL/XS vs. XL shape, there can be seen to be some general features. The XL/XS ratio falls to a clear minimum shortly before the peak of the flare. No extrapolation is required to get this minimum for XL/XS except for the X45 and X20 flares and even then the extent of the extrapolation required is minimal.

For flares greater than about X10, extrapolation, shown by dashed or solid lines, has been needed in Figure 12 to estimate the XL/XS ratio at the peak because, as previously mentioned, XS saturates at about 0.49 mW/m^2. Obviously there is some uncertainty in the extrapolations but, as in figure 4, account has been taken of the non-saturating cases in Figure 12, including no discontinuities in the rate of change of slope near the peak. Also, in all cases except perhaps the X20 case, the peak XL values are known because XL has not saturated.

In the case of the X20 flare (2 April 2001) the XL extrapolation (from X17) is fairly minimal. Thus the XL/XS ratios at the flare peaks have likely been reasonably well estimated.

Both the minimum value of XL/XS for a flare and the XL/XS ratio at the peak are smaller the larger the flare. In Figure 13 the minimum value of the XL/XS ratio, R_{min}, and the XL/XS ratio at the (XL) peak of the flare, R_{peak}, are plotted against XL at the flare peak for some representative flares. Four plot symbols are used. The solid circles and the large X45 symbol are from 3-second GOES 12 data in the active period 22 October to 4 November 2003, plus an X1.3 flare on 27 May 2003. The open circles are from 1-minute GOES 12 data in July, October and November of 2004. The nine solid diamonds are from 1-minute GOES 8 data from 6 Nov 97 (X9), 18 Aug 98 (X5), 14 Jul 00 (X6), 2, 6 and 15 Apr 01 (X20, X5.6, X14), 28 Aug 01 and 13 Dec 01 (X5, X6), and 23 Jul 02 (X5). The solid lines are reasonable fits to the data points.

From Figure 13, it can be seen that the XL/XS ratios for both R_{min} and R_{peak} are consistent with the great flare of 4 November 2003 having a magnitude of about X45 as determined previously by *Thomson et al*. [2004] by VLF phase extrapolation of the XL flux. This XL/XS ratio consistency check is somewhat independent of the VLF ionospheric technique but has a higher uncertainty. A re-examination of the XL/XS ratio plot for the great flare in Figure 4 shows that if it had been extrapolated to only (say) X30, R_{min} would have hardly changed and so would still have indicated a magnitude of at least X45 in the R_{min} versus peak XL graph in the top panel of Figure 13.

6. Summary and Conclusions

The great solar flare of 4 November 2003 was the largest ever recorded by the X-ray detectors on the GOES satellites which have been in operation since 1976. Unfortunately the current GOES X-ray detectors saturate at about X17.4 and the great flare was markedly larger than this; so some means of extrapolation is needed to estimate its size. NOAA's Space Environment Center, who provide the GOES detectors and hence the most widely recognized international records of solar flare X-ray fluxes, arrived at an estimate of X28 for the peak by extrapolating their recorded fluxes beyond saturation. The flare X-rays create significant extra ionization in the Earth's ionosphere, particularly in the lower D-region where VLF radio waves reflect thus lowering their reflection height. It has been previously shown that the reflection height lowering and the peak VLF phase advances during flares are nearly linearly related to the logarithm of the flare's peak 'long' (0.1-0.8 nm) X-ray flux [*McRae and Thomson*, 2004]. It has also been shown [*Thomson et al.*, 2004] that the phase shifts during large flares are nearly linearly related to the VLF phase changes during the flares. This relation looks likely to apply over a very great range of solar flare X-ray fluxes (and D-region height lowering) without saturation. This has enabled the continuous, smoothly changing VLF phase to be used to extrapolate the 'long' (0.1-0.8 nm) X-ray flux from which a magnitude of X45 was obtained [*Thomson et al.*, 2004].

Because the wavelengths of the dominant ionizing X-rays at the VLF reflection height near the peak of the great flare are likely to be in the 'short' X-ray band (XS), it seemed sensible to also extrapolate this band's flux and find its peak value for the flare. This was done successfully in Figure 3, but as flare magnitudes are normally given in terms of their 'long' band peak flux (XL) a value of the XL/XS ratio at the peak was needed. This was found and used to show that this route gave a magnitude of X47±8 for the flare, consistent with the previous (long band) VLF ionospheric extrapolation.

VLF long path phase measurements can still provide very good X-ray flux extrapolation from saturation even when the Sun is quite low in the sky (8-26 degrees above the horizon). Further, quite useful extrapolation results were obtained from a completely independent receiver even though the (partly polar) path was partly in darkness (though more than 50% sunlit). However, in such a case it is important that the day/night ratio on the path is changing only very slowly during the flare.

The lowering of the D-region reflection height due to the flare X-ray fluxes was found to continue, essentially linearly, up to the X45 flux level, nearly a factor of 10 further than had previously been found up to X5. At the peak of the X45 flare, H' had lowered to a height of about 53 km, or about 17 km below typical mid-day, unperturbed conditions. The D-region sharpness parameter, β, which was previously thought to increase to saturation at about 0.52 km^{-1}, was found to increase further again up to about 0.57 km^{-1} at X45, possibly due to the X-ray flux spectrum falling off rapidly for wavelengths shorter than about 0.05 nm (the lower limit of the GOES 'short' band).

Finally the XL/XS ratios were examined for a number of flares from small to very large, and it became clear that the XL/XS ratios themselves were reasonably well defined functions of XL, and so could be used to make quite useful estimates of flare peaks (without reference to the ionosphere or VLF measurements). These XL/XS ratio plots were also found to be consistent with the great flare being at least as large as X45.

Acknowledgements. We are very grateful to NOAA's Space Environment Center, particularly to Dr Rodney Viereck, for their help and for providing not only the 1-min but also the 3-s GOES X-ray data, which made possible the (flux) calibration of our VLF phase data. We would also like to thank Mr Dave Hardisty of our institution for the design and implementation of the digital MSK multi-channel modulator/demodulator which carries our VLF signals live from our field station.

References

Bahr, J. L., J. B. Brundell, S. F. Hardman, and R. L. Dowden, Multi-instrument coincident detection of sprites, *Phys. Chem. Earth (B), 25*, 417-422, 2000.

Banks, P. M. and G. Kockarts, *Aeronomy,* Academic Press, N.Y., 1973.

Dowden, R. L., S. F. Hardman, C. J. Rodger, and J. B. Brundell, Logarithmic decay and Doppler shift of plasma associated with sprites, *J. Atmos. Sol-Terr. Phys.*, *60*, 741-753, 1998.

McRae, W. M. and N. R. Thomson, VLF phase and amplitude: daytime ionospheric parameters, *J. Atmos. Sol-Terr. Phys.*, *62*, 609-618, 2000.

McRae, W. M. and N. R. Thomson, Solar flare induced ionospheric D-region enhancements from VLF phase and amplitude observations, *J. Atmos. Sol-Terr. Phys.*, *66*, 77-87, 2004.

Mitra, A. P. *Ionospheric effects of solar flares*, D. Reidel, Dordrecht, 1974.

Morfitt D. G. and C. H. Shellman, MODESRCH, an improved computer program for obtaining ELF/VLF/LF mode constants in an Earth-Ionosphere Waveguide, Naval Electronics Laboratory Center Interim Rep. 77T, NTIS, Accession No. ADA032573, National Technical Information Service Springfield, Va. 22161, USA, 1976.

Rishbeth, H. and O. K. Garriott, *Introduction to Ionospheric Physics*, Academic Press, N.Y. and London, 1969.

Thomson, N. R., Experimental daytime VLF ionospheric parameters. *J. Atmos. Terr. Phys., 55*, 173-184, 1993.

Thomson, N. R. and M. A. Clilverd, Solar flare induced ionospheric D-region enhancements from VLF amplitude observations. *J. Atmos. Sol-Terr. Phys., 63*(16): 1729-1737, 2001.

Thomson, N. R., C. J. Rodger, and R. L. Dowden, Ionosphere gives size of greatest solar flare. *Geophys. Res. Lett.* 31(6), L06803, doi:10.1029/2003GL019345, 2004.

Watt, A. D., *VLF Radio Engineering,* Pergamon Press, Oxford, 1967.

Wait J.R. and K. P. Spies, Characteristics of the Earth-ionosphere waveguide for VLF radio waves. *NBS Tech. Note* 300, 1964.

Zinn, J., C. D. Sutherland, and S. Ganguly, The solar flare of August 18, 1979: incoherent scatter radar data and photochemical model comparisons, *J. Geophys. Res., 95* (D10), 16705-16718, 1990.

Large Solar Flares and their Ionospheric D-region Enhancements

Neil R. Thomson and Craig J. Rodger
Physics Department, University of Otago, Dunedin, New Zealand

Mark A. Clilverd
Physical Sciences Division, British Antarctic Survey, Cambridge, UK

On 4 November 2003, the largest solar flare ever recorded saturated the GOES satellite X–ray detectors making an assessment of its size difficult. However, VLF radio phase advances effectively recorded the lowering of the VLF reflection height and hence lowest edge of the Earth's ionosphere. Previously these phase advances were used to extrapolate the GOES 0.1-0.8 nm ('XL') fluxes from saturation at X17 to give a peak magnitude of X45±5 for this great flare. Here it is shown that a similar extrapolation, but using the other GOES X–ray band, 0.05-0.4 nm ('XS'), is also consistent with a magnitude of X45. Also reported here are VLF phase measurements from two paths near dawn: 'Omega Australia' to Dunedin, NZ, (only just all sunlit) and NPM, Hawaii, to Ny Alesund, Svalbard (only partly sunlit) which also give remarkably good extrapolations of the flare flux, suggesting that VLF paths monitoring flares do not necessarily need to be in full daylight. D-region electron densities are modeled as functions of X-ray flux up to the level of the great X45 flare by using flare-induced VLF amplitudes together with the VLF phase changes. During this great flare, the 'Wait' reflection height, *H'*, was found to have been lowered to ~53 km, or ~17 km below the normal mid-day value of ~70 km. Finally, XL/XS ratios are examined during some large flares including the great flare. Plots of such ratios against XL can give quite good estimates of the great flare's size (X45), but without use of VLF measurements.

1. Introduction

During solar flares the X-ray flux received at the Earth increases dramatically, often within a few minutes, and then decays again in times ranging from a few tens of minutes to several hours (http://sec.noaa.gov/Data/goes.html). These X-rays have major effects in the Earth's upper atmosphere but are absorbed before they reach the ground. X-ray detectors on the GOES satellites have been recording the fluxes from solar flares since about 1976. However, during the very largest flares, such as the great flare of 4 November 2003, the GOES detectors saturate thus resulting in considerable uncertainty in the peak X-ray flux.

VLF (Very Low Frequency) radio waves (3-30 kHz) typically propagate with good signal-to-noise ratio over ranges up to 10-15 Mm or more in the Earth-ionosphere waveguide, bounded above by the D-region and below by the Earth's surface [e.g., *Watt*, 1967]. By day, the propagation paths are largely stable and the received phases are reproducible, in quiet conditions away from dawn and dusk, to a very few microseconds or better than about 10 degrees [e.g., *Watt*, 1967; *McRae and Thomson*, 2000; 2004]. However, when a solar flare occurs (on a sunlit path), the extra ionization generated by the X-rays lowers the effective reflection height of the ionosphere and advances the phase at the receiver by an amount that depends on the intensity of the X-ray flux [e.g., *Mitra*, 1974]. For daytime solar flares, both the height lowering and the phase advance (at least for path lengths greater than a few Mm) have been found to be nearly proportional to the logarithm of the X-ray flux [*McRae and Thomson*, 2004] up to at least the level of an X5 flare which lowered the effective reflection height from about 70 km (mid-day) to about 58 km [*McRae and Thomson*, 2004].

These D-region flare-induced ionospheric changes show no saturation effects thus allowing measurements of the received VLF phase changes to be used to extrapolate the GOES X-ray fluxes beyond saturation to the peak of the great flare. *Thomson et al.* [2004] used this technique on the GOES fluxes in the band 0.1-0.8 nm together with the daytime VLF paths across the Pacific to Dunedin, NZ, from the transmitters NLK (Seattle, 24.8 kHz), NPM (Hawaii, 21.4 kHz), and NDK (North Dakota, 25.2 kHz). They found that this technique gave a magnitude of X45±5 (4.5±0.5 mW/m^2 in the 0.1-0.8 nm band) for the great flare as compared with the value of X28 (2.8 mW/m^2 in the 0.1-0.8 nm band) estimated by NOAA's Space Environment Center (SEC) (http://sec.noaa.gov/weekly/pdf2003/prf1471.pdf).

The two previously largest flares were both about X20 (2.0 mW/m^2 in the 0.1-0.8 nm band), occurring on 16 August 1989 and 2 April 2001. Flares smaller than X1 (0.1 mW/m^2 in the 0.1-0.8 nm band) are designated in the ranges M1.0-M9.9 or C1.0-C9.9 when their 0.1-0.8 nm band fluxes are in the ranges 10-99 μW/m^2 and 1-9.9 μW/m^2, respectively (http://sec.noaa.gov/weekly/Usr_guide.pdf). Generally the ionospheric VLF phase technique is sensitive down to about C1 (1 μW/m^2) [e.g., *McRae and Thomson,* 2004] or about 1/4500 of the flux of the great flare of 4 November 2003. Below this C1 X-ray flux level (i.e., during normal quiet times), the D-region is maintained by day mainly by Lyman-α radiation (121.6 nm) from the Sun ionizing the minor neutral constituent, nitric oxide (in contrast with the flare X-rays which ionize all constituents, including N_2 and O_2) [e.g., *Banks and Kockarts,* 1973].

The GOES satellites record the X-ray fluxes in two wavelength bands: (1) 0.1-0.8 nm, referred to as 'long' or 'XL', and (2) 0.05-0.4 nm, referred to as 'short' or 'XS'. The 'long' band has the greater fluxes and is, as explained above, used in the usual C, M, X flare designations. The 'short' band fluxes are more penetrating and so are more representative of the wavelengths doing the ionizing at the bottom edge of the D-region during a large flare [e.g., *Banks and Kockarts,* 1973]. The XL/XS power ratio varies from around 20-40 at the C1 level down to around 2-3 for the largest flares. This is discussed in more detail in section 5. In the present day GOES satellites (GOES 10 and 12), the 'XL' fluxes saturate at about X17 (1.7 mW/m^2) whereas the 'XS' fluxes saturate just below 0.5 mW/m^2 which typically corresponds to flare sizes of around X8-X12.

In section 2, the use of VLF phase perturbations is extended to extrapolate the 'XS' 0.05-0.4 nm X-ray flux during the great flare, beyond saturation to its peak. By making a reasonable estimate for the XL/XS ratio at the peak, the peak XS flux is translated into a new estimate of peak XL flux, and thus flare magnitude. Later, in section 5, these XL/XS ratios, particularly during large flares, are further examined and found to be able to give surprisingly good estimates of (conventional) flare sizes, in particular the size of the great flare of 4 November 2003.

In section 3, we test the VLF-phase extrapolation technique on VLF paths with higher solar zenith angles (i.e., with the Sun nearer the horizon) to potentially considerably increase the number of suitable VLF observing paths for extrapolating the X-ray fluxes of very large flares.

In section 4, we extend the work of *McRae and Thomson* [2004] who reported H' and β values (measures of the D-region reflection height and 'sharpness' respectively) as functions of X-ray flux from around C1-C2 up to about X5. The VLF amplitudes and phases of three new large flares (X10, X20, and X45) are analyzed here to extend this range of D-region electron density parameters by a further factor of nearly 10 in X-ray flux.

2. X-ray Flux Extrapolation using VLF Phase Records

Figure 1 shows the VLF radio propagation paths used in this study, in particular, the 12.3 Mm path across the sunlit Pacific Ocean to Dunedin, New Zealand from the 24.8 kHz US Navy transmitter, NLK, in Seattle.

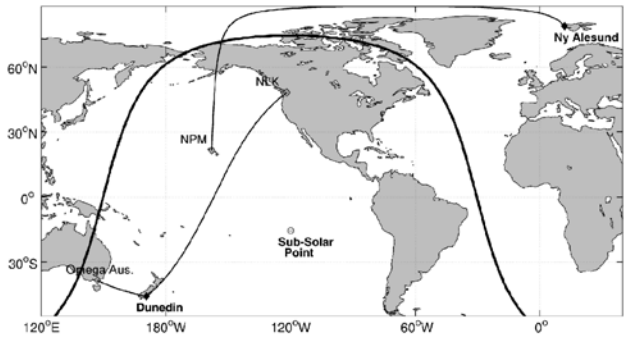

Figure 1. The VLF radio propagation paths used here together with the day-night terminator (bold line).

Figure 2 [*Thomson et al.,* 2004] shows the 0.1-0.8 nm flux (right hand axis, log scale) as a function of time during the great flare of 4 November 2003. Also shown are the accompanying phase variations of NLK received at Dunedin. The two curves were superposed by linearly scaling the phase, with an appropriate constant factor, and offsetting the phase by another appropriate constant factor.

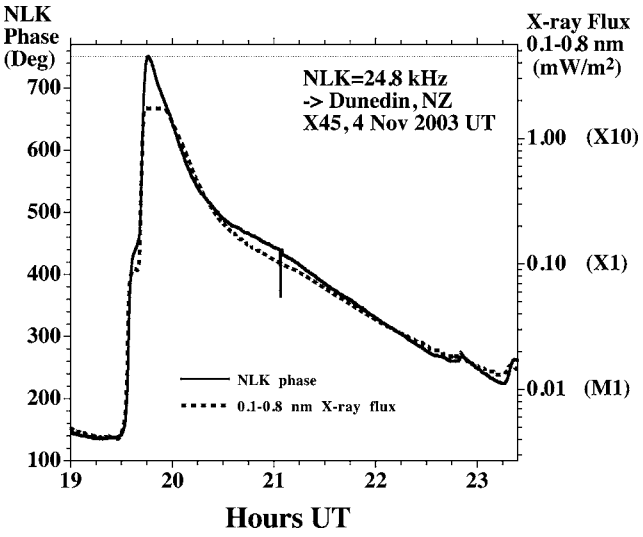

Figure 2. The phase of NLK, Seattle, as received at Dunedin, NZ, during the great flare on 4 November 2003, superposed on the XL (0.1-0.8 nm) GOES X-ray flux.

The phases were recorded with AbsPAL receivers which are similar to OmniPAL VLF data loggers [*Dowden et al.*, 1998] but modified so that they lock to GPS 1-second pulses [*Bahr et al.*, 2000]. The 3-second resolution X-ray data in figure 2 have been scaled in amplitude to match the 1-minute data on the NOAA-SEC web site, and thus the standard (C,M,X) X-ray flare magnitudes.

The VLF phase in Figure 2 can be seen to track the GOES 0.1-0.8 nm X-ray flux up until the X-ray detector goes into saturation at about X17. Assuming the phase continues to track the (unavailable) XL flux beyond saturation, the peak flux is 4.5±0.5 mW/m^2 or X45±5 as found by *Thomson et al.* [2004] who also found very similar results (including a peak around X45) using the Dunedin recorded phases of NPM

(Hawaii, 8.1 Mm, 21.4 kHz) and NDK (North Dakota, 13.5 Mm, 25.2 kHz) to extrapolate the GOES 0.1-0.8 nm X-ray flux.

Figure 3 is similar to Figure 2, except that the VLF phase (NLK to Dunedin) is now fitted to the 'short' or 'XS' band X-ray flux (0.05-0.4 nm). As can be seen, the phase again tracks the XS flux well, enabling the flux to be extrapolated from

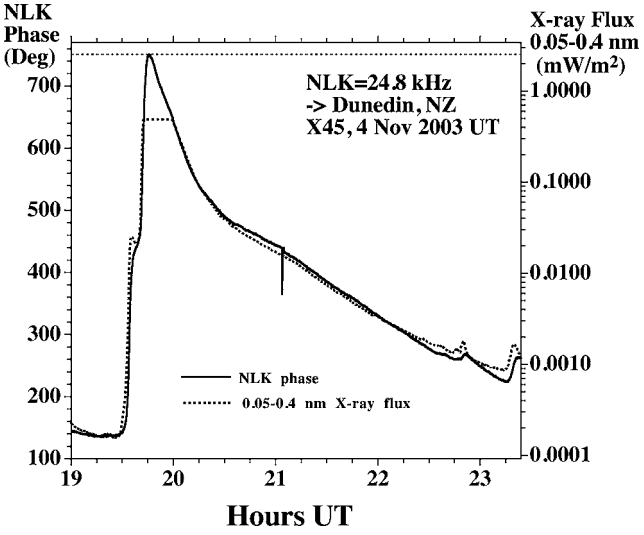

Figure 3. Similar to Figure 2 except that the *XS* band (0.05-0.4 nm) GOES X-ray flux is compared with the VLF phase of NLK, Seattle, as received in Dunedin, NZ.

saturation (about 0.49 mW/m^2) up to the peak which can thus be seen to be about 2.45 mW/m^2 (with an error of about ±0.3 mW/m^2). X-ray flux in this XS band is likely to be doing the bulk of the ionizing in the enhanced lower D–region, at altitudes of 40-70 km [e.g., *Banks and Kockarts*, 1973]. Although there is more energy in the XL band (0.1-0.8 nm), these longer wavelength X–rays do not penetrate so far into the atmosphere.

It is interesting to explore how the ratio of 'long' X-ray flux to 'short' X-ray flux (i.e., XL/XS) varies during the flare. In Figure 4 this XL/XS ratio is plotted against the 'long' band flux, XL. The ('open' circle) data points are from the 3–s X–ray fluxes from NOAA-SEC (scaled in size to match their standard 1-min values). As the flare rises towards its maximum the XL/XS ratio reduces, moving up the lower trace; the XL/XS ratio is lower (i.e., the flux is harder) while the flare fluxes are rising (for given values of XL) as compared with when the flare is decaying.

The cusp on the rising trace at about the X1 level (0.1 mW/m^2) corresponds to where the fluxes happen to briefly plateau, for this particular flare (see Figures 2 and 3), during their otherwise rapid rises. The near 90-degree change of direction of the data points as the flare rises past about X10 (1 mW/m^2) is due to first the XS flux saturating and then, around X17, the XL flux saturating too. When both fluxes come out of saturation, the XL/XS ratio moves down the upper trace as the flare decays.

The dashed line around the peak of the flare is a likely extrapolation of the XL/XS ratio beyond saturation. In making this extrapolation the following (reasonably probable)

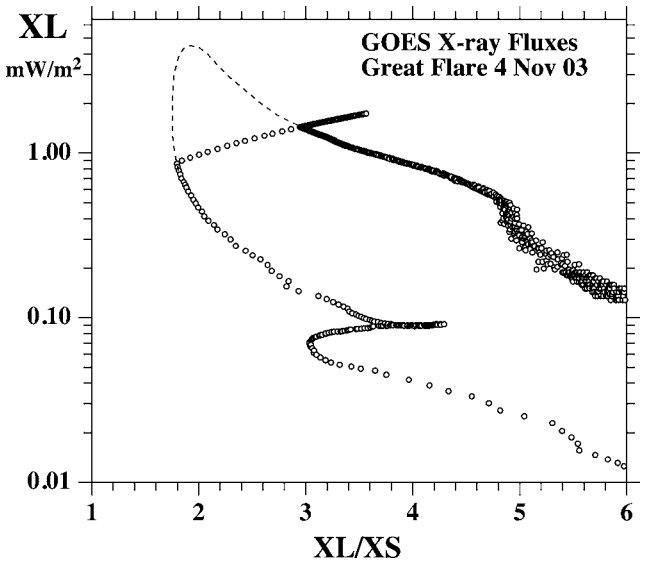

Figure 4. The 'long' band (0.1-0.8 nm) X-ray flux, XL, plotted against the XL/XS ratio, where XS is the 'short' band (0.05-0.4 nm) X-ray Flux, from GOES 12 near the peak of the great flare on 4 November 2003. Time increases clockwise around the plot, starting in the lower right corner.

constraints were used as guides: (1) the slope of the XL/XS versus XL plot should not change suddenly and (2) the general appearance/shape of the XL/XS ratio near the peak should be similar to that for other large flares (as displayed in section 5). Although the peak value of XL is shown (tentatively) at X45 in Figure 4, it would make little difference to the resulting value of the XL/XS ratio at the XL peak if this peak value were anywhere in the range X20-X50. Thus it can be seen that a reasonable estimate of the XL/XS ratio at the peak of the great flare is about 1.92 ± 0.1. However, this ratio, when combined with the 'short' flux peak value of 2.45 mW/m^2 as extrapolated in Figure 3, gives XL = 1.92 x 2.45 = 4.7 mW/m^2 or a magnitude of X47±8 (after allowing for uncertainty in both the XS peak flux and the XL/XS ratio at the peak). This indirect estimate of X47 is reasonably consistent with the more direct (VLF phase-guided, 'long' flux) extrapolation of X45±5 made by *Thomson et al*. [2004].

3. VLF Phase near Dawn/Dusk and X-ray Flux Extrapolation

The original VLF phase extrapolations of the great flare's (long band) X-ray flux, which gave the peak as X45, used VLF paths from Hawaii, Seattle and North Dakota to New Zealand for which the maximum solar zenith angle was about 65 degrees while the average solar zenith angle was about 40-50 degrees, meaning the paths were well sunlit with the Sun averaging 40-50 degrees above the horizon.

The question arises as to whether it is necessary for the Sun to be so high in the sky in order to get a satisfactory VLF phase extrapolation (in cases where the X-ray flux detectors saturate). Not surprisingly solar zenith angle does affect VLF phase and this occurs progressively with changing daytime solar zenith angle; it is not simply a matter of being either day or night [*McRae and Thomson*, 2000 and 2004]. However,

although the effects on the D-region of the ionosphere and hence the changes in VLF phase become smaller for flares at high solar zenith angles (since the X-rays have to travel obliquely and thus further through the atmosphere to penetrate to and ionize at a given height), the effects seem likely to be *proportionately* smaller.

For example, if the solar zenith angle were sufficiently great that the VLF phase change for the X-ray flux increasing from (say) 4 $\mu W/m^2$ to 1.7 mW/m^2 (i.e., GOES detector saturation) was half that for (nearly) overhead Sun, then it seems likely that the VLF phase change from the GOES saturation level to the peak flux (say 4.5 mW/m^2) would also be half that for (nearly) overhead Sun. This would be in line with the observations of *McRae and Thomson* [2004] who found that the VLF phase perturbations were fairly closely proportional to the logarithm of the X-ray flux at least up to about X5 (0.5 mW/m^2 in the usual 0.1-0.8 nm band). However, their results applied for solar zenith angles less than about 60-70 degrees and fluxes up to X5.

An opportunity to test VLF paths with higher solar zenith angles arises with the 2.2 Mm 'Omega Australia' (13 kHz, 38.5^o S, 146.9^o E) to Dunedin, NZ, path for which the solar zenith angles were in a range of about 64-82 degrees near the time of the great flare peak (1945 UT, 4 November 2003). This is shown in figure 5 where the extrapolation again comes out close to X45 thus suggesting that such high solar zenith angle paths can give good results. The transmitter referred to

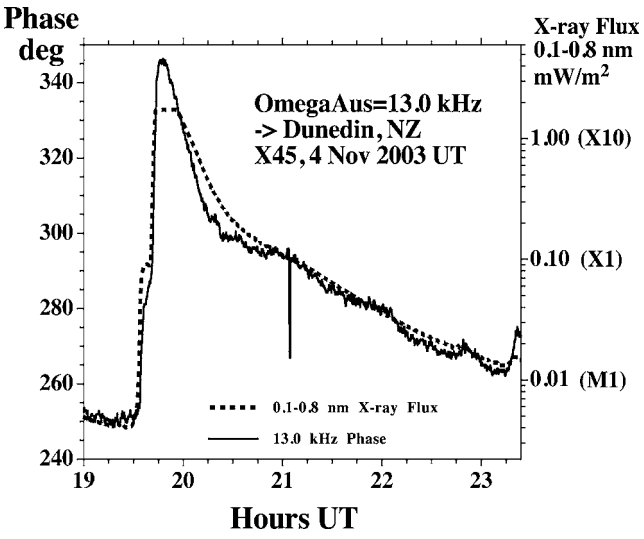

Figure 5. Extrapolation of the great flare X-ray flux using the phase of 'Omega Australia' at Dunedin near dawn.

here as 'Omega Australia' is the transmitter that used to be the real Omega Australia until 30 September 1997. In 2003 it was using 100 baud MSK on a fixed frequency of 13 kHz rather than the old Omega pulse sequence. Unfortunately it was no longer as phase stable as the real Omega transmitters were. However, this does not seem to be a problem because the phase drift is fairly constant (about 46 degrees per hour) and this has been largely removed before Figure 5 was plotted.

It now seems appropriate to test if VLF phase extrapolation at still higher solar zenith angles might give useful, though possibly more approximate, results even when part of the path is in darkness. An OmniPAL receiver in Ny Alesund, Svalbard, recorded the phase of NPM, Hawaii, at the time of the great flare. About one third of the nearly 9 Mm path was in darkness at the receiver end. A superposed plot of the long band X-ray flux and the NPM phase is shown in Figure 6. It can be seen that, even for this day-night path, the VLF phase fit and extrapolation is quite good. Certainly the flare size would come out at X50±10 rather than X45 but this is only a ~10% difference for this very inhomogeneous path. From Figure 6 it can be seen that the NPM VLF phase changes are about 70 degrees per decade of X-ray flux change for this partly sunlit, 9 Mm, high solar zenith angle path. In contrast, for the fully sunlit, lower solar zenith angle, 8 Mm, NPM to Dunedin path, the VLF phase changes were about twice as large, at 130 degrees per decade of X-ray flux change [*Thomson et al.*, 2004]. These phase changes are none-the-less both proportional to the corresponding (logarithms of their) X-ray flux changes.

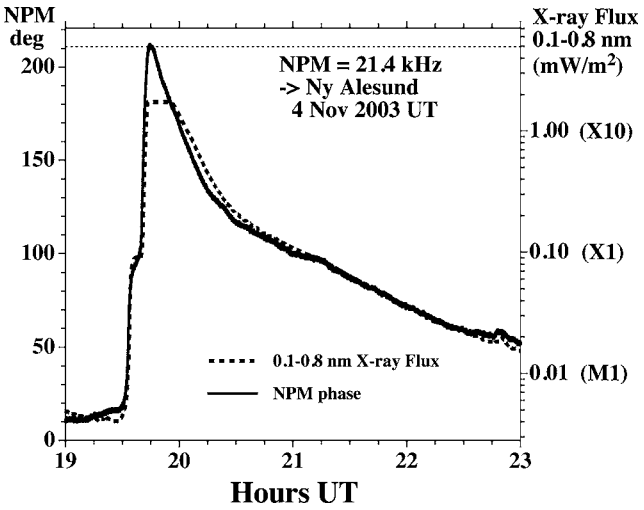

Figure 6. Extrapolation of the great flare X-ray flux using the phase of NPM, Hawaii, at Ny Alesund, Spitzbergen (with about 1/3 of the path in darkness).

For this path the NPM phase is stable but the OmniPAL receiver phase was drifting about 76 degrees/hour when averaged over a few days. In Figure 6, a correction of just 70 degrees/hour has been applied to get the best fits before and after the flare. This difference between 70 and 76 degrees/hour is partly due to changing solar zenith angle during the flare and partly to measurement uncertainty.

While a highly inhomogeneous day-night VLF path such as NPM to Ny Alesund gives only marginally satisfactory results on extrapolation, it is none-the-less interesting that they are so close to acceptable. This tends to imply that the relatively minor inhomogeneities in an all-day path, even at quite high solar zenith angles, are unlikely to detract significantly from the accuracy of VLF-phase-guided X-ray flux extrapolations.

The nearly satisfactory extrapolation results from the day-night NPM-Ny Alesund path do not imply that all day-night paths will give similarly useful results. Because of the near polar location of Ny Alesund (latitude ~79^o N) and the time of the flare, the sunrise/sunset terminator was moving rather slowly (less than about 0.2 Mm/hour) along this path.

In contrast, for the nearly 6 Mm day-night path from NWC (19.8 kHz, North West Cape of Australia) to Dunedin, the terminator was moving nearly 1.3 Mm/hour during the flare, and so the day-night phase changes are comparable or greater than the flare induced phase changes. Also, the day-night phase changes during a large flare can be expected to be significantly different from those in unperturbed conditions, because of the much lower D-region heights (and hence different mode conversions), and thus a useful separation of the flare effects from the day-night effects would be difficult.

4. D-region Electron Density Parameters as a Function of Solar X-ray Flux

The X-rays from solar flares ionize the neutral atmosphere at D-region heights (40-90 km) greatly increasing the electron densities there and thus markedly lowering the effective VLF reflection height. This lowering of the reflection height is the principal cause of the VLF phase advances observed during flares. However, the electron density profile at the lower edge of the D-region also 'sharpens' during flares in the sense that the rate of increase of electron density with height increases, and this also effects the VLF phase and amplitude at the receiver [eg *Thomson and Clilverd*, 2001 ; *McRae and Thomson*, 2004].

The VLF signals used here propagate in the Earth-ionosphere waveguide which is bounded below by the Earth (typically ocean) and above by the D-region. We model this using the NOSC (Naval Ocean Systems Center, San Diego, USA) computer programs (MODESRCH, MODEFINDER, LWPC – long wave propagation capability) which take the input path parameters, calculate appropriate full-wave reflection coefficients for the waveguide boundaries, and then search for those modal angles which give a phase change of 2π across the guide, taking into account the curvature of the Earth [e.g. *Morfitt and Shellman*, 1976]. These NOSC programs can take arbitrary electron density profiles supplied by the user to describe the D-region profile and thus the ceiling of the waveguide. However, for accurately predicting (or explaining) VLF amplitudes and phases, this approach effectively involves too many variables to be manageable in our present state of knowledge of the D-region. We thus follow the work of the NOSC group by characterizing the D-region with a Wait ionosphere defined by just two parameters, the 'reflection height', *H'*, in km, and the exponential sharpness factor, β, in km^{-1} [*Wait and Spies*, 1964]. This has been found to give very satisfactory results for normal daytime propagation over a good range of solar zenith angles [*Thomson*, 1993; *McRae and Thomson*, 2000] and for solar flares up to about X5 [*Thomson and Clilverd*, 2001; *McRae and Thomson*, 2004]. Here we extend the flare-time VLF phase and amplitude results of *McRae and Thomson* [2004] by nearly a factor of ten in X-ray flux up to the X45 level of the great flare of 4 November 2003.

4.1 VLF Amplitude Changes during the Great Flare

Figure 7 shows the amplitude (left-hand ordinate) of the 24.8 kHz VLF signal recorded at Dunedin, NZ, during the great flare of 4 November 2003. Also plotted, for comparison, is the 'long' (0.1-0.8 nm) GOES-12 X-ray flux (right-hand ordinate). The contrast with the phase plot for the same period in Figure 2 is evident. The phase varies very nearly proportionately with

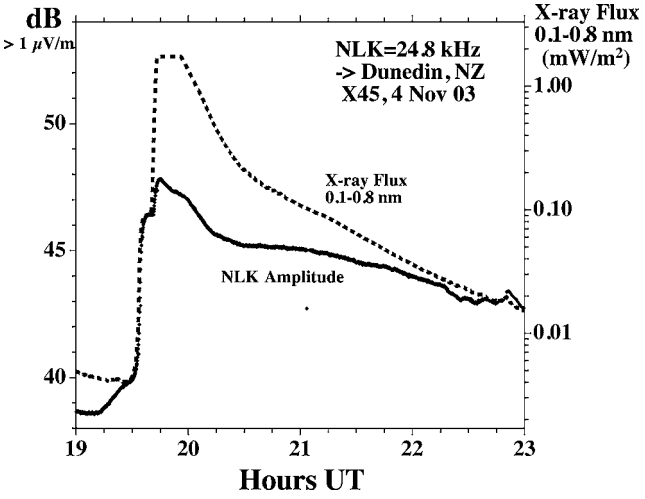

Figure 7. Amplitude of NLK, Seattle, recorded at Dunedin, NZ, together with the GOES X-ray flux during the great flare.

the (logarithm of the) X-ray flux while the amplitude does not. Thus the phase is useful and convenient for extrapolating the X-ray flux when the GOES detectors saturate but the amplitude is not. None-the-less, these flare-time VLF amplitudes and their accompanying phase perturbations readily allow the determination of β and *H'* at the peak of the flare, as described below.

4.2 Flare Induced VLF Amplitude and Phase Changes up to X45

Figure 8 shows the VLF phase and amplitude perturbations for the NLK to Dunedin path for three recent very large flares as well as the flares (all ≤X5) previously reported by *McRae and Thomson* [2004]. The three new very large flares shown are the X20 of 2 April 01, the X10 of 29 Oct 03, and the great flare of 4 Nov 03. Other recent very large flares such as the X17.2 of 28 Oct 03 and the X14.4 of 15 Apr 01 were not suitably timed for daylight VLF paths for our receivers in Dunedin, NZ.

Special care has been required in establishing and plotting the phase changes for the very large flares in Figure 8, as opposed to the smaller flares. Typically before the smaller flares and away from solar maximum, where the ≤X5 flares were recorded, the X-ray flux preceding the flare is (appreciably) less than the C1 level. In these conditions the pre-flare D-region is maintained principally by Lyman–α and so is at a standard unperturbed 'base' level. The phase changes observed and calculated are thus between this fairly standard unperturbed level [see *McRae and Thomson*, 2004, for details] and the flare peak. However, for flares occurring during periods of high solar activity, such as the very large flares reported here, the pre-flare X-ray flux is normally appreciably greater than C1 and so needs to be taken into account. For example, for the great flare, the pre-flare flux was about C4, and so the observed phase change ('C4-to-peak') needed to be increased by the (small) expected 'unperturbed-to-C4' phase change (from the left-hand side of the phase plot in Figure 8) before plotting the great flare (on the right-hand side of this plot) in Figure 8.

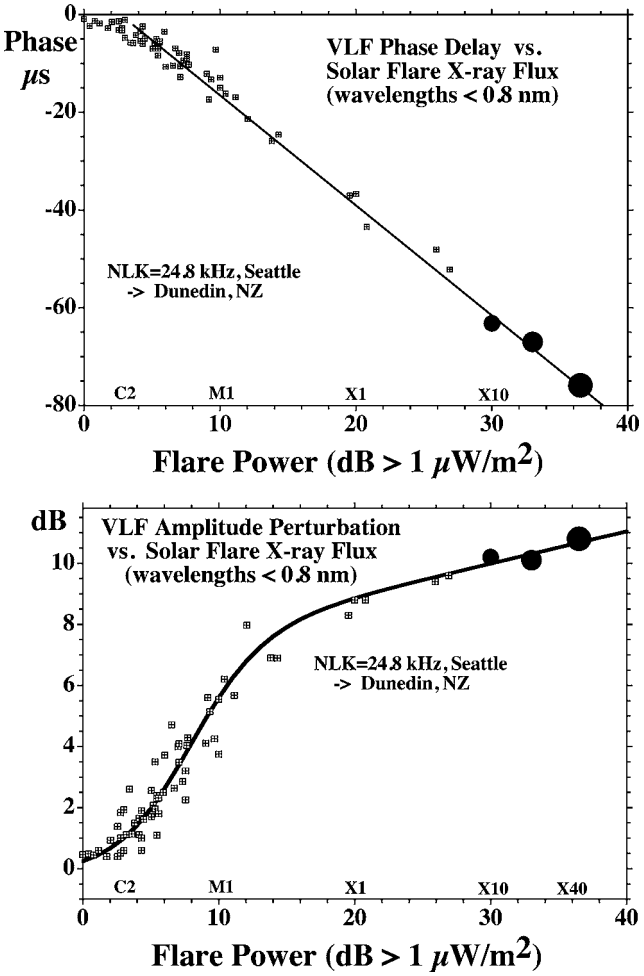

Figure 8. Phase delay perturbations and received VLF amplitude versus peak X-ray flux.

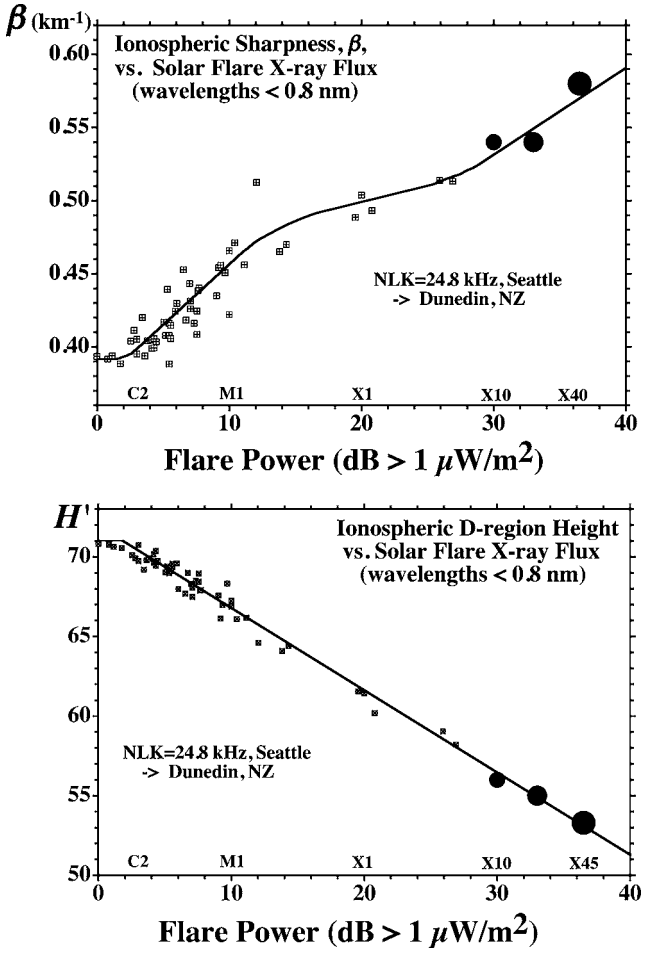

Figure 9. Ionospheric D-region sharpness, β, and height, H', as functions of peak solar flare power.

As can be seen in Figure 8, the phase trend evident in the previous work [*McRae and Thomso*n, 2004] continues (for a further factor of ~10 in flare power). However, the amplitude increase, in the lower panel of Figure 8, at high flare powers, does not fully flatten off for flare sizes >X5 as had previously been indicated [*McRae and Thomson*, 2004], but continues to rise slowly.

4.3 Flare Induced β and H' up to X45

Figure 9 shows plots of the values of β and H' required for MODEFINDER to calculate the observed (as shown in figure 8) absolute amplitudes at the flare peaks and the observed (as shown in Figure 8) phase changes at the flare peaks. Although the process of finding β and H' using MODEFINDER has an element of trial and error, the process is none-the-less fairly fast and straightforward. As is found from MODEFINDER, the phase changes are monotonic in H', and much more dependent on H' than β, while the amplitude changes are typically more dependent on β than H'. This makes it possible to iteratively and quickly find values of β and H' which cause MODEFINDER to output the observed amplitudes and the observed phase changes. The key to this is starting with appropriate values of β and H' for the unperturbed D-region. These are now fairly well established [e.g., *Thomson*, 1993; *McRae and Thomson*, 2004] and, when these are used as the starting points here, the resulting searches for the flare-time values of β and H' prove to be fast (few iterations), stable and unique.

As can be seen in the lower panel of Figure 9, the nearly linear reduction of H' with (the logarithm of the) flare flux (0.1-0.8 nm) continues from the upper limit of X5 in the previous study [*McRae and Thomson*, 2004] to at least the X45 of the great flare in the present study. However, in the upper panel of Figure 9 it can be seen that, although β levels off to a significant degree around X1-X5 as in the previous study, it then starts to rise again with increasing flare power for the very large flares (>>X5).

β increasing with flare power at low flare powers, and the (near) flattening off of β around the X1 flux level are still likely to be caused, as previously suggested [*Thomson and Clilverd*, 2001], by these X-ray fluxes becoming thoroughly dominant over both cosmic rays and Lyman-α as the ionizing source in the D-region, under these conditions. If Lyman-α were the sole source of ionization in the unperturbed D-region then the unperturbed profile slope would be similar to that when X-rays dominate. However, in the real unperturbed D-region, galactic cosmic rays make additional ionization mainly in the lowest parts [*Rishbeth and Garriott*, 1969] so that the unperturbed electron density falls with decreasing height at a

rate which is slower than for Lyman-α (or X-rays) alone. Such normal unperturbed profiles, in which the electron density increases relatively slowly with height, result in relatively low values of β when modeling using β and H'.

The discussion in the last paragraph provides an explanation of why β increases with increasing flare power until the effects of the X-ray flux swamp the effects of the galactic cosmic rays (and the Lyman-α) at which point β would be expected to increase no further and thus appear 'saturated'. It is suggested that the fact that β is observed to increase further for very large flares may be due to there being little X-ray flux at wavelengths shorter than about 0.05 nm (the lower wavelength limit of the 'short' GOES band). Only wavelengths shorter than this could penetrate significantly below a height of about 50 km and their absence would result in extremely low electron densities in these lowest parts of the VLF reflection region.

4.4 Flare Time Electron Density Comparisons

Wait and Spies [1964] defined a height dependent conductivity parameter:

$$\omega_r(z) = \omega_0^2(z)/\nu(z) = 2.5 \times 10^5 \exp[\beta(z-H')]$$

where $\omega_0(z)$ is the (angular) electron plasma frequency and $\nu(z)$ is the effective electron-neutral collision frequency, both being functions of the altitude, z, in km. This assumes $\omega_r(z)$ varies exponentially with height at a rate determined by the constant, β (in km^{-1}). H' is the height (in km) at which $\omega_r(z) = 2.5 \times 10^5$ s^{-1} and is often used as a convenient measure of the 'height' of the D-region. The collision frequency depends on the neutral air density which decreases (approximately) exponentially with height. A reasonable expression for the collision frequency, as used in LWPC and MODEFINDER is

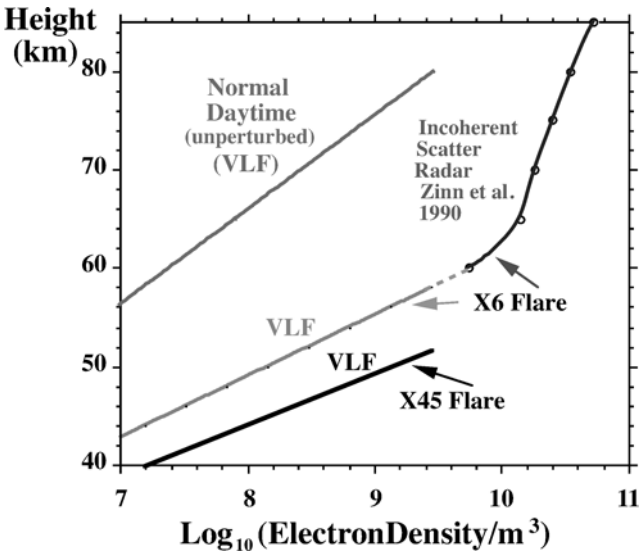

Figure 10. VLF-determined electron densities during the great X45 flare of 4 November 2003 compared with normal unperturbed electron densities. Also shown are electron densities from an incoherent scatter radar during an X6 flare and those predicted from VLF observations.

$\nu(z) = 1.82 \times 10^{11} \exp(-0.15z)$ [*Morfitt and Shellman*, 1976]. The (angular) plasma frequency is related to the electron density by $\omega_0^2(z) = N(z)e^2/(\varepsilon_0 m) \approx 3180\ N(z)$. Hence the electron density increases exponentially with height in the D-region as

$$N(z) = 1.43 \times 10^{13} \exp(-0.15H') \exp[(\beta - 0.15)(z - H')].$$

In Figure 10 are plotted the electron densities for (1) a typical unperturbed mid-solar cycle day ($\beta = 0.39$ km^{-1}, $H' = 71$ km [*McRae and Thomson*, 2004]), (2) an X6 flare as determined by *Zinn et al.* [1990] from a set of incoherent scatter observations, (3) an X6 flare from the H' and β values determined from VLF measurements as in Figure 9 [*McRae and Thomson*, 2004], and (4) the great X45 flare of 4 November 2003.

4.5 A Possible Extrapolation to Even Larger Flares

Figure 11 is essentially the same H' versus solar flare X-ray flux plot as in the lower panel of Figure 9 except that the best fit line has been extrapolated to very much larger solar X-ray fluxes than have ever been recorded. This illustrates just how well our atmosphere protects us on the Earth's surface from the X-ray bursts of extremely large flares. Even if a flare were so large that the 0.1-0.8 nm solar X-ray flux reached the level of the total current output of the Sun (i.e., the solar constant, ~1400 W/m^2), the lower edge of the ionosphere, and hence the height of extinction of the X-rays would still be greater than 20 km.

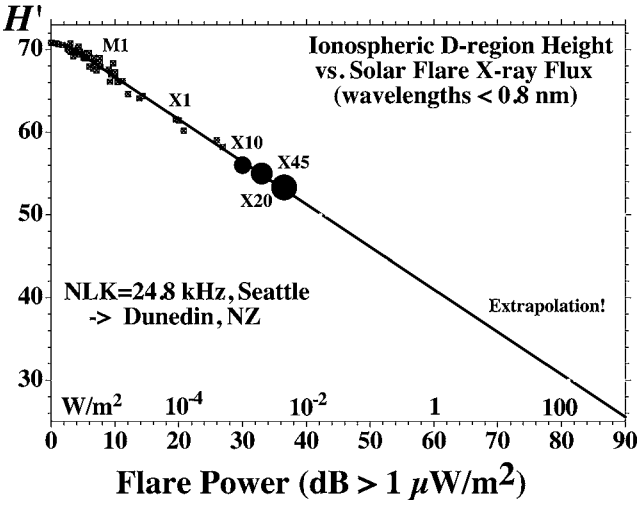

Figure 11. Same as lower panel of Figure 9 except extrapolated to much higher flare magnitudes.

5. Long/Short (XL/XS) X-ray Flux Ratios during Flares

As shown in Figure 4 and discussed in Section 2, the ratio of the 'long' X-ray flux to the 'short' X-ray flux, or XL/XS ratio, varies during the flare reaching a minimum near the flare flux peak. Similar such XL versus XL/XS plots are shown for a number of large flares in Figure 12. Five of the flares come from the same very active period, 20 October 2003 – 5 November 2003, as the great flare of 4 November 2003. They

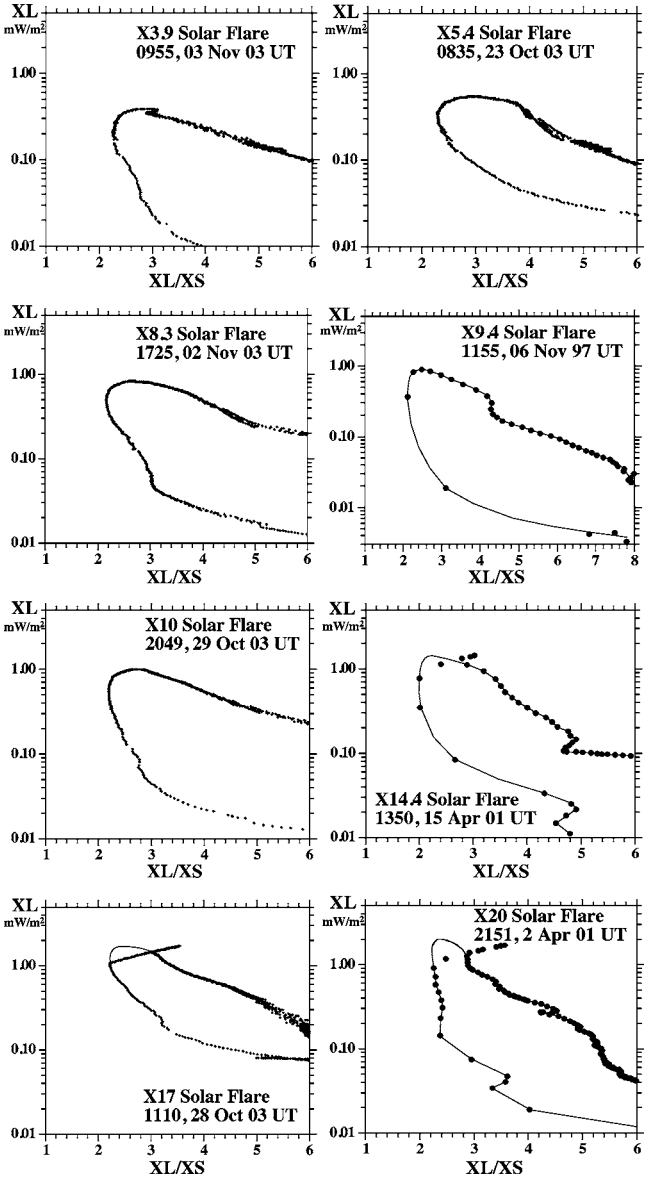

Figure 12. As in Figure 4, XL and XS are the 'long' and 'short' band X-ray fluxes. Again, XL is plotted against the ratio XL/XS. GOES 12 has been used for the five flares from 2003, and GOES 8 for the three earlier flares. Time again increases clockwise around each plot.

include the X17 flare of 28 October 2003 and the X10 flare of 29 October 2003 which are the 4th and 10th largest flares ever recorded by the GOES satellites (since 1976). Also included in this period are an X8.3, an X5.4, and an X3.9. They have been included partly because of their large sizes, partly because 3-second resolution data was available and partly because they were recorded on the GOES 12 satellite which is designated by NOAA-SEC as the current primary satellite and was the satellite used as the calibration source by *Thomson et al.* [2004] for their ionospherically estimated X45 determination.

Also shown in Figure 12 are the XL/XS ratios plotted against XL for the X20 flare of 2 April 2001, the X14 flare of 15 April 2001, and the X9.4 flare of 6 November 1997. For these three

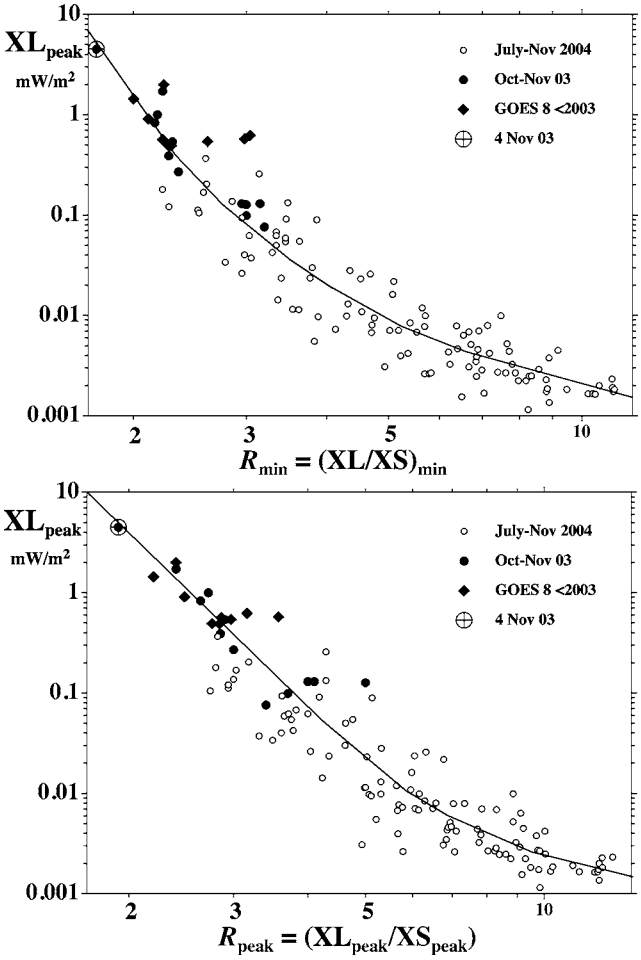

Figure 13. The peak 'long' band X-ray flux, XL_{peak}, plotted against (a) the minimum value of XL/XS near the flare peak and (b) the value of XL/XS at the flare peak.

flares the data comes from the GOES 8 satellite at 1-minute resolution.

In all cases the XL/XS ratios are lower for the rising flare fluxes than for the falling fluxes, just as for the great flare in Figure 4. As can be seen, the slopes of the XL/XS curves typically change progressively in the vicinity of the flux peaks. (For the X20, X17 and X14 flares, XS saturated near the peaks and so the curves have been extrapolated as was done for the great flare in Figure 4.) While no two flares have exactly the same XL/XS vs. XL shape, there can be seen to be some general features. The XL/XS ratio falls to a clear minimum shortly before the peak of the flare. No extrapolation is required to get this minimum for XL/XS except for the X45 and X20 flares and even then the extent of the extrapolation required is minimal.

For flares greater than about X10, extrapolation, shown by dashed or solid lines, has been needed in Figure 12 to estimate the XL/XS ratio at the peak because, as previously mentioned, XS saturates at about 0.49 mW/m^2. Obviously there is some uncertainty in the extrapolations but, as in figure 4, account has been taken of the non-saturating cases in Figure 12, including no discontinuities in the rate of change of slope near the peak. Also, in all cases except perhaps the X20 case, the peak XL values are known because XL has not saturated.

In the case of the X20 flare (2 April 2001) the XL extrapolation (from X17) is fairly minimal. Thus the XL/XS ratios at the flare peaks have likely been reasonably well estimated.

Both the minimum value of XL/XS for a flare and the XL/XS ratio at the peak are smaller the larger the flare. In Figure 13 the minimum value of the XL/XS ratio, R_{min}, and the XL/XS ratio at the (XL) peak of the flare, R_{peak}, are plotted against XL at the flare peak for some representative flares. Four plot symbols are used. The solid circles and the large X45 symbol are from 3-second GOES 12 data in the active period 22 October to 4 November 2003, plus an X1.3 flare on 27 May 2003. The open circles are from 1-minute GOES 12 data in July, October and November of 2004. The nine solid diamonds are from 1-minute GOES 8 data from 6 Nov 97 (X9), 18 Aug 98 (X5), 14 Jul 00 (X6), 2, 6 and 15 Apr 01 (X20, X5.6, X14), 28 Aug 01 and 13 Dec 01 (X5, X6), and 23 Jul 02 (X5). The solid lines are reasonable fits to the data points.

From Figure 13, it can be seen that the XL/XS ratios for both R_{min} and R_{peak} are consistent with the great flare of 4 November 2003 having a magnitude of about X45 as determined previously by *Thomson et al*. [2004] by VLF phase extrapolation of the XL flux. This XL/XS ratio consistency check is somewhat independent of the VLF ionospheric technique but has a higher uncertainty. A re-examination of the XL/XS ratio plot for the great flare in Figure 4 shows that if it had been extrapolated to only (say) X30, R_{min} would have hardly changed and so would still have indicated a magnitude of at least X45 in the R_{min} versus peak XL graph in the top panel of Figure 13.

6. Summary and Conclusions

The great solar flare of 4 November 2003 was the largest ever recorded by the X-ray detectors on the GOES satellites which have been in operation since 1976. Unfortunately the current GOES X-ray detectors saturate at about X17.4 and the great flare was markedly larger than this; so some means of extrapolation is needed to estimate its size. NOAA's Space Environment Center, who provide the GOES detectors and hence the most widely recognized international records of solar flare X-ray fluxes, arrived at an estimate of X28 for the peak by extrapolating their recorded fluxes beyond saturation. The flare X-rays create significant extra ionization in the Earth's ionosphere, particularly in the lower D-region where VLF radio waves reflect thus lowering their reflection height. It has been previously shown that the reflection height lowering and the peak VLF phase advances during flares are nearly linearly related to the logarithm of the flare's peak 'long' (0.1-0.8 nm) X-ray flux [*McRae and Thomson*, 2004]. It has also been shown [*Thomson et al.*, 2004] that the phase shifts during large flares are nearly linearly related to the VLF phase changes during the flares. This relation looks likely to apply over a very great range of solar flare X-ray fluxes (and D-region height lowering) without saturation. This has enabled the continuous, smoothly changing VLF phase to be used to extrapolate the 'long' (0.1-0.8 nm) X-ray flux from which a magnitude of X45 was obtained [*Thomson et al.*, 2004].

Because the wavelengths of the dominant ionizing X-rays at the VLF reflection height near the peak of the great flare are likely to be in the 'short' X-ray band (XS), it seemed sensible to also extrapolate this band's flux and find its peak value for the flare. This was done successfully in Figure 3, but as flare magnitudes are normally given in terms of their 'long' band peak flux (XL) a value of the XL/XS ratio at the peak was needed. This was found and used to show that this route gave a magnitude of X47±8 for the flare, consistent with the previous (long band) VLF ionospheric extrapolation.

VLF long path phase measurements can still provide very good X-ray flux extrapolation from saturation even when the Sun is quite low in the sky (8-26 degrees above the horizon). Further, quite useful extrapolation results were obtained from a completely independent receiver even though the (partly polar) path was partly in darkness (though more than 50% sunlit). However, in such a case it is important that the day/night ratio on the path is changing only very slowly during the flare.

The lowering of the D-region reflection height due to the flare X-ray fluxes was found to continue, essentially linearly, up to the X45 flux level, nearly a factor of 10 further than had previously been found up to X5. At the peak of the X45 flare, H' had lowered to a height of about 53 km, or about 17 km below typical mid-day, unperturbed conditions. The D-region sharpness parameter, β, which was previously thought to increase to saturation at about 0.52 km^{-1}, was found to increase further again up to about 0.57 km^{-1} at X45, possibly due to the X-ray flux spectrum falling off rapidly for wavelengths shorter than about 0.05 nm (the lower limit of the GOES 'short' band).

Finally the XL/XS ratios were examined for a number of flares from small to very large, and it became clear that the XL/XS ratios themselves were reasonably well defined functions of XL, and so could be used to make quite useful estimates of flare peaks (without reference to the ionosphere or VLF measurements). These XL/XS ratio plots were also found to be consistent with the great flare being at least as large as X45.

Acknowledgements. We are very grateful to NOAA's Space Environment Center, particularly to Dr Rodney Viereck, for their help and for providing not only the 1-min but also the 3-s GOES X-ray data, which made possible the (flux) calibration of our VLF phase data. We would also like to thank Mr Dave Hardisty of our institution for the design and implementation of the digital MSK multi-channel modulator/demodulator which carries our VLF signals live from our field station.

References

Bahr, J. L., J. B. Brundell, S. F. Hardman, and R. L. Dowden, Multi-instrument coincident detection of sprites, *Phys. Chem. Earth (B), 25*, 417-422, 2000.

Banks, P. M. and G. Kockarts, *Aeronomy,* Academic Press, N.Y., 1973.

Dowden, R. L., S. F. Hardman, C. J. Rodger, and J. B. Brundell, Logarithmic decay and Doppler shift of plasma associated with sprites, *J. Atmos. Sol-Terr. Phys.*, *60*, 741-753, 1998.

McRae, W. M. and N. R. Thomson, VLF phase and amplitude: daytime ionospheric parameters, *J. Atmos. Sol-Terr. Phys.*, *62*, 609-618, 2000.

McRae, W. M. and N. R. Thomson, Solar flare induced ionospheric D-region enhancements from VLF phase and amplitude observations, *J. Atmos. Sol-Terr. Phys.*, *66*, 77-87, 2004.

Mitra, A. P. *Ionospheric effects of solar flares*, D. Reidel, Dordrecht, 1974.

Morfitt D. G. and C. H. Shellman, MODESRCH, an improved computer program for obtaining ELF/VLF/LF mode constants in an Earth-Ionosphere Waveguide, Naval Electronics Laboratory Center Interim Rep. 77T, NTIS, Accession No. ADA032573, National Technical Information Service Springfield, Va. 22161, USA, 1976.

Rishbeth, H. and O. K. Garriott, *Introduction to Ionospheric Physics*, Academic Press, N.Y. and London, 1969.

Thomson, N. R., Experimental daytime VLF ionospheric parameters. *J. Atmos. Terr. Phys., 55*, 173-184, 1993.

Thomson, N. R. and M. A. Clilverd, Solar flare induced ionospheric D-region enhancements from VLF amplitude observations. *J. Atmos. Sol-Terr. Phys., 63*(16): 1729-1737, 2001.

Thomson, N. R., C. J. Rodger, and R. L. Dowden, Ionosphere gives size of greatest solar flare. *Geophys. Res. Lett.* 31(6), L06803, doi:10.1029/2003GL019345, 2004.

Watt, A. D., *VLF Radio Engineering,* Pergamon Press, Oxford, 1967.

Wait J.R. and K. P. Spies, Characteristics of the Earth-ionosphere waveguide for VLF radio waves. *NBS Tech. Note* 300, 1964.

Zinn, J., C. D. Sutherland, and S. Ganguly, The solar flare of August 18, 1979: incoherent scatter radar data and photochemical model comparisons, *J. Geophys. Res., 95* (D10), 16705-16718, 1990.